Bioinspired Catalysts for Phosphoryl Transfer Reactions

Inaugural-Dissertation

zur
Erlangung der Doktorwürde
der
Naturwissenschaftlich-Mathematischen Gesamtfakultät
der
Ruprecht-Karls-Universität
Heidelberg

Vorgelegt von
Diplom-Chemikerin
Malgorzata Jagoda
aus Tarnow, Polen
2005

Short summary in English

Phosphoryl transfer reactions are ubiquitous in biology and are usually catalyzed by metalloenzymes. For a number of phosphoryltransfer enzymes, including the exonuclease subunit of DNA polymerase I, a mechanism involving two metal ions and double Lewis-acid activation of the substrate, combined with leaving group stabilisation, has been proposed.

Aim of this thesis was the study of low-molecular-weight models of phosphoryl transfer metalloenzymes. The focus was in particular on the macrocyclic dicopper(II) complex **LCu$_2$**, which is the first transesterification catalyst for highly inert dialkyl phosphates and a mimic of the exonuclease subunit of DNA polymerase I.

For the first time, a crystal structure of **LCu$_2$** with a coordinated phosphodiester was obtained. [**L**Cu$_2$(1,3-μ-DMP)(NO$_3$)](NO$_3$)$_2$ (**2**) contains a 1,3- bridging phosphodiester.

By extensive UV-Vis and pH metric titrations, the metal complex species present in methanolic **LCu$_2$**/DMP solution have been identified. In particular it has been shown, that [**L**Cu$_2$(DMP)(OCH$_3$)]$^{2+}$ is the active species and that coordinated methanolate (and not free methanol or methanolate) is the nucleophile which attacks the P-atom of the substrate. DFT calculations (in cooperation with the group of Prof. Smith, IWR Heidelberg) confirm that the 1,3-DMP bridged complex is the dominant species in solution.

By extensive kinetic studies including rate dependence on catalyst concentration, saturation kinetics, pH dependence on rate and dependence on rate on substrate structure, solid experimental data have been obtained which support the proposal of a reaction mechanism related to exonuclease subunit of DNA polymerase I.

The applicability of **LCu$_2$** as a catalyst for the phosphorylation of various alcohols by dimethyl phosphate has been evaluated. A unique functional group tolerance of the catalyst and selectivity for dialkyl phosphates over alkyl carboxylates is observed.

Screening of ATP hydrolysis by Zr(IV) and Eu(III) complexes was examined using a robotic liquid-handling workstation. It was found that a phosphate detection assay using molybdate is compatible with the presence of these high-valent metal ions. ATPase activity of the metal is modulated by the ligands, and the most efficient catalyst is the Zr complex of the tetracarboxylate ligand **L6** at both pH 4 and pH 7. This is in contrast to Zr promoted DNA hydrolysis where polycarboxylate ligands have been shown to quench strongly the phosphoesterase activity of the metal ion.

Kurzfassung auf deutsch

Phosphoryl-Transferreaktionen sind in der Biologie allgegenwärtig und werden üblicherweise von Metalloenzymen katalysiert. Für eine Vielzahl von Phosphoryltransfer Enzymen, die Exonuclease Untereinheit der DNA-Polymerase I eingeschlossen, wurde ein Mechanismus vorgeschlagen, der durch zwei Metallionen eine doppelt lewissaure Aktivierung des Substrats mit einer Stabilisierung der Abgangsgruppe kombieniert.

Das Ziel dieser Arbeit war, niedermolekulare Modelle von Phosphoryltransfer-Metalloenzymen zu untersuchen. Das Hauptaugenmerk lag dabei auf dem makrocyclischen Dikupfer(II)-Komplex **LCu_2**, dem ersten Komplex, der als Modellkomplex der Exonuclease Untereinheit der DNA Polymerase I die Umesterung inerter Dialkylphosphate katalysiert.

Es konnte zum ersten Mal eine Kristallstruktur von **LCu_2** mit koordinierten Phosphodiestern erhalten werden. [**L**Cu_2(1,3-μ-DMP)(NO_3)](NO_3)$_2$ (**2**) enthält einen 1,3-verbrückenden Phosphodiester.

Über umfangreiche UV-Vis und pH-Titrationen wurden die in methanolischer Lösung von **LCu_2** und DMP vorliegenden Metallkomplex Spezies identifiziert. Es konnte gezeigt werden, dass [**L**Cu_2(DMP)(OCH_3)]$^{2+}$ die aktive Spezies ist, und dass koordiniertes Methanol (und nicht freies Methanol oder Methanolat) das Nucleophil ist, das das Phosphoratom des Substrates angreift. DFT-Rechnungen (in Zusammenarbeit mit der Gruppe von Prof. Smith, IWR Heidelberg) bestätigen den 1,3-DMP verbrückten Komplex als die dominierende Spezies in Lösung.

Eingehende kinetische Untersuchungen, u.a. zur Abhängigkeit der Reaktionsgeschwindigkeit von der Konzentration des Katalysators, zur Sättigungs-Kinetik, zur Abhängigkeit der Reaktionsgeschwindigkeit vom pH-Wert sowie der Substratstruktur,

lieferten experimentelle Daten, die einen vorgeschlagenen Reaktionsmechanismus mit Bezug zur Exonuclease-Untereinheit der DNA-Polymerase I untermauern.

Außerdem wurde die Anwendbarkeit von **LCu_2** als Katalysator für die Phosphorylierung verschiedener Alkohole mit Dimethylphosphat untersucht. Es konnte eine einzigartige Toleranz des Katalysators gegenüber funktionellen Gruppen sowie eine einzigartige Selektivität für Dialkylphosphate gegenüber Alkylcarboxylaten beobachtet werden.

In einem zweiten Projekt wurde an einem Pipettierroboter ein Screening-Verfahren für die ATPase Aktivität von Zirconium(IV)- und Europium(III)-Komplexen entwickelt. Es wurde gezeigt, dass Molybdat als Reagenz für den Phosphat-Nachweis mit diesen hochvalenten Metallionen kompatibel ist. Die ATPase Aktivität der Metallionen wird stark durch den Liganden beeinflusst. Zirconium-Komplexe eines Tetracarboxylat-Liganden **L6** wurden sowohl bei pH 4 als auch pH 7 als aktivste Spezies identifiziert. Dieses Ergebnis steht im Gegensatz zu den Beobachtungen für die Zirconium vermittelte DNA-Hydrolyse, bei der Polycarboxylatliganden die Phosphoresterase-Aktivität des Metalllions unterdrücken.

Bioinspired Catalysts for Phosphoryl Transfer Reactions

Inaugural-Dissertation

zur
Erlangung der Doktorwürde
der
Naturwissenschaftlich-Mathematischen Gesamtfakultät
der
Ruprecht-Karls-Universität
Heidelberg

Vorgelegt von
Diplom-Chemikerin
Malgorzata Jagoda
aus Tarnow, Polen
2005

Tag der mündlichen Prüfung: 21.10.2005

Bioinspired Catalysts for Phosphoryl Transfer Reactions

Gutachter: Prof. Dr. Roland Krämer

Prof. Dr. Nils Metzler-Nolte

Die experimentellen Untersuchungen zu der vorliegenden Arbeit wurden in der Zeit von September 2001 bis Mai 2005 im Anorganisch-Chemischen Institut der Ruprecht-Karls-Universität Heidelberg durchgeführt.

Herrn PROF. DR. ROLAND KRÄMER, unter dessen Anleitung diese Arbeit angefertigt wurde, danke ich herzlich für zahlreiche Anregungen, Diskussionen, sein Interesse an meiner Arbeit und die materielle Unterstützung.

Index of contents

List of Figures

List of schemes

List of tables

List of Abbreviation

ADP	Adenosine-5´-diphosphate
AMP	Adenosine-5´-monophosphate
ATP	Adenosine-5´-triphosphate
BNPP	Sodium Bis-(p-nitrophenyl)phosphate
DBP	Sodium dibenzyl phosphate
DMP	Sodium dimethyl phosphate
DNA	Deoxyribonucleic acid
EPR	Electron Paramagnetic Resonance
HPLC	High Performance Liquid Chromatography
MALDI	Matrix-Assisted Laser Desorption/Ionisation
NMR	Nuclear Magnetic Resonance
Ph	Phenyl
UV/Vis	UltraViolet/Visible
$^{s}_{s}$pH	experimental meter reading in methanol (correction parameter of 2.24 added) with an electrode standardized with aqueous buffers
$^{s}_{s}$pD	experimental meter reading in d_4- methanol (correction parameter of 2.24 added) with an electrode standardized with aqueous buffers

1. Introduction

1.1. Enzyme-catalyzed phosphoryl transfer reactions

Nucleophilic substitutions at phosphorus comprise one of the most important classes of reactions in biology. For example, cleavage and formation of the phosphate diester backbone of nucleic acid is catalyzed by nucleases and polymerases and are critical in replication, transcription and DNA repair. Phosphate transfer reactions are catalyzed by GTPases, ATPases, small molecule kinases and small molecule phosphatases.[1] These enzymes play diverse roles in energy regulation, cell signalling, ion and small molecule transport, and nucleotide synthesis.

1.1.1. Classes of enzymes involving reactions at phosphorus

In figure 1.1 are summarized the classes of enzymes that catalyze displacement reactions at phosphorus atom. The enzymes that handle phosphoric monoesters fall into three categories: the phosphatases, where water is acceptor of the phosphoryl group (these include enzymes such as alkaline phosphatase that are merely hydrolytic, and enzymes such as ATPases where the free energy available is coupled to some other metabolic function); the kinases where a nucleoside triphosphate is the phosphoryl donor and some molecule other than water is the acceptor; and the mutases, for which the acceptor is an intrinsic functional group of the donor molecule. The enzymes that handle phosphoric diesters are either hydrolytic (e.g. nucleases) or nucleotidyl transfer catalysts.[2]

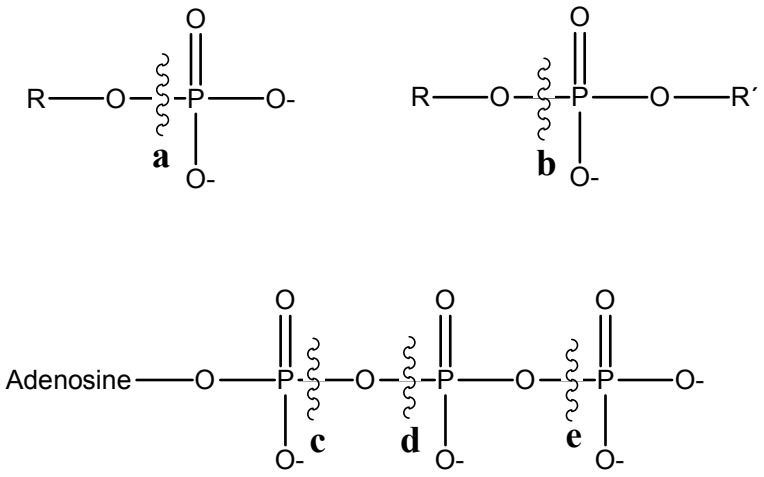

a phosphokinases
phosphatases
nucleotidases
phosphomutases

b nucleases
phosphodiesterases
phospholipases

c nucleotidyl transferases
nucleotidyl cyclases

d pyrophosphokinases

e phosphokinases
ATPases

Figure 1.1. Classes of enzymes that catalyze transfer reactions at phosphorus.

1.1.2. Klenow fragment of DNA polymerase I

DNA polymerases catalyze the template-directed addition of nucleotides onto the 3´-OH group of the DNA primer terminus. Those enzymes belong to four families: polymerases I (family A), polymerases α (family B), polymerases β (family X) and reverse transcriptases.[3,4] Although polymerases from different families are structurally quite diverse, several common

features have emerged. The polymerase domain from each enzyme resembles a right hand protein and may be further divided into palm, fingers, and thumb subdomains (Fig. 1.2), as was originally described for the large fragment of Escherichia coli polymerase I (Klenow fragment).[5] The polymerase I has three enzymatic activities: DNA polymerase; the Klenow fragment (the large C- terminal fragment) has both, the DNA polymerase and the 3´-5´exonuclease activities, and the smaller amino terminal fragment has the 5´-3´exonuclease activity.

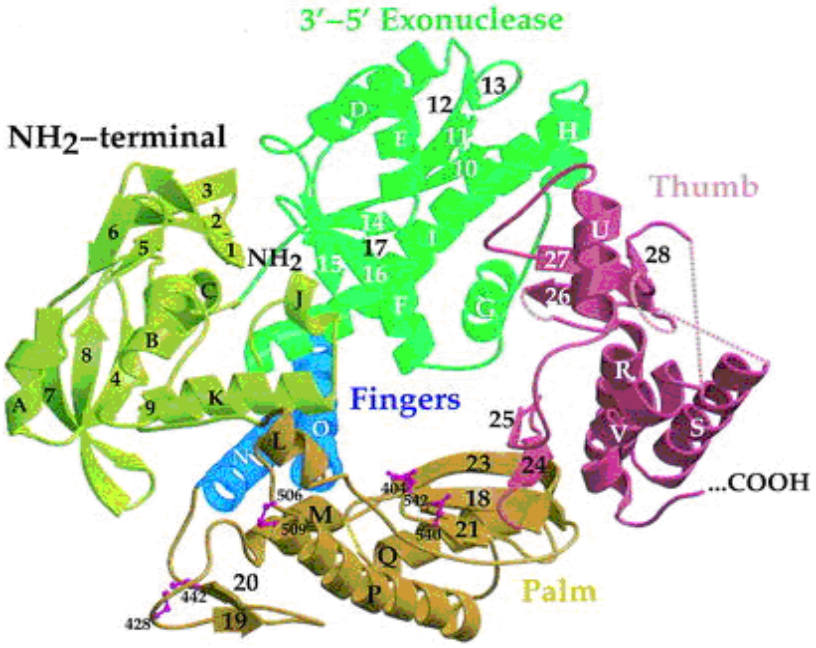

Figure 1.2. General structure of DNA polymerases.[6]

The Klenow fragment is folded into two distinct domains, the smaller one binds deoxynucleoside monophosphate and metal. The larger domain forms a structure containing a very deep cleft that is large enough to accommodate the double-stranded DNA, the product of DNA synthesis.

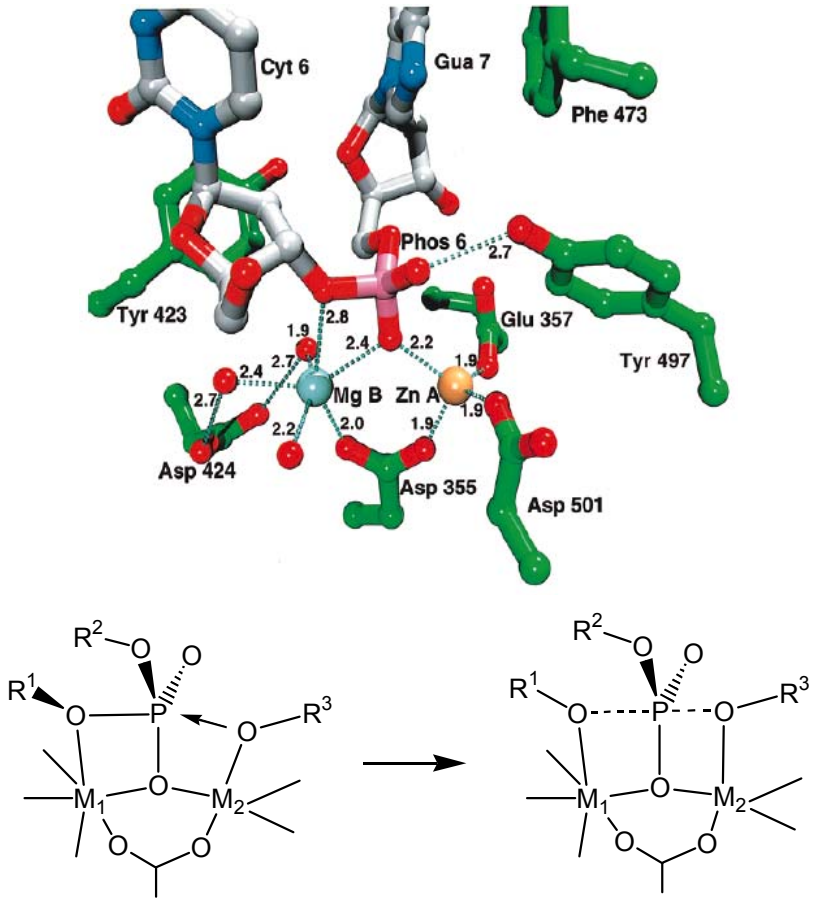

Figure 1.3. Top: View of the 3´-5´exonuclease active site with bound deoxydinucleotide. Bottom: Proposed mechanism of phosphodiester hydrolysis.

All polymerases appear to share the same mechanism for nucleotidyl transfer reactions, involving two divalent metal ions,[7] and it is thought to be an associative mechanism, proceeding through a pentacovalent intermediate.[8] The active site of the 3´-5´exonuclease is shown in figure 1.3.[9] The deoxynucleoside monophosphate binds to the smaller N-terminal domain of the Klenow fragment in the same position as the 3´ terminal nucleotide of a single-stranded substrate. In the absence of substrate or product, the exonuclease domain has one firmly bound divalent metal ion (site A) while the deoxynucleoside monophophate complex shows a second divalent metal ion (site B) bound ~ 4 Å from site A. Divalent metal ions ($Mg^{2+,}$ Mn^{2+} or Zn^{2+}) are essential for exonuclease activity and their removal by EDTA or by mutation of ligating amino acids results in the loss of the deoxynucleoside monophosphate binding and loss of exonuclease activity in solution.[10] The metal ions provide double Lewis-

acid activation of the bridging phosphate, site A generates a coordinated hydroxide nucleophile and site B stabilizes the alcoholate leaving group (Scheme 3.5). The trigonal-bipyramidal transition state (or intermediate) of the nucleophilic substitution reaction is efficiently stabilized. Subsequently this (or a closely related) mechanism has been proposed, mostly on basis of crystallographic evidence, for other phosphoryl transfer enzymes in which two active site metal ions are about 4 Å apart. It was observed in phosphate monoester cleavage by alkaline phosphatase[11], that a transesterification step is involved, which was as well proposed for restriction endonucleases[12], for DNA polymerases[13,14] and was discussed as a possible mechanism of RNA cleavage by ribozymes.[15]

1.2. Dinuclear models for phosphoryl transfer

In the past decades many enzyme-catalyzed processes have been mimicked with synthetic molecules.[16,17,18] The cleavage or transesterification of phosphate diesters is of particular interest. Under neutral conditions phosphate diesters are negatively charged and resistant toward hydrolysis, which explains their presence in nature as the repeating linkers in DNA and RNA. In this respect, the development of artificial catalysts that can cleave phosphate diester bond is a fundamental challenge. Moreover, artificial enzymes that can cleave DNA and RNA at specific sites may find application as tools in biotechnology or as therapeutic antisense oligonucleotides.[19]

The first report on catalytic phosphate ester cleavage by two cooperating metal ions came from the group of Breslow[20]. They used a phenyl spacer to orient two macrocyclic ligands known to form extremely stable Zn(II) complexes. At pH 8.0, the resulting dinuclear Zn(II) complex **I** (Fig. 1.4) is 4.4 and 7 times as effective as its monomer in the hydrolysis of the

neutral charged esters diphenyl p-nitrophenyl phosphate and p-nitrophenyl acetate, respectively.

Cleavage of ribonucleotide dimers by intramolecular transesterification to cyclic mononucleotide phosphates was studied by Komiyama and coworkers.[21] The dinuclear Zn(II) complex **III** (Fig.1.4) efficiently cleaves adenyl(3′-5′)adenosine for which the authors propose a mechanism comprising Lewis acid activation of the phosphoryl group and the leaving group stabilization, but no experimental evidence for such a mechanism is given.

The first report of a dinuclear Zn (II) complex applied in an antisense oligonucleotide was published as well by the group of Komiyama.[22] They coupled two equivalents of **II** (Fig.1.4) to m-xylene and tethered the dinucleating ligand to the 5′ ends of DNA oligomers. Incubation with a complementary RNA oligonucleotide resulted in sequence-selective cleavage of the RNA target. The cleavage is due to cooperative action of the Zn (II) centers within the DNA-RNA duplex and even at high concentration of free Zn(II) ions the cleavage is selective.

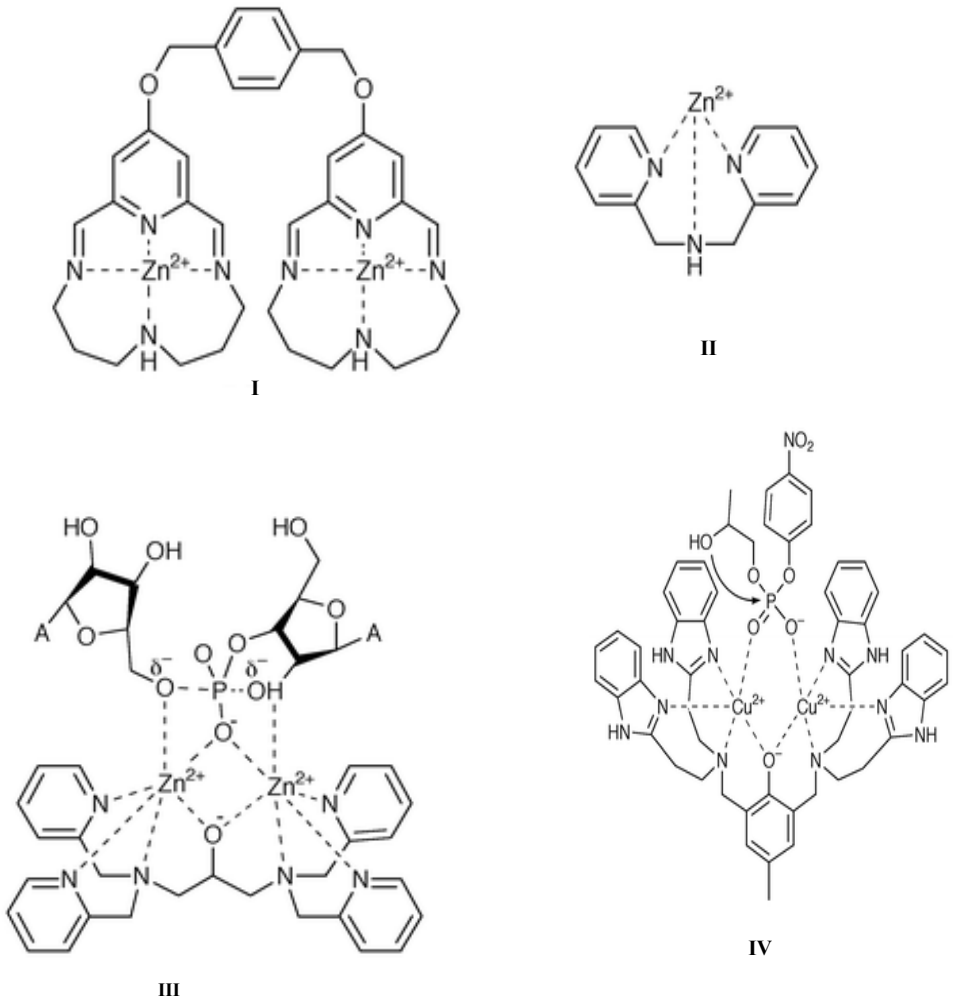

Figure 1.4. Examples of dinuclear models for phosphoryl transfer enzymes.

The group of Chin was one of the first reported on the high catalytic activity of Cu(II) complexes in phosphodiester cleavage. In complex **IV** (Fig. 1.4), two Cu(II) centers are bridged by a phenoxide and display a high cooperativity in the intramolecular transesterification of the RNA model 2-hydroxypropyl p-nitrophenyl phosphate (HPNP).[23] Despite an enormous rate acceleration of approximately 2 x 10^4 in the cleavage of HPNP, the cleavage of RNA dinucleotides was not catalyzed, probably because of steric hindrance.

1.2.1. Model systems for Klenow fragment of DNA polymerase I

A structural model for phosphate diester binding to the Klenow fragment of DNA polymerase I was reported by Lippard and coworkers.[24] In the complex, two Cu(II) ions are bridged by hydroxide and diphenyl phosphate (Fig. 1.5). One oxygen atom of from the latter is bound to the metal ions in the unusual 1,1-μ-O- bridging mode.

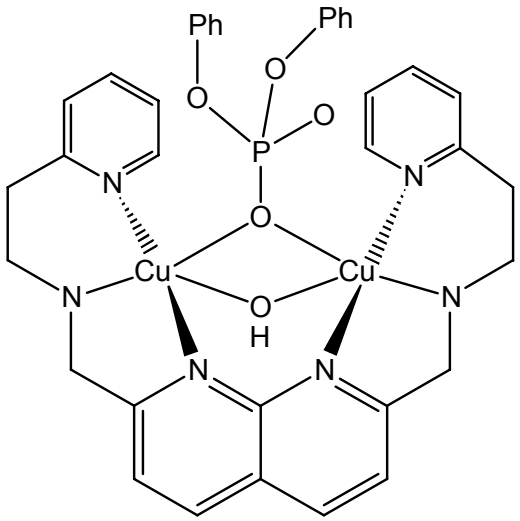

Figure 1.5. Structure of $[Cu_2(\mu\text{-}OH)\{\mu\text{-}(PhO)_2PO_2\}(BPAN)]^{2+}$ cation.[24]

Many other important studies using simple coordination compounds gave insight into various modes of the two-metal ions activation in the phosphoryltransfer reactions. In most cases, the substrates were reactive phosphate esters, either with good leaving groups (such as nitrophenolate) or with neighbouring -OH as a catalytic auxiliary group (as present in RNA), or supercoiled plasmid DNA which is activated by intrinsic strain. Although simple dialkyl phosphates such as $O_2P(OCH_3)^{2-}$ represent more appropriate models for many biological phosphate transfer reactions than activated aryl phosphates, a very few examples of the cleavage of such phosphates by synthetic reagents have been reported. The reason is that these

substrates are highly inert: stoichiometric hydrolysis has been observed only with strongly Lewis-acidic tri- and tetravalent metal ions at high temperature or low pH.[25,26,27]

1.2.2. Model systems for ATPase activity

Hydrolysis of adenosine-5´-triphosphate (ATP) occurs via highly efficient metalloenzymatic reactions catalyzed by ATPases and plays a key role in numerous processes: photosynthesis phosporylation (chloroplast ATPase), oxidative phosphorylation (mitochondrial ATPase), muscle action (myosin ATPase), etc. However, despite a large knowledge based on metalloenzyme crystal structures, kinetic and binding data, and extensive studies with model systems, the detailed role of the metal ion is still unclear.[28,29] Williams[30] has demonstrated that ATP hydrolysis promoted by multiple metal ions in an associative mechanism is highly sensitive to catalysis by Mg(II) ions in aqueous solution. The rate of hydrolysis of ATP by dinuclear Co(III) complex is 3000-fold faster in $MgCl_2$ solution than in KCl solution (Fig. 1.6).

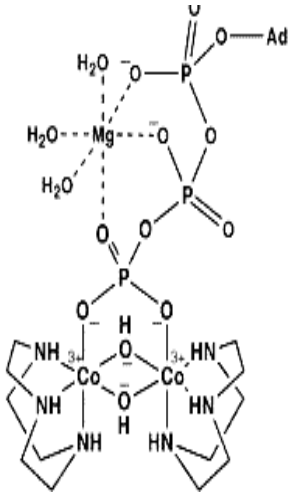

Figure 1.6. Binding of Mg(II) to Co(III)-ATP complex

It is recognized that macrocyclic and polymacrocyclic polyammonium cations selectively bind a variety of inorganic and organic anions with high affinity.[31,32] Hosseini et al.[33] found that the 24-memberd ditopic macrocycle [24]N_6O_2 forms supramolecular complexes by strongly binding ATP and provides significant rate enhancement in its cleavage to ADP and phosphate (Fig. 1.7). The structural properties of the complex apparently favour nucleophilic catalysis, and the central neutral amino group in this ditopic receptor displaces ADP by reaction at the terminal phosphate group of the bound substrate. The resulting phosphoramidate derivative hydrolyses in water to regenerate the catalyst and to complete the cycle. Studies on the effect of an addition of metal ions show the greatest rate enhancement for manganese (II) which doubled the rate of ATP hydrolysis.

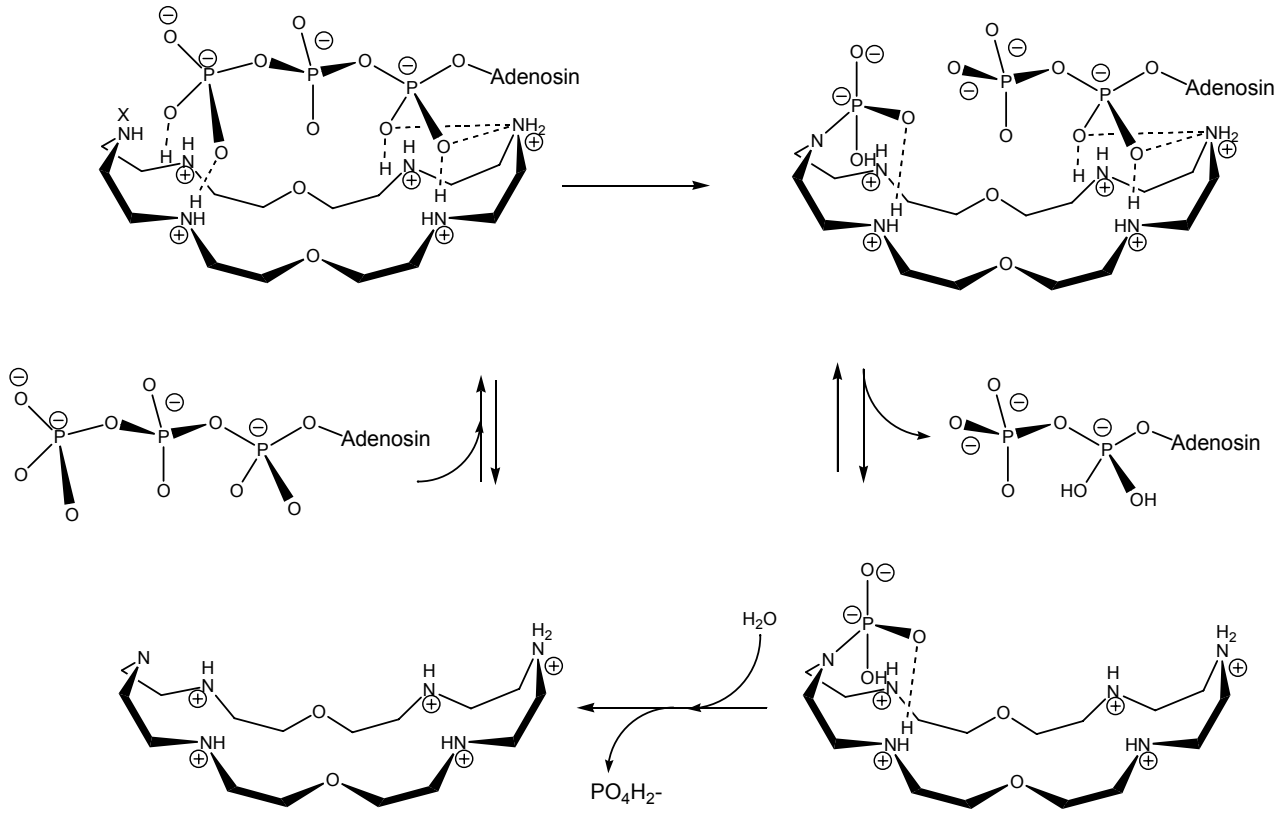

Figure 1.7. Schematic representation of the sequence of reactions for ATP dephosphorylation.

1.3. Chemistry of aqueous zirconium(IV) solutions

This area of zirconium chemistry has long been confused by a lack of structural information and by complexities due to pH dependent formation of various aggregates. At pH < 1 $[Zr(OH)]^{3+}$ is formed whereas at higher pH formation of species such as $[Zr_3(OH)_4]^{8+}$ and $[Zr_4(OH)_8]^{8+}$ is observed.[34] The structure determination of $ZrOCl_2 \cdot 8H_2O$[35] was an important step forward since it showed that this salt contained the tetranuclear cation $[Zr_4(OH)_8(H_2O)_{16}]^{8+}$ (Fig. 1.8).

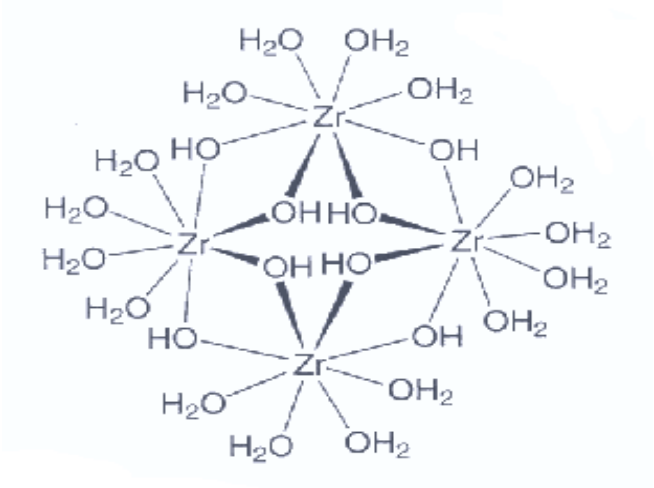

Figure 1.8. Structure of $[Zr_4(OH)_8(H_2O)_{16}]^{8+}$ cation.

The four zirconium atoms are linked ba bridging OH groups, and four water molecules at each Zr complete the 8-fold coordination.

2. Aim of this study

The dinuclear, macrocyclic complex **LCu_2** was previously found to be the only available catalyst for the transesterification of the highly inert substrate dimethyl phosphate. The unique reactivity of this complex was atribiuted to a reaction mechanism similar to that proposed for the Klenow fragment of DNA polymerase I, and other dinuclear phosphoryl transfer enzymes. Therefore, the complex was hypothesized to serve as the first low molecular-weight model for the investigation of the two-metal mechanism suggested for many phosphoryl transfer enzymes.

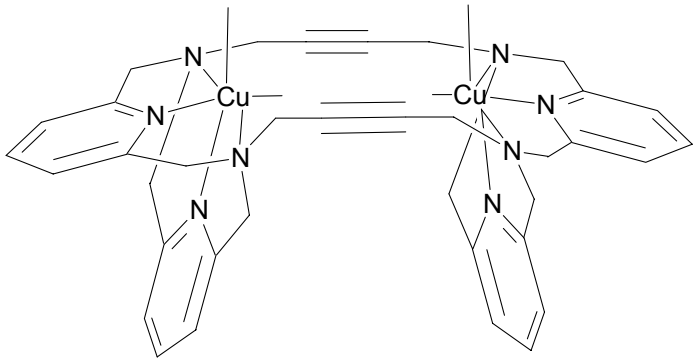

LCu_2

Aim of this work was to support the suggested reaction mechanism by structural, speciation, kinetic and theoretical studies, and to explore the applicability of the **LCu_2** to the phosphorylation of alcohols by dimethyl phosphate, a readily available and insensitive reagent.

In addition, ATP cleavage by high-valent metal ions such as Zr(IV) which display the highest phosphoesterase activities in DNA cleavage should be explored. Screening ATPase activity of Zr(IV) complexes with various polycarboxylate, polyammonium and polyhydroxo ligands should be performed using high-throughput techniques.

3. Catalytic transesterification of phosphate esters by a dicopper(II) macrocyclic complex

3.1. Ligand synthesis (L)

The synthesis of dinucleating octaaza macrocycle **L** from a hexaazamacrocyclic precursor[36] was performed according to the procedure described by S. Warzeska[37]. **L** is obtained by N-alkylation with 2,6-pyridinedimethyl ditosylate (2 equiv.) in acetonitrile in the presence of Na_2CO_3 in up to 49% yield (Scheme 3.1). In the NMR spectra of L in $CDCl_3$, very broad signals are observed beside the expected signals of **L**. These signals have been attributed to H_2O incorporation by **L** and dynamic behaviour of inclusion complex, but the presence of "organic" impurities could previously not be ruled out. To address this problem, a sample of **L** was analyzed by HPLC. HPLC-MS analysis of the product indicates formation of only negligible amounts (<5%) of "oligomeric" byproducts (Scheme 3.1(such) which could not be removed by crystallization or column chromatography. The peak at m/z = 1161 is attributed to traces of a covalent "dimer" formed by reaction of two molecules of the hexaazamacrocycle with four molecules of the ditosylate.

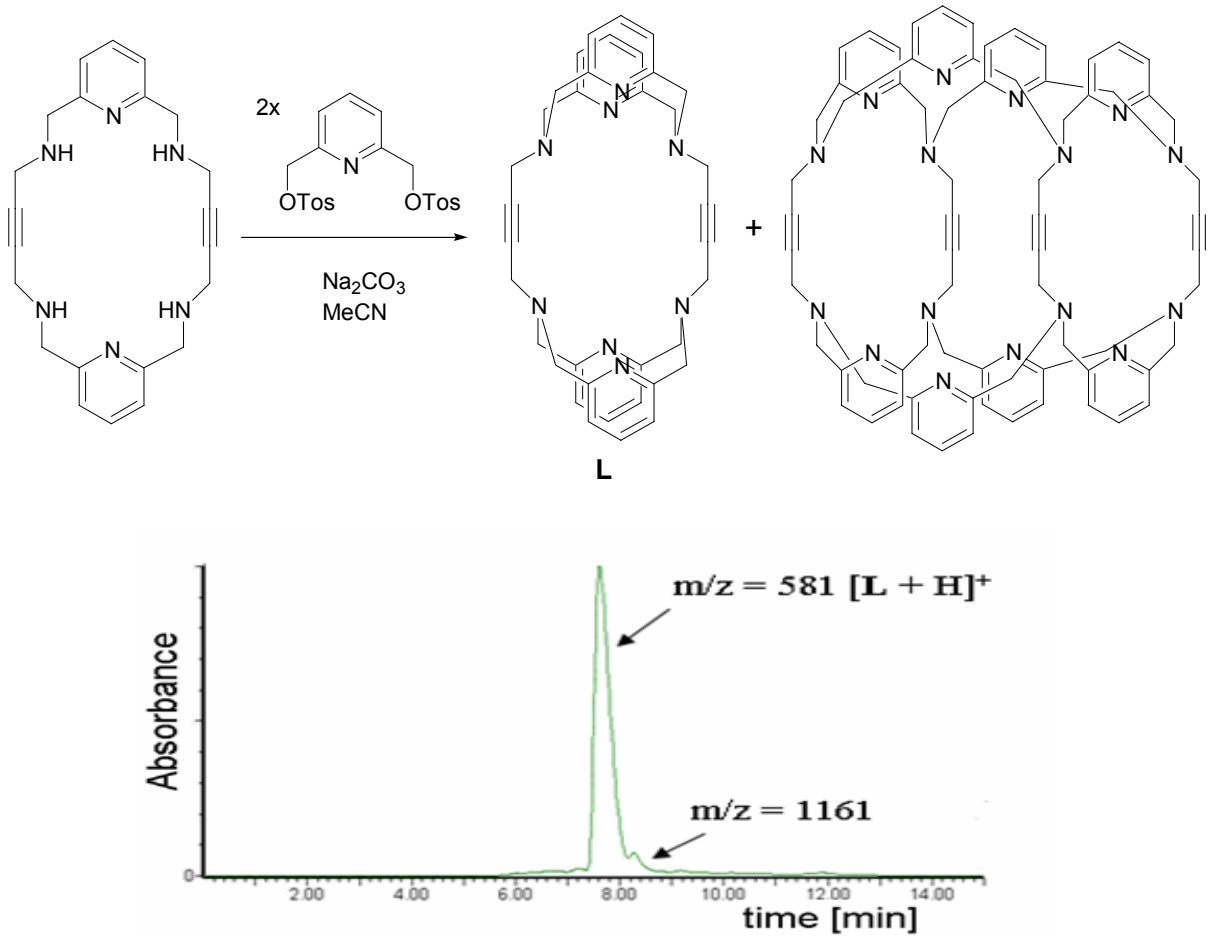

Scheme 3.1. Synthesis of **L** and HPLC-MS analysis of reaction products.

3.2. Synthesis and structure of 1

The dinuclear Cu(II) complex $[(\mathbf{L})Cu_2(NO_3)_2](NO_3)_2 \cdot 2\ CH_3OH$ **(1)** was obtained by reaction of **L** with 2 equiv. $Cu(NO_3)_2$ trihydrate in methanol as described[38]. This complex which is used as a phosphoryltransfer catalyst could be isolated in pure, crystalline form (Figure 3.1) but only in low yield. This is attributed to a suprising kinetic stability of the Cu(II) complexes of **L**. Instead of smooth formation of the thermodynamically most stable product, a mixture of species is obtained, possibly involving mononuclear, trinuclear and hydroxo- complexes. ESI spectra of a methanolic solution containing **L** and 2 equiv. $Cu(NO_3)_2$ display signals of $[(\mathbf{L})Cu]^{2+}$, $[(\mathbf{L})Cu(OH^-)(H_2O)]^+$ and $[(\mathbf{L})Cu_2(NO_3^-)_2(OH^-)]^+$. The

yield of **1** could not be improved by variation of reaction conditions (e.g. synthesis at prolonged reaction time at 50°C.

To illustrate the ability of weakly basic oxoanions to form a 1,1-μ– oxygen bridge between the Cu ions of **LCu$_2$**, the structure of **1** (previously determined by S. Warzeska) is given in figure 3.1.

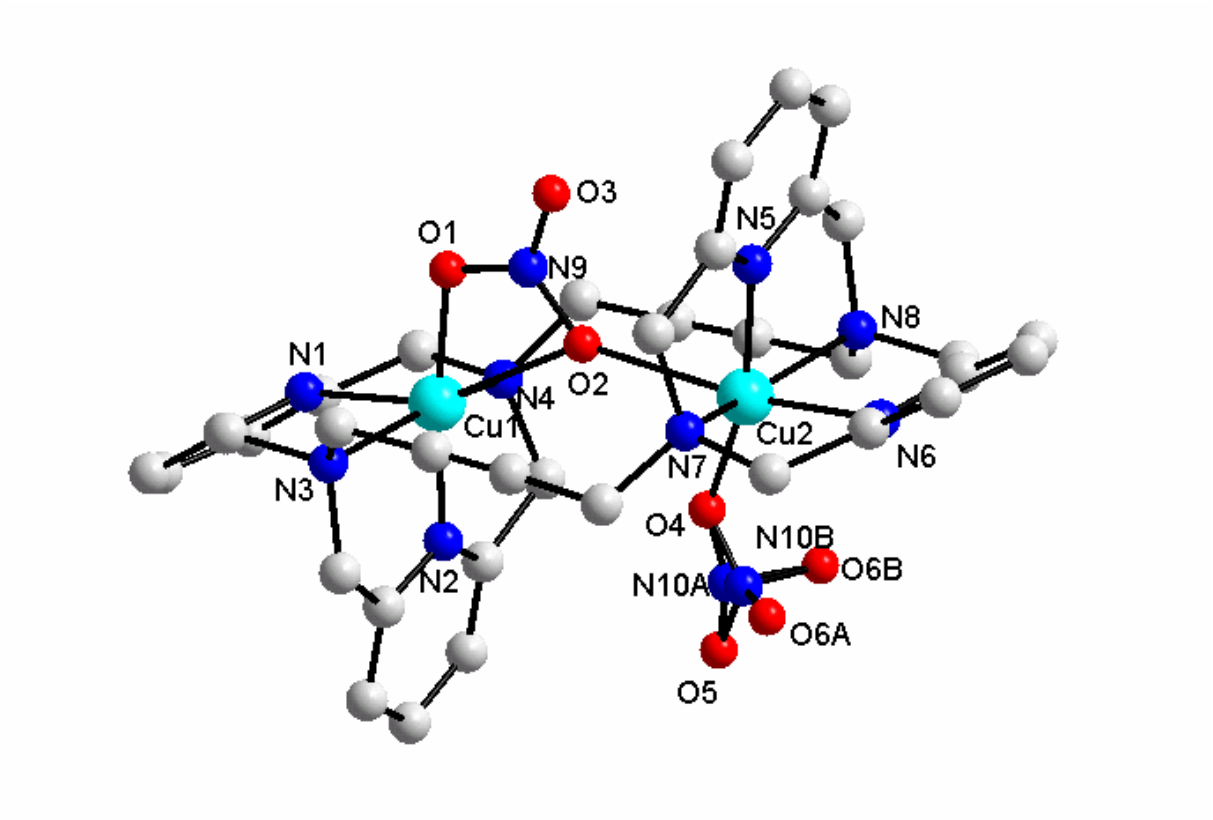

Figure 3.1. Crystal structure of [(**L**)Cu$_2$(NO$_3$)$_2$]$^{2+}$ complex cation of **1**.[38] Hydrogen atoms are omitted for clarity.

3.3. Solution chemistry of Cu(II) complex of L

3.3.1. UV-Vis titration of L with $Cu(NO_3)_2$

Complex formation in methanol/chloroform (the latter was added to improve solubility of **L**) was followed by spectrophotometric titration of **L** with a solution of copper(II) nitrate. A 1:1 L-Cu(II) complex is formed smoothly and rapidly (Fig. 3.2).

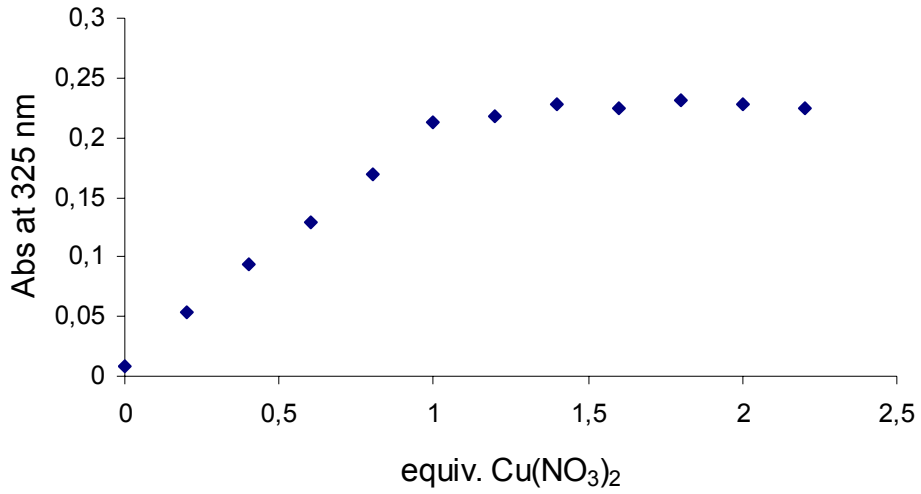

Figure 3.2. Absorbance diagram at 325 nm for addition of 0-2.2 equiv. $Cu(NO_3)_2$ to **L** (0.1 mM) in methanol / chloroform (9:1).

Incorporation of a second Cu(II) ion appears to be more difficult to achieve and facilitated by prolonged heating to 50°C. Distinct spectral changes are observed but no longer indicative of a smooth conversion.

3.3.2. EPR Spectra

EPR spectra of frozen solution of in situ prepared [**L**Cu]$(NO_3)_2$ are well resolved and indicate formation of a single species with g = 2,29 and A = 154 G, typical for in plane N_2O_2-coordination of Cu(II)[39] (Figure 3.3). Therefore, an elongated octahedral coordination by one diazapyridinophane subunit and two solvent (or nitrate) coligands is assumed, with in-plane coordination by the latter O-donors and two pyridine N atoms. Frozen methanolic solutions containing **L** and 2 equiv. Cu(II) show poorly resolved, complicated EPR spectra.

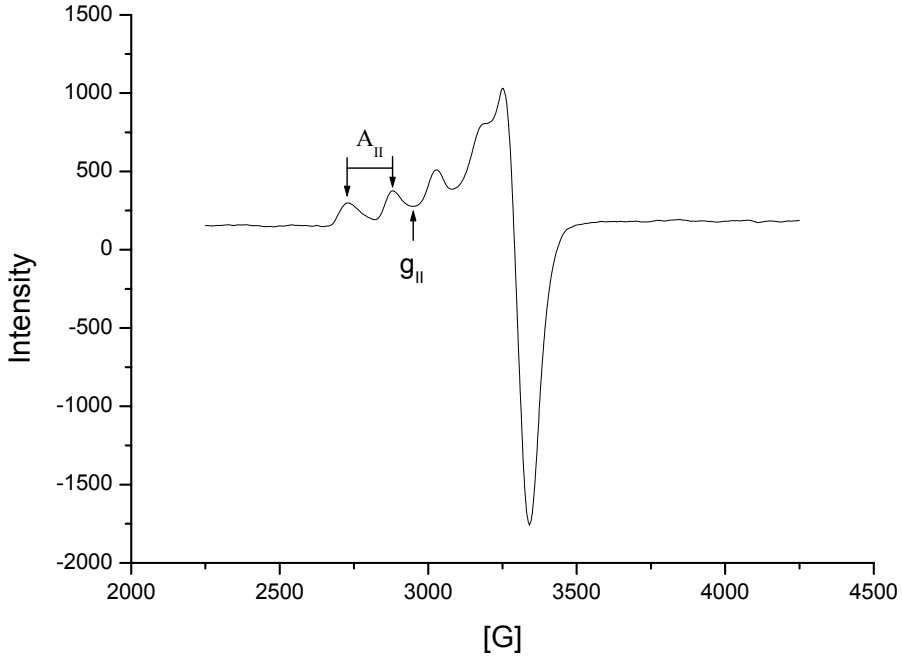

Figure 3.3. EPR spectrum of glassy methanol solution (T = 77 K) containing **L** / $Cu(NO_3)_2$ (2mM each).

3.3.3. UV-titration of 1 with $NaOCH_3$

A titration of **1** with $NaOCH_3$ was performed in methanol. Addition of up to 1 equiv. $NaOCH_3$ to **1** reveals only minor spectral changes, with absorbance decreasing continuously

(Figure 3.4, right), suggesting the formation of a 1:1 (**L**)$Cu_2(OCH_3)$ complex. (**L**)$Cu_2(OCH_3)$ converts smoothly to (**L**)$Cu_2(OCH_3)_2$ at 1-2 equiv. $NaOCH_3$ (Figure 3.4, left), with a characteristic maximum of the bis(methanolate)complex at 335 nm (ε_{335} = 4200 cm^{-1}). No significant spectral changes are observed on addition of > 2 equiv. $NaOCH_3$. The spectrum at 2.2 equiv. $NaOCH_3$ does not change significantly on addition of 25 equiv. NaDMP, indicating that DMP does not strongly compete with the second OCH_3^- for **LCu_2** binding.

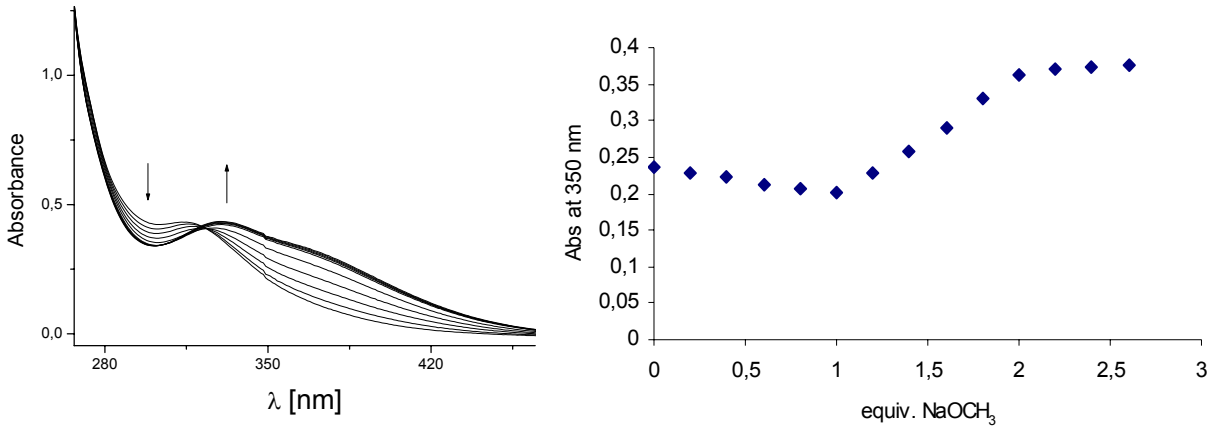

Figure 3.4. Left: spectrophotometric titration of **1** (0.1mM) in methanol with $NaOCH_3$ (in 0.2 equiv. steps; only the curves for 1-2.5 equiv. $NaOCH_3$ are shown). Right: absorbance diagram at 350 nm for addition of 0-2.5 equiv. $NaOCH_3$ to **1** (0.1 mM).

3.3.4. pH titration of 1 with $NaOCH_3$

In addition to the spectrophotometric studies, pH measurements in the methanolic solutions were performed, following a more recently recommended method[40b] using a standard glass electrode calibrated with aqueous buffers and a correction value of +2.24 added to the pH meter reading. Approximate pK_a values of the solution species were determined by measuring their half neutralization.

pH measurements involving metal complexes have been applied to 1 mM solutions of **1**. From the pH titration of **1** with $NaOCH_3$, pK_a values 6.0 (± 0.3) and ≈ 12 (corresponding to the pH values on addition of 0.5 and 1.5 equiv., Figure 3.5) were derived for the equilibria $LCu_2(CH_3OH)$ / $LCu_2(OCH_3)$ + H^+ and $LCu_2(OCH_3)$ / $LCu_2(OCH_3)_2$ + H^+.

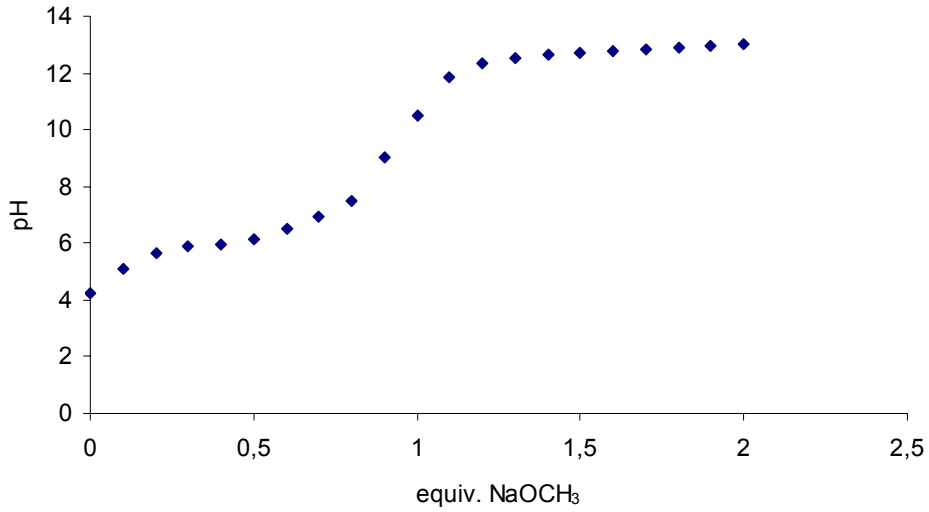

Figure 3.5. pH titration in methanol of **1** (1 mM) with $NaOCH_3$. T = 25°C

3.4. Synthesis and structure of a dimethyl phosphate (DMP) complex of 1

3.4.1. Synthesis of DMP complex of 1.

Many attempts to isolate phosphate ester complexes of **LCu_2** were unsuccessful, except in case of the dimethyl phosphate complex **2**. The dimethyl phosphate complex was crystallized from a methanolic 1:1 mixture of **1** and NaDMP. Whithin 3 days blue-green crystals of $[(\mathbf{L})Cu_2(1,3\text{-}\mu\text{-DMP})(NO_3)](NO_3)_2$ **2** were obtained, which could however not be fully characterized because they were obtained in very low yield and its crystallization was not reproducible.

3.4.2. Crystal structure of $[(L)Cu_2(1,3\text{-}\mu\text{-}DMP)(NO_3)](NO_3)_2 \cdot CH_3OH \cdot H_2O$ (2).

The structure of **2** was solved by direct method and refined by full matrix least-squares based on F^2 with all measured reflections. Crystal data and structure refinement for **2** are given in Table 3.1.

Table 3.1. Crystal data and structure refinement for **2**.

Empirical formula	$C_{39}\ H_{48}\ Cu_2\ N_{11}\ O_{15}\ P$	
Formula weight	1068.93 g/mol	
Temperature	100(2) K	
Wavelength	0.71073 Mo Kα (Å)	
Crystal system	Orthorhombic	
Space group	P b c a	
Unit cell dimensions	a = 14.5986(16)Å	α= 90°.
	b = 20.862(2) Å	β= 90°.
	c = 28.726(3) Å	γ = 90°.
Volume	8748.7(16) $Å^3$	
Z	8	
Density (calculated)	1.623 g/m^3	
Absorption coefficient	1.093 mm^{-1}	
F(000)	4416	
Crystal size	0.22 x 0.08 x 0.03 mm^3	
Theta range for data collection	1.84 to 25.03°.	
Index ranges	0<=h<=17, 0<=k<=24, 0<=l<=34	
Reflections collected	7742	
Independent reflections	7742 [R(int) = 0.0000]	
Completeness to theta = 25.03°	100.0 %	
Max. and min. transmission	0.9732 and 0.7911	
Refinement method	Full-matrix least-squares on F^2	
Data / restraints / parameters	7742 / 0 / 617	
Goodness-of-fit on F^2	0.821	
Final R indices [I>2sigma(I)]	R1 = 0.0568, wR2 = 0.1047	
R indices (all data)	R1 = 0.1485, wR2 = 0.1239	
Largest diff. peak and hole	0.709 and -0.753 e.$Ĺ^{-3}$	

The complex $[(L)Cu_2(1,3\text{-}\mu\text{-}DMP)(NO_3)](NO_3)_2 \cdot CH_3OH \cdot H_2O$ crystallizes in an orthorhombic system. The cell unit contains eight molecules of **2**. Crystal structure of the $[(\mathbf{L})Cu_2(1,3\text{-}\mu\text{-}DMP)(NO_3)]^{2+}$ complex cation of (**2**) is shown in figure 3.6. Selected bond lenghts and angles are given in table 3.2.

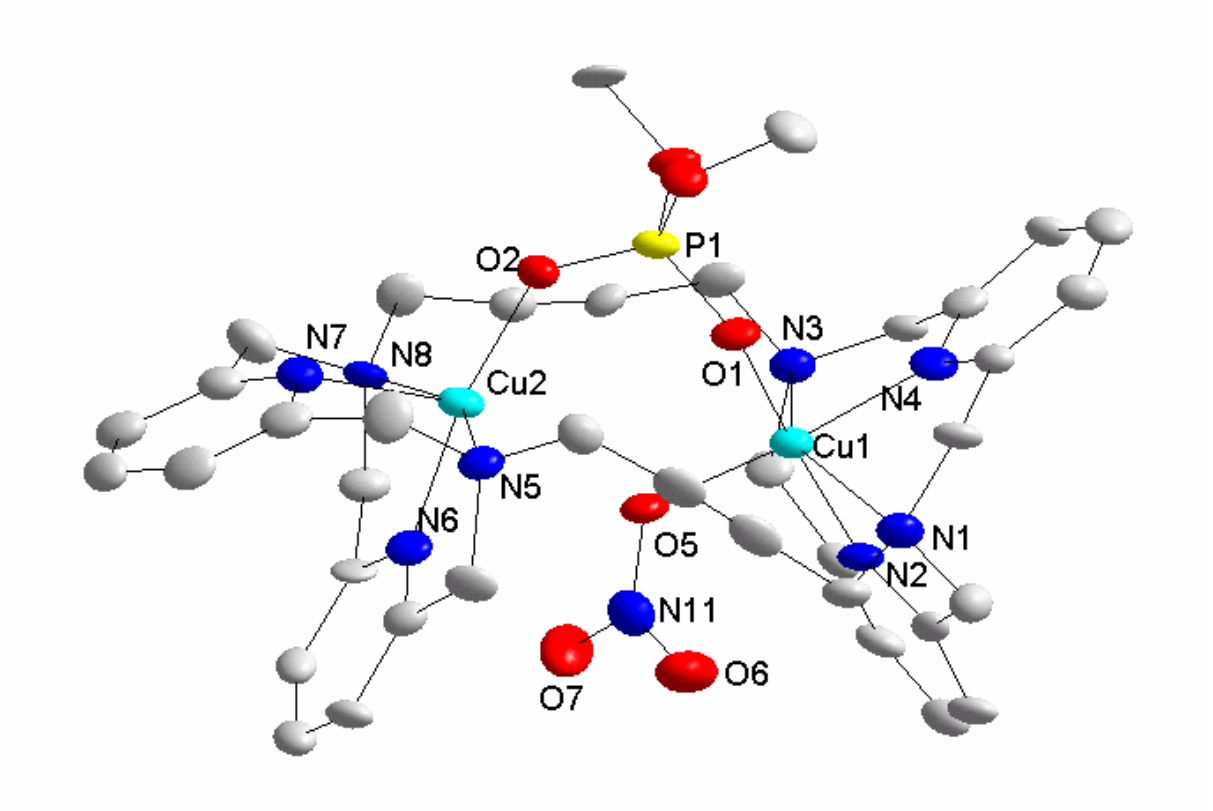

Figure 3.6. Crystal structure of the $[(\mathbf{L})Cu_2(1,3\text{-}\mu\text{-}DMP)(NO_3)]^{2+}$ complex cation of (**2**) Hydrogen atoms are omitted for clarity.

Table 3.2. Selected bond lenghts and angles for **1**.

Selected bond lengths Å	
Cu(1)-O(1) 1.922(4)	Cu(2)-O(2) 1.883(4)
Cu(1)-N(2) 1.978(5)	Cu(2)-N(6) 1.924(5)
Cu(1)-O(5) 1.996(4)	Cu(2)-N(7) 2.169(5)
Cu(1)-N(4) 2.008(5)	Cu(2)-N(5) 2.218(5)
Cu(1)-N(1) 2.352(5)	Cu(2)-N(8) 2.227(5)
Cu(1)-N(3) 2.435(5)	
Selected angles (°)	
O(1)-Cu(1)-N(2) 174.5(2)	N(1)-Cu(1)-N(3) 143.75(18)
O(1)-Cu(1)-O(5) 90.31(17)	O(2)-Cu(2)-N(6) 168.86(19)
N(2)-Cu(1)-O(5) 93.40(19)	O(2)-Cu(2)-N(7) 107.17(18)
O(1)-Cu(1)-N(4) 89.47(19)	N(6)-Cu(2)-N(7) 83.8(2)
N(2)-Cu(1)-N(4) 87.4(2)	N(5)-Cu(2)-N(8) 153.07(19)
O(5)-Cu(1)-N(4) 171.9(2)	

Dimethyl phosphate coordinates by O(1) and O(2) in a 1,3-bridging fashion, with distances Cu(1)-O(1) 1.922(4) Å and Cu(2)-O(2) 1.883(4) Å .The nitrate ligand forms only one short Cu(1)-O(5) bond (1.996(4) Å), the distance of O(5) to Cu(2) is 3.007Å and thus nonbonding. This results in a mixed coordination of the Cu ions. The coordination of Cu(1) ion is elongated octahedral with four short in-plane bonds and two elongated apical bonds to the sp^3 nitrogens of the tetradentate diazapyridinophane-type subunit. Such a coordination is comparable to that reported for mononuclear Cu(II) complexes of 2,11-diaza[3.3](2,6)pyridinophanes[41]. The five coordinated Cu(2) ion adopts distorted square pyramidal structure. The coordination sphere of two Cu ions is shown in figure 3.7.

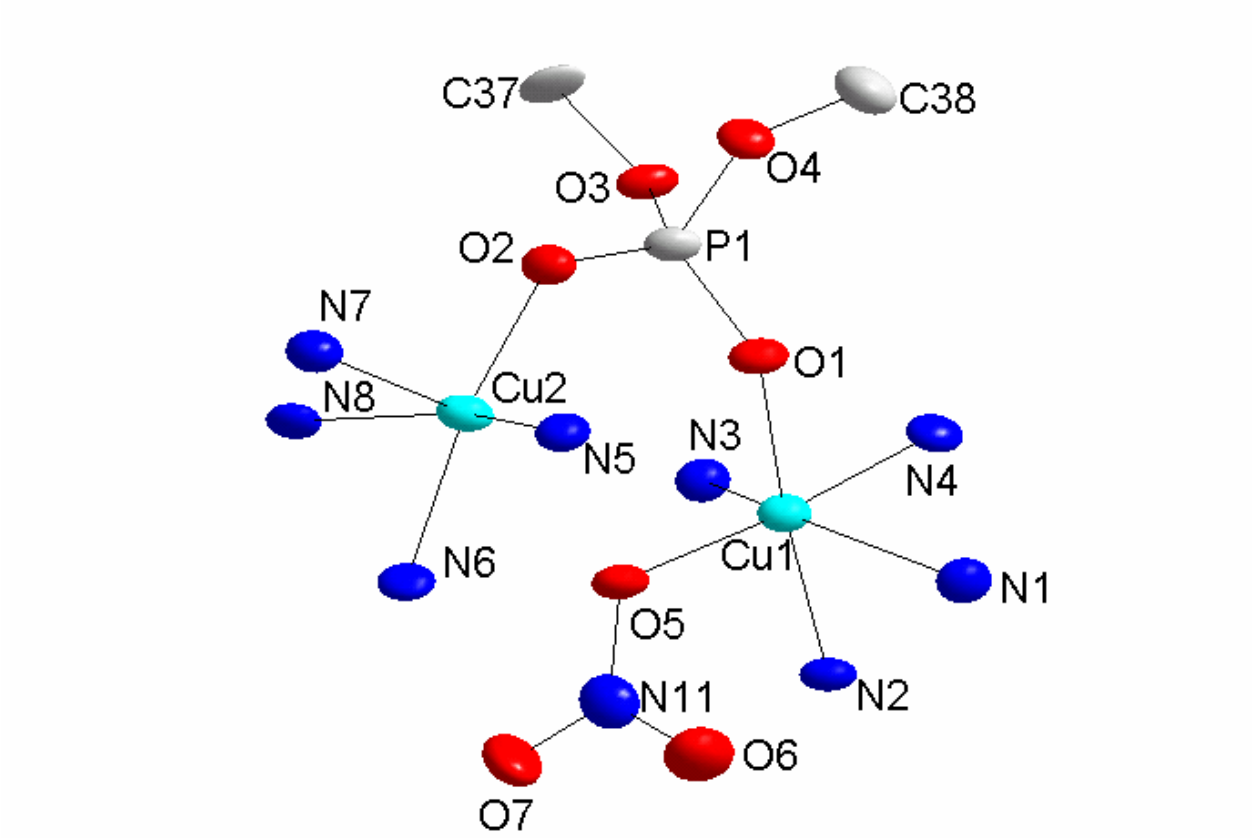

Figure 3.7. Coordination sphere of Cu ions in **2**.

3.5. Solution chemistry of DMP complex of 1

3.5.1. Spectroscopic titration of 1 with DMP

To investigate the interaction of **1** with dimethylphosphate in solution, a UV-Vis titration of the complex with NaDMP in methanol was performed. Interaction of $\mathbf{LCu_2}$ with oxoanions is generally followed on the basis of a broad absorbance in the range 300-350 nm (ε in the order of 4000 M^{-1} cm^{-1}) which is interpreted as an oxygen-to-copper(II) charge transfer band. In case of **1**, the band is very broad and appears as a shoulder centered at about 325 nm. On addition of up to ~1 equiv. DMP to **1**, the shoulder decreases continuously (Figure 3.8),

suggesting the formation of a 1:1 LCu_2-DMP complex. Addition of more DMP smoothly generates a new species with an absorbance maximum at 310 nm (ε_{310} = 4200 M^{-1} cm^{-1}). Complete conversion (i.e. no further increase of 310 nm absorbance) requires large excess of DMP.

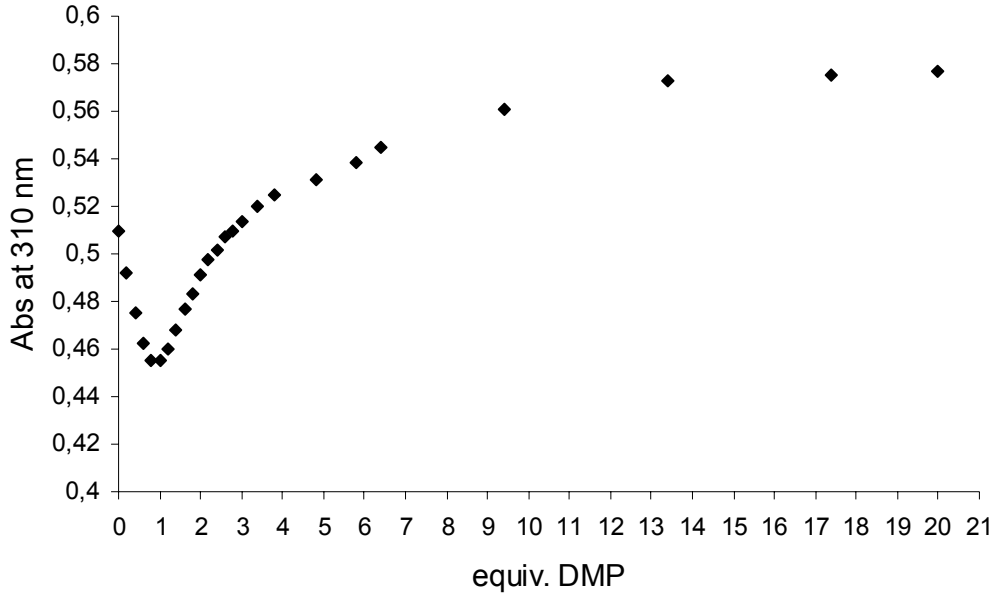

Figure 3.8. Absorbance diagram at 310 nm of a methanolic solution of **1** (0.1mM) on addition of 0-20 equiv.DMP (in 0.2 equiv.steps).

The same changes of absorbance with isosbestic points are observed, when the 1:1 **LCu_2**-DMP solution is titrated with 0-1 equiv. $NaOCH_3$ (Figure 3.9). Therefore, it can be concluded that a methanolate complex $[(\mathbf{L})Cu_2(DMP)(OCH_3)]^{2+}$ is formed in both cases, either by addition of one equiv. OCH_3^- or a large excess of DMP which is a weak base and deprotonates a Cu-coordinated MeOH solvent molecule. In figure 3.9, spectra are selected which correspond to the addition of 0 to ~ 0.6 equivalents $NaOCH_3$ to the **1** / DMP 1:1 mixture. Titration curves obtained on subsequent $NaOCH_3$ addition no longer pass the isosbestic points and absorbance no longer increases linearly, possibly due to competing

formation of a bis-methanolate complex. Frozen methanolic solutions containing **1** and excess NaDMP show poorly resolved, complicated EPR spectra.

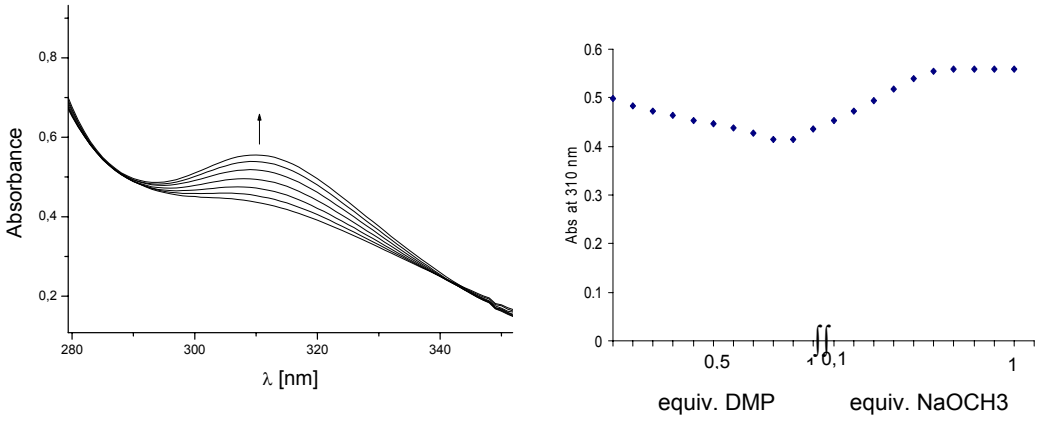

Figure 3.9. Left: spectrophotometric titration of a methanol solution of **1**/DMP (0.1 mM each) with $NaOCH_3$ (0-0.6 equiv.) in 0.1 equiv. steps. Right: absorbance diagram at 310 nm of a methanolic solution of **1** (0.1mM) on addition of 0-1 equiv. DMP, and on subsequent addition of 0-1 equiv. $NaOCH_3$ (in 0.1 equiv. steps).

3.5.2. pH titration of DMP complex of 1

pH measurements were performed in the methanolic solutions, following a more recently recommended method[40b] using a standard glass electrode calibrated with aqueous buffers and a correction value of +2.24 added to the pH meter reading.

There were some problems with the reproducibility of these measurements but data quality was sufficient for the determination of approximate pK_a values for some of the solution species involved by measuring their half neutralisation. A pK_a = 4.9 (± 0.2) of HDMP at 1 mM concentration in methanol (no salts added) was determined by titration of NaDMP with

the strong acid *p*-toluene sulfonic acid. As expected this value is somewhat higher than the one reported (3.95) for phosphoric acid diphenyl ester[40a].

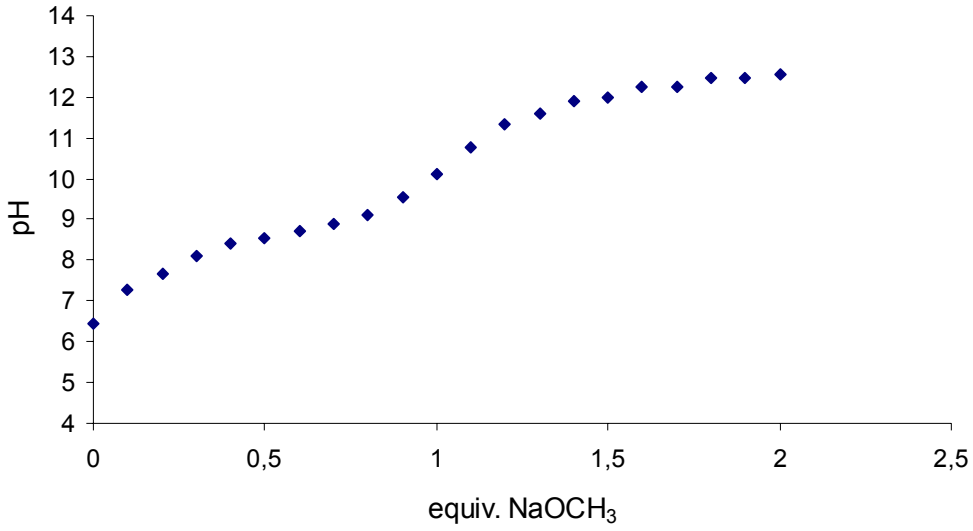

Figure 3.10. pH titration in methanol of 1 mM **1**/NaDMP (1:1) with $NaOCH_3$. T = 25°C

From the pH titration of LCu_2DMP (1mM), formed in situ from **1** and NaDMP, with $NaOCH_3$ (Figure 3.10), pK_a values 8.5 (± 0.3) and ≈ 12 (corresponding to the pH on addition of 0.5 and 1.5 equiv. $NaOCH_3$) were derived for the equlibria $LCu_2(DMP)$ / $LCu_2(DMP)(OCH_3) + H^+$ and $LCu_2(DMP)(OCH_3)$ / $LCu_2(OCH_3)_2 + H^+$.

Conversion of $LCu_2(OCH_3)$ or $LCu_2(DMP)(OCH_3)$ to $LCu_2(OCH_3)_2$ requires strongly basic conditions and the pK_a value could not be determined accurately. A summary of the suggested acid-base equilibria in the presence of DMP is given in scheme 3.2.

$$LCu_2(DMP) \rightleftharpoons LCu_2(DMP)(OCH_3) + H^+ \qquad pK_a = 8.5$$

$$LCu_2(DMP)(OCH_3) \rightleftharpoons LCu_2(OCH_3)_2 + H^+ + DMP \qquad pK_a \approx 12$$

Scheme 3.2. Suggested protonation equilibria of **LCu_2** in methanolic solution in the presence of DMP

A calculated pH dependent distribution of the three complex species of scheme 4 supports a smooth conversion of $LCu_2(DMP)$ into $LCu_2(DMP)(OCH_3)$ on half neutralization to pH 8.5, while formation of $LCu_2(OCH_3)_2$ becomes significant at pH > 11 (Figure 3.11).

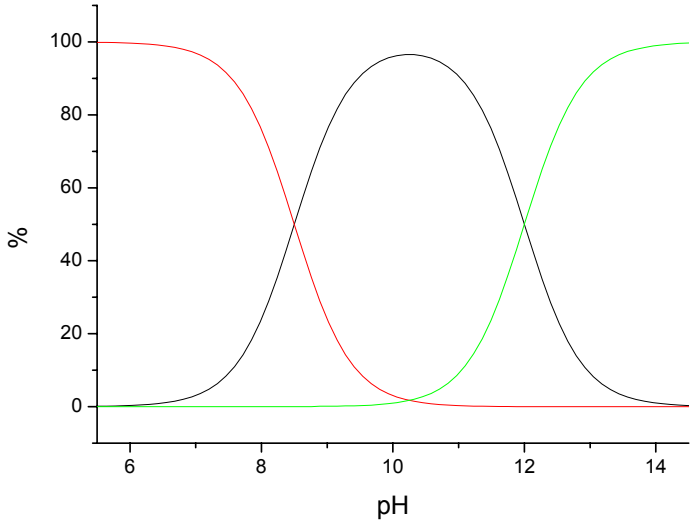

Figure 3.11. pH dependent species distribution: — $LCu_2(DMP)$, — $LCu_2(DMP)(OCH_3)$, — $LCu_2(OCH_3)_2$ (calculated using pKa values 8.5 and 12, see scheme 3.2).

3.6. Catalytic transesterification of dimethyl phosphate in CD_3OD

The activity of **LCu_2** for the transesterification of the dimethyl phosphate (DMP) was followed by ^1H NMR spectroscopy in d_4-methanol. Reaction solutions typically contained 2 mM **1** and 50 mM sodium dimethyl phosphate. Significant broadening of the $(CH_3O)_2PO_2^-$ doublet (coupling with ^{31}P nucleus) is attributed to coordination to paramagnetic Cu(II), with rapid exchange of the phosphodiester ligand on the NMR time scale. Even at -50°C it was not possible to distinguish coordinated and excess "free" phosphate by NMR spectroscopy. It was previously shown[38] that **LCu_2** in aqueous solution readily incorporates hydroxide even at rather low pH values < 2. (**L**)Cu_2(OH) does not form a DMP complex in water and is consequently not a hydrolysis catalyst, which contrasts to the behavior of (**L**)$Cu_2(OCH_3)$ in methanol.

Transesterification of DMP is followed by release of CH_3OD (Figure 3.12) as previously described by U. Kühn[44]. Identity and ratio relative to DMP of reaction products $(CH_3O)(CD_3O)PO_2^-$ and $(CD_3O)_2PO_2^-$, which differ only in their isotope composition, is confirmed by mass spectrometry (ESI-MS). These observations support a nucleophilic substitution mechanism at phosphorus with a CH_3O^- leaving group and CD_3O^- as incoming nucleophile. Experimental observations rule out an alternative pathway with nucleophilic attack of CD_3O^- at a carbon atom of DMP which would produce the monoester $(CH_3O)PO_3^{2-}$ (not observed by mass spectrometry) and dimethylether-d_3 (expected at 3.2 ppm but not observed in ^1H NMR if the reaction is performed in a sealed NMR tube). For reaction times <10 days at 25°C an approximately linear increase of methanol concentration (determined by integration of ^1H NMR signals) with time is observed, corresponding to 7 turnovers after 9 days without loss of catalyst activity. In view of the hydrolytic stability of DMP, **LCu_2** very

efficiently promotes the transesterification. The previously determined half-life of catalyst-bound DMP of about 100 minutes at 55 °C could be confirmed.

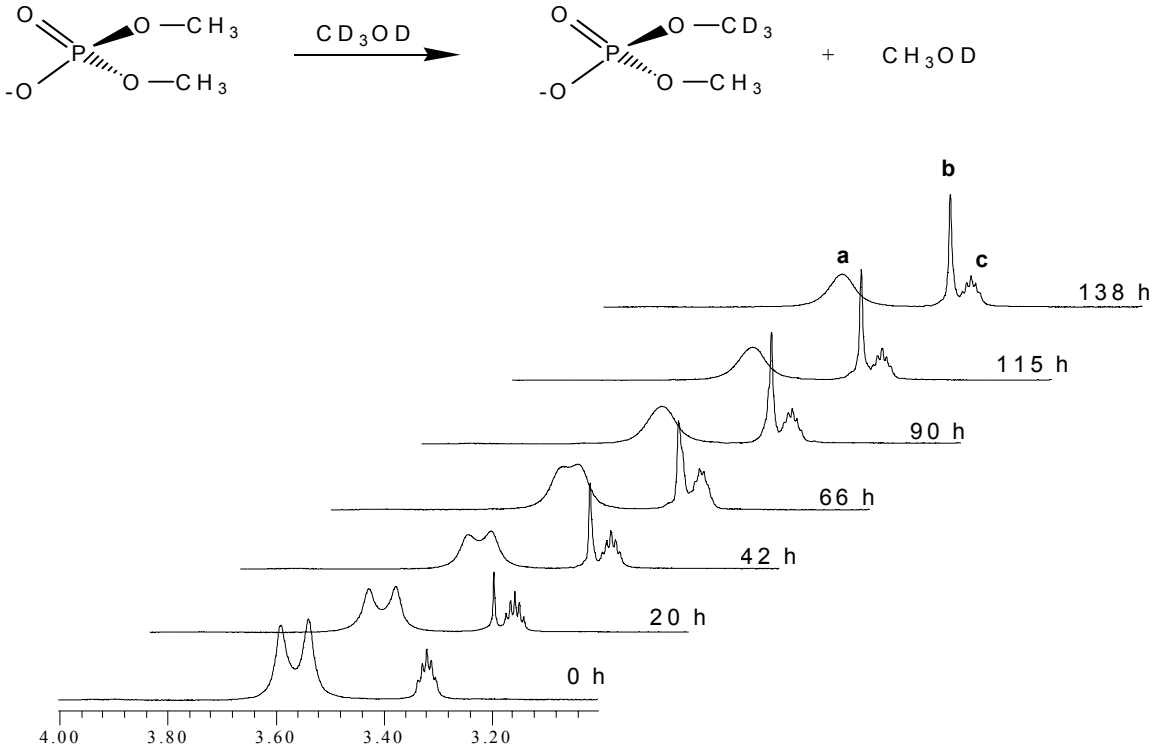

Figure 3.12. ^{1}H NMR spectra of reaction solutions containing 50 mM DMP and 2mM **1** in D_3COD at 25°C. a) broad signal of $(CH_3O)_2PO_2^-$ b) released CH_3OD at 3.39 ppm c) residual CD_2HOD pentet of deuterated solvent.

The extrapolated first-order rate constant for uncatalyzed P-O bond cleavage by hydroxide at pH 7 in water at 25°C is in the order of 10^{-18} s^{-1} [16a]. Data for methanolysis of DMP are not available but may lie in the same range since the second-order rate constant of diphenyl phosphate cleavage by CH_3O^- is very close to the value for the hydroxide reaction in water[40a]. In control experiments, copper(II) nitrate, free **L** and the in-situ prepared mononuclear complex (**L**)$Cu(NO_3)_2$ did not cleave DMP, and no trace of methanol was detectable after 4 weeks. Cleavage of simple dialkylphosphates by M^{2+} complexes has not been observed

before. Few examples for the hydrolysis of dimethyl phosphate by strongly Lewis-acidic tri- and tetravalent metal ions have been reported, in stoichiometric reactions and often at high temperature or low pH. Examples include Co(III) ($t_{1/2}$ (DMP) = 40 days, 60°C, pH 5.9)[25], Ce(IV) ($t_{1/2}$ (DMP) = 22 min, 60°C, pH 1.8)[26], Mo(IV) ($t_{1/2}$ (DMP) = 18 d, 70°C, pH 4.0)[27].

3.6.1. Dependence of initial rate of DMP cleavage on catalyst concentration.

The measurements of dependence of initial rate (dc/dt) of DMP cleavage were performed in d_4-methanol at 55°C. Concentration of DMP was kept constant (50 mM), while [**LCu$_2$**] was between 1-3 mM. The $^{s}_{s}$pD value of the CD_3OD solution at 25°C was 9.9 ± 0.2, adjusted by addition of *p*-toluonesulfonic acid to the solution at 1 and 1.5 mM **1.** To the pH meter reading of the CD_3OD solution correction value 2.24 was added.

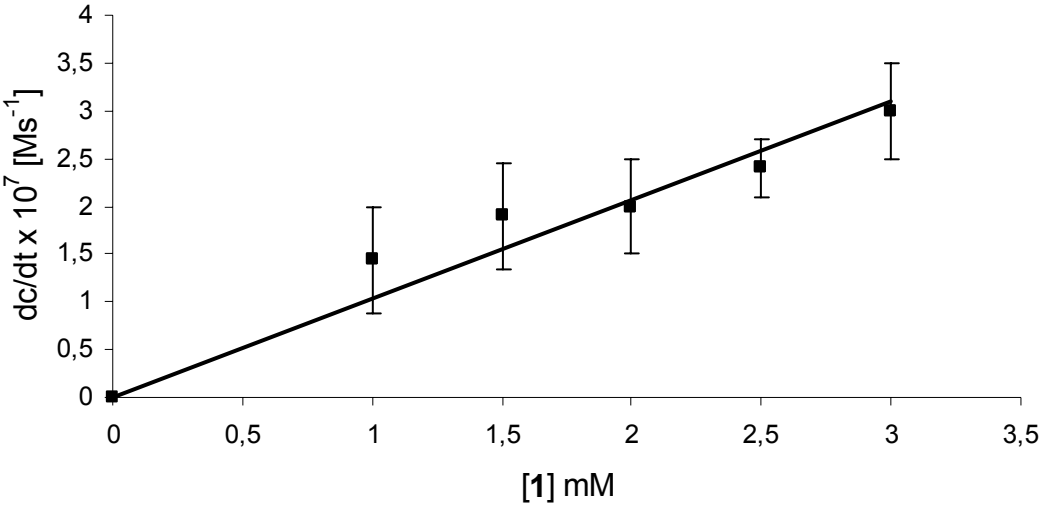

Figure 3.13. Dependence of initial rate (dc/dt) at 55 °C of DMP (50 mM) cleavage in CD_3OD on concentration of **1**, $^{s}_{s}$pD = 9.9 ± 0.2.

The reaction of DMP cleavage is a first-order since the cleavage rate increases linearly with concentration of catalyst **1** (1 to 3 mM) at a constant DMP concentration (Figure 3.13).

3.6.2. Saturation kinetics for the hydrolysis of DMP by 1

In a typical kinetic assay, appropriate amount of sodium dimethyl phosphate was added to 2mM stock solution of **1** in CD_3OD and the solution was kept at 55°C. The $^{s}_{s}$pD of the solution was 9.9 ± 0.3 at 25°C. The pD of the solution dropped to < 9.5 when [DMP]<10 mM, therefore data at <10mM DMP are not included.

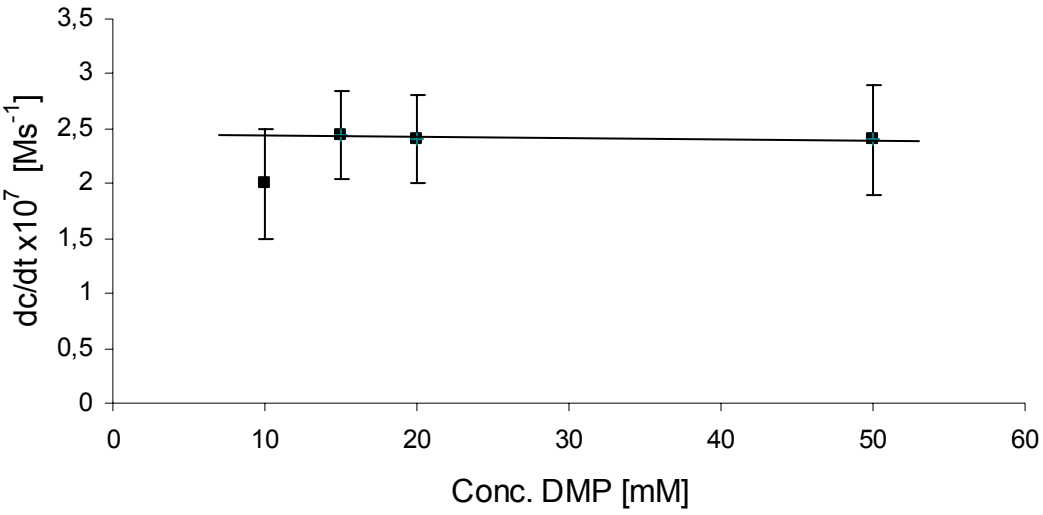

Figure 3.14. Saturation kinetics for the hydrolysis of DMP by **1** (2 mM) in CD3OD at 55 °C.

Since cleavage rate is nearly the same for 10, 25 and 50 mM DMP, the **LCu_2** catalyst (2 mM) is saturated with substrate and k_{cat} = 1.2 (±0.5) · 10^{-4} s^{-1} at 55°C is readily derived, which is the cleavage rate constant of DMP substrate bound to **LCu_2** (Figure 3.14).

3.6.3. Depedence of DMP transesterification rate on pH

Exploring the dependence of the DMP transesterification rate on pH was complicated by the use of deuterated methanol and elevated temperature (55°C) to avoid very long reaction times in the kinetic assays. While the published method for pH determination using a glass electrode applies to CH_3OH and 25°C, there is a lack of recommendations for CD_3OD and for temperature changes in this context. Therefore, solutions of **1** (2 mM) and NaDMP (50 mM) in CH_3OH and CD_3OD, respectively were compared. The $^{s}_{s}$pH in the CH_3OH medium was adjusted by addition $NaOCH_3$ or *p*-toluenesulfonic acid stock solutions. Then the same amount of $NaOCD_3$ and *p*-toluenesulfonic acid to the reaction solution in CD_3OD was added, and the rate of DMP cleavage in these solutions was measured.

Rates in CD_3OD are related to the $^{s}_{s}$pH valus of corresponding CH_3OH solution in figure 3.15. Included in this diagram is a pH-dependent speciation curve for (**L**)Cu_2(DMP)(OCH_3), calculated using pK_1 = 8.5 and pK_2 = 12 for the acid / base equilibria in scheme 3.2. It is difficult to predict how the deuterated solvent, the elevated temperature and the higher ionic strength affect the pK values and pH measurement. Note, however, that the shape of this speciation curve is similar to that of the pH-rate dependence in figure 3.15. Therefore, we consider (**L**)Cu_2(DMP)(OCH_3) as the active species. The pH rate profile in figure 3.15 is not consistent with either a free CD_3OD or a free CD_3O^- nucleophile. In the latter case, the rate should increase 10-fold when pH increases by one unit; even if this effect is partially compensated by a decrease in concentration of the active complex species, it cannot be fitted to the profile.

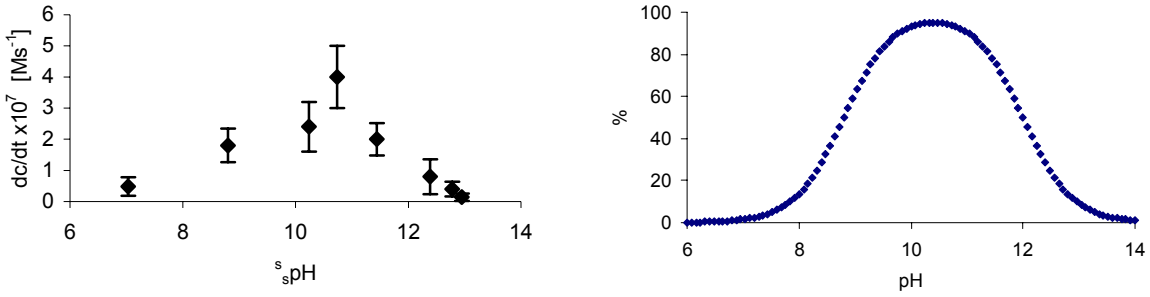

Figure 3.15. Left: $^{s}_{s}$pH values given in this figure were adjusted by adding methanolic stock solutions of $NaOCH_3$ or *p*-toluenesulfonic acid to **1** / NaDMP (2 / 50 mM) in methanol. Reactions solutions were prepared by adding the same amount of $NaOCD_3$ or *p*-toluenesulfonic acid (stock solutions in CD_3OD) to **1** / NaDMP (2 / 50 mM) in CD_3OD. Initial rate (dc/dt) at 55°C of DMP cleavage in the CD_3OD reaction solution is related to the $^{s}_{s}$pH values of the corresponding CH_3OH solutions. Right: calculated pH dependent speciation of (**L**)Cu_2(DMP)(OCH_3), % of total **LCu$_2$**., based on the first and second pKa values 8.5 and 12 of (**L**)Cu_2(DMP).

3.7. Catalytic methanolysis of other phosphodiesters

3.7.1. Catalytic transesterification of dibenzyl phosphate (BDP) in CD_3OD

The activity of **LCu$_2$** for the transesterification of the dibenzyl phosphate (DBP) was tested in d_4-methanol. Reaction solutions typically contained 2 mM **1** and 50 mM sodium dibenzyl phosphate. Transesterification was followed by ^{1}H-NMR spectroscopy (Figure 3.16) and formation of mono-transesterified products in the initial stage of the reaction confirmed by electrospray mass spectrometry. $k_{cat} = 2 \cdot 10^{-5}$ s^{-1} was calculated by integration of ^{1}H-NMR signal of released HO-C$\underline{H_2}$-ph at 4.6 ppm.

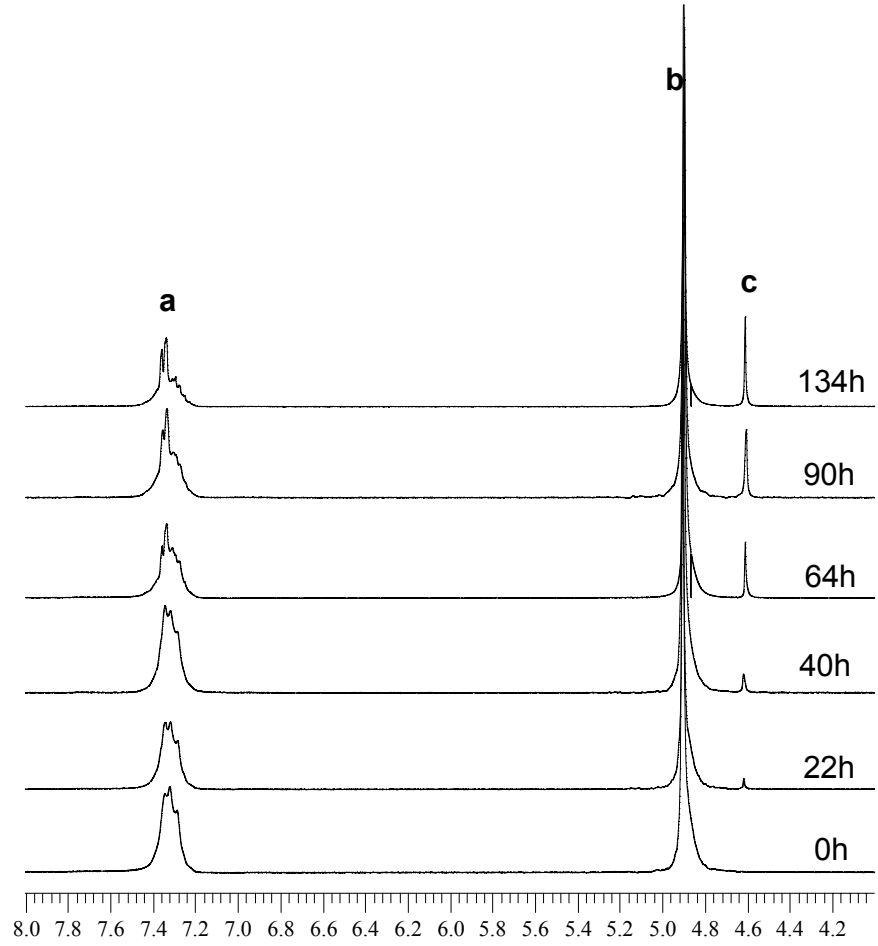

Figure 3.16. ^{1}H-NMR spectra of reaction solutions containing 50 mM DBP and 2mM **1** in D_3COD at 55°C. a) broad signal of aryl-H b) overlapping signals of residual H_2O and of DBP methylene groups c) relesead HO-C$\underline{H_2}$-Ph at 4.6 ppm.

3.7.2. Catalytic transesterification of bis(p-nitrophenyl)phosphate (BNPP) in CD_3OD

Transesterification of bis(p-nitrophenyl)phosphate (BNPP) is followed by release of HO-*p*-$C_6H_4NO_2$ by ^{1}H-NMR spectroscopy (Figure 3.17). Formation of the mono-transesterified product in the initial stage of the reaction was followed by the integration of NMR signals and confirmed by electrospray mass spectrometry. Reaction solutions typically contained 2 mM **1** and 50 mM sodium bis(p-nitrophenyl)phosphate. Broadening of aryl-H signals in the ^{1}H NMR spectrum (8.20 and 7.40 ppm) indicates coordination of BNPP to $\mathbf{LCu_2}$. The cleavage

of BNPP was detectable after 52 hours at 55°C (signals of released nitrophenol at 8.16 and 6.85 ppm were observed). With this data, k_{cat} was calculated to be $3 \cdot 10^{-6}$ s^{-1}.

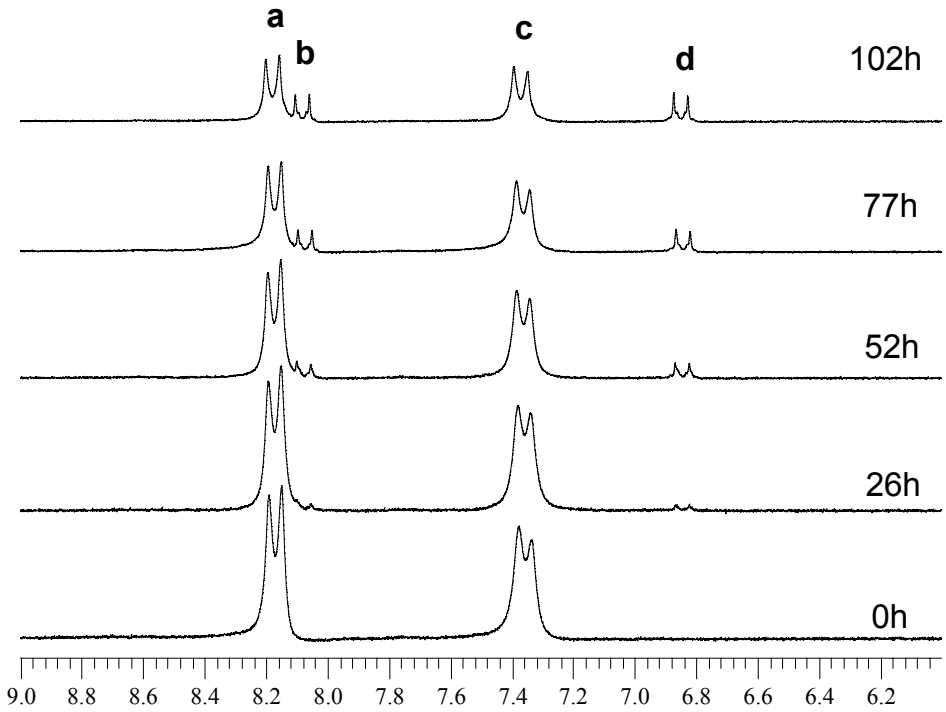

Figure 3.17. ^{1}H NMR spectra of reaction solutions containing 50 mM BNPP and 2mM **1** in D_3COD at 55°C. a,c) broad signal of aryl-H of BNPP b,d) released nitrophenol at 8.16 and 6.85 ppm.

3.8. Influence of the alcoholate (RO^-) leaving group on catalytic rate of phosphodiester transesterification

In phosphodiester cleavage there is usually a strong dependence of rate on the pK_a of the alcohol leaving group. A linear dependence of log k on pK_a is observed in hydroxide cleavage[16a], and the hydrolysis of dimethylphosphate (extrapolated data, pK_a methanol = 15.50) is 5-6 orders of magnitude slower than of bis(p-nitrophenyl)phosphate with pK_a (nitrophenol) = 7.16. A similar factor in rate has been reported for Co(III) promoted dimethyl

phosphate and bis(p-nitrophenyl)phosphate hydrolysis[16a], i.e. rate accelerations by the metal are comparable for substrates with good and poor leaving groups. This trend is qualitatively confirmed by the observation that metal ions or complexes that efficiently cleave phosphodiesters with good leaving groups usually do not cleave simple dialkyl phosphates, or that this reaction is too slow to be detected. Metal promoted methanolysis of phosphodiesters is less well explored but recent studies by Brown and coworkers[40a,42] indicate that e.g. lanthanide ions are efficient promoters of aryl phosphate methanolysis or cyclophosphate ring opening, while simple -O-alkyl substitutents are not released.

Table 3.3. Absolute and relative k_{cat} values for methanolysis of phosphodiesters $O_2P(OR)(OR')^-$ catalyzed by **1**, in dependence on leaving group –OR. CD_3OD, [**1**] = 2mM, $[O_2P(OR)_2^-]$ = 50 mM, T = 55°C.

-OR,-OR'	k_{cat} [s^{-1}]	Relative k_{cat}	References
$-OCH_3$	$1.2\cdot10^{-4}$	1	Ref. 44 and this work
$-OCH_2CH_3$	$1.2\cdot10^{-6}$	0,01	Ref. 44
-O-*p*-$C_6H_4NO_2$	$3\cdot10^{-6}$	0,025	this work
$-OCH_2C_6H_5$	$2\cdot10^{-5}$	0,17	this work
$-OCH_3$	$1.5\cdot10^{-5}$	0,13	Ref 44
-O*p*-$C_6H_4NO_2$	$2.2\cdot10^{-5}$	0,18	

In this context, the properties of transesterification catalyst **1** are rather unusual. Absolute and relative k_{cat} values including data of a previous investigation are listed in table 3.3. Dimethyl phosphate and dibenzyl phosphate have similar pK_a values of the alcohol component in water (methanol: 15.50, benzyl alcohol: 15.40)[43], but dimethyl phosphate cleavage is 6 times faster. Apparently the steric bulk of the substituents have a strong

influence on methanolysis rate. Diethyl phosphate is even 100 times less reactive[44] than dimethyl phosphate, possibly due to a combination of steric effects and a higher basicity of the ethoxide group (pK_a ethanol = 15.93). Surprisingly, bis(p-nitrophenyl)phosphate with a very good p-nitrophenolate leaving group due to the low pK_a of the corresponding phenol, is converted at 40 times lower rate than dimethyl phosphate. Such an inversion of reactivity of dialkyl and diaryl phosphates has never been observed before and is attributed to a very significant influence of steric bulk at the alpha C-atom of the –OR substituent. In the substrate lithium methyl p-nitrophenylphosphate, both methanolate (8 times slower than in case of DMP) and p-nitrophenolate (7 times faster than in case of bis(nitrophenyl)phosphate) are released.[44] Apparently, not only the steric effect of the leaving alcohol but also overall steric crowding in the transition state has a significant effect on catalytic rate. An explanation of these observations would be a transition state stabilisation in phosphodiester methanolysis similar to that proposed for the Klenow fragment, including metal coordination of the alcoholate leaving group. According to molecular models, coordination of a bulky nitrophenolate leaving group (in contrast to methanolate) in phosphodiester methanolysis by **1** is disfavoured by steric hindrance of nitrophenyl substitutents and CH_2 groups of the macrocycle.

3.9. Phosphorylation of alcohols by DMP

Since DMP is a readily available and insensitive reagent, we explored its utility for the catalytic phosphorylation of various alcohols. Reactions were performed using the alcohols as solvents since solutions of the alcohols in DMSO or in DMF were much less or inefficient for the desired phosphorylations. Product formation was followed by electrospray mass

spectrometry. Compared with the transesterification in CD_3OD, reactions with other alcohols were very slow at 55°C and therefore followed only to < 2% conversion. In case of benzyl alcohol, the phosphate esters were separated and the formation of $O_2P(OC\underline{H}_3)(OC\underline{H}_2C_6H_5)^-$ was confirmed by ^1H NMR spectroscopy (d, 3.6 ppm and d, 4.8 ppm). Products of alcohol phosphorylation detected by ESI-MS are shown in scheme 3.3.

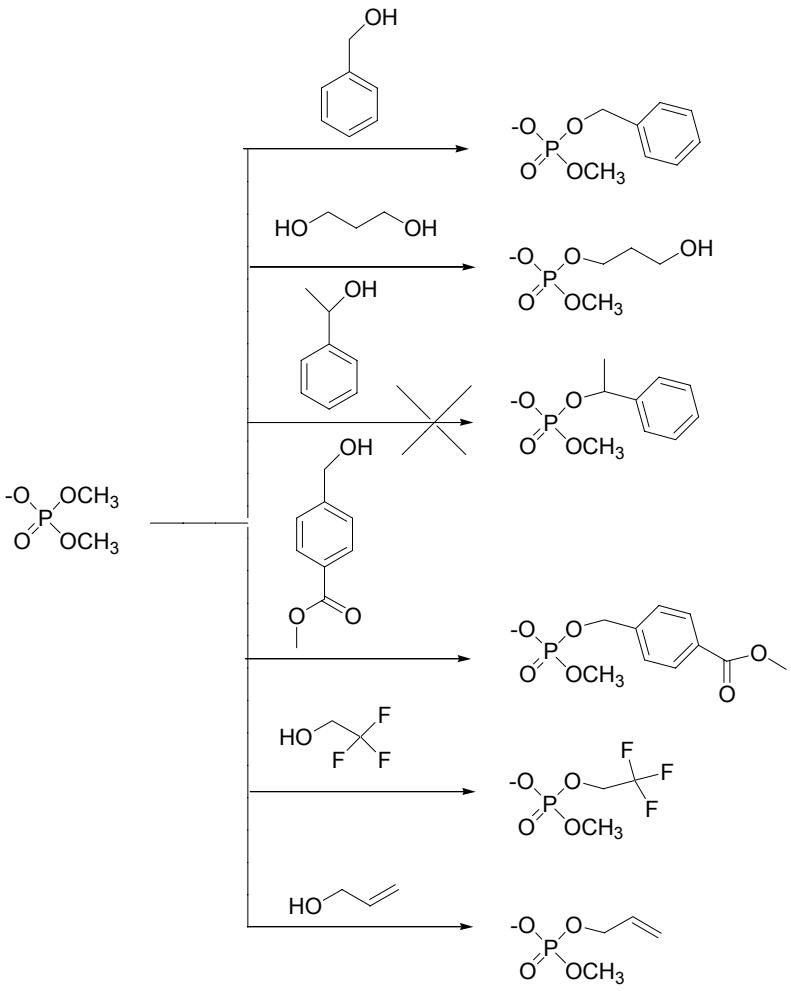

Scheme 3.3. Products of catalytic alcohol phosphorylations by DMP. Procedure: 2mM **1** and 50mM NaDMP were dissolved in the coresponding alcohol and kept at 55°C for at least 1 week. Products were qualitatively detected by electrospray mass spectrometry, conversion was estimated < 2% in all cases.

Reactions are too slow to be of practical use but interesting observations concerning the selectivity have been made. Only primary alcohols yield phosphorylation products, no trace of product is found with the secondary alcohol 1-(hydroxy)ethylbenzene as a substrate. Obviously, steric bulk at the alpha-C-atom of the alcohol nucleophile prevents transesterification.

A remarkable property of catalyst **1** is a specific transesterification of a dialkyl phosphate in the presence of an alkyl carboxylate ester in the case of 4-(hydroxymethyl)benzoic acid methyl ester. This reaction was performed in a 1:1 mixture of the latter alcohol (which is a solid at 55°C) and benzyl alcohol. The only detectable transesterification products are the phosphodiesters $O_2P(OCH_3)(OCH_2C_6H_5)^-$ and $O_2P(OCH_3)(OCH_2C_6H_4CO_2CH_3)^-$, the latter with an intact methyl carboxylate functionality. No traces of benzyl carboxylate products are detected. This is remarkable in view of the relative stabilities $1:10^7$ of methyl acetate and dimethyl phosphate (extrapolated data for cleavage at P) toward hydrolytic cleavage. While certain Cu(II) complexes accelerate the hydrolysis of alkyl carboxylic esters 10^9-fold[45], **1** is inactive in the transesterification of e.g. methyl acetate in CD_3OD.

3.10. Mechanistic discussion

The mechanism of phosphodiester methanolysis catalyzed by **1** must be compatible with the following observations:

- very large rate enhancement for DMP methanolysis
- the reactive species is $[(\mathbf{L})Cu_2(OCH_3)\{(RO)_2PO_2\}]^{2+}$. Attack of external methanol or methoxide at coordinated phosphodiester is ruled out by the pH-rate-profile

- steric bulk at the α-C-atom of the leaving group -OR strongly reduces catalytic rate.

A reaction mechanism (Scheme 3.4) which is related to the Klenow fragment mechanism, in particular with respect to the transition state stabilization is suggested.

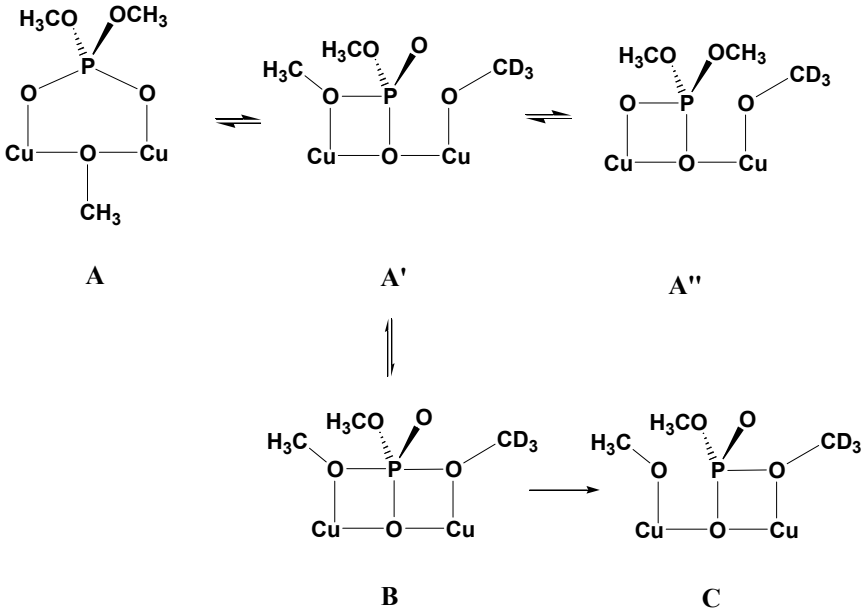

Scheme 3.4. Proposed mechanism for the transesterfication of $(CH_3O)_2PO_2^-$ in CD_3OD catalyzed by **LCu₂** (**L** is omitted for clarity).

The pK_a value of coordinated MeOH in the complex (**L**)$Cu_2(CH_3OH)$ is in the order of 6, much higher then $pK_a \approx 1.6$ of **LCu₂**-coordinated water[46]. Incorporation of bridging OCH_3^- could be somewhat disfavoured for steric reasons. Therefore it is suggested, that the reactive complex $[(\mathbf{L})Cu_2(DMP)(OCH_3)]^{2+}$ exists in an equilibrium of an ´´unproductive`` species **A** containing a bridging methanolate (and being structurally related to **2**) and a productive species **A'** in which bridging methanolate is replaced by a 1,1-bridging DMP. Existence of an energy rich intermediate of a metal complex species in which a P-O-CH_3 group of DMP coordinates to Cu^{2+} in the ground state, related to that observed in the Klenow fragment, is confirmed by the DFT calculations. DFT calculations of species suggested in scheme 3.4 have been performed by Dr. P. Imhof (from the group of Prof. J.Smith, IWR Heidelberg).

Moreover, species **B** was identified by DFT calculations as an intermediate rather than transition state. A reaction pathway which includes the relative DFT energies of species **A**, **A`** and **B** is suggested in scheme 3.5. Attempts to calculate the pathways including transition states between **A**, **A`** and **B** were unsuccessful. We believe that the activation energies for the interconversion of **A** and **A`** or **A`**and **B**, respectively, are low due to the outstanding tolerance of Cu^{2+} to changes in coordinative bond distances (dynamic Jahn-Teller effect) and coordination number (5 to 6 and vice versa). Compared to the cleavage of free DMP by OH^- in water, the energy gap between ground state and trigonal-bipyramidal phosphorane intermediate reduces from 37 kcal/mol[45] to 18 kcal/mol. Therefore, DFT calculations support the idea that the proposed mechanism accounts for the dramatic rate enhancement observed for DMP methanolysis by **1**.

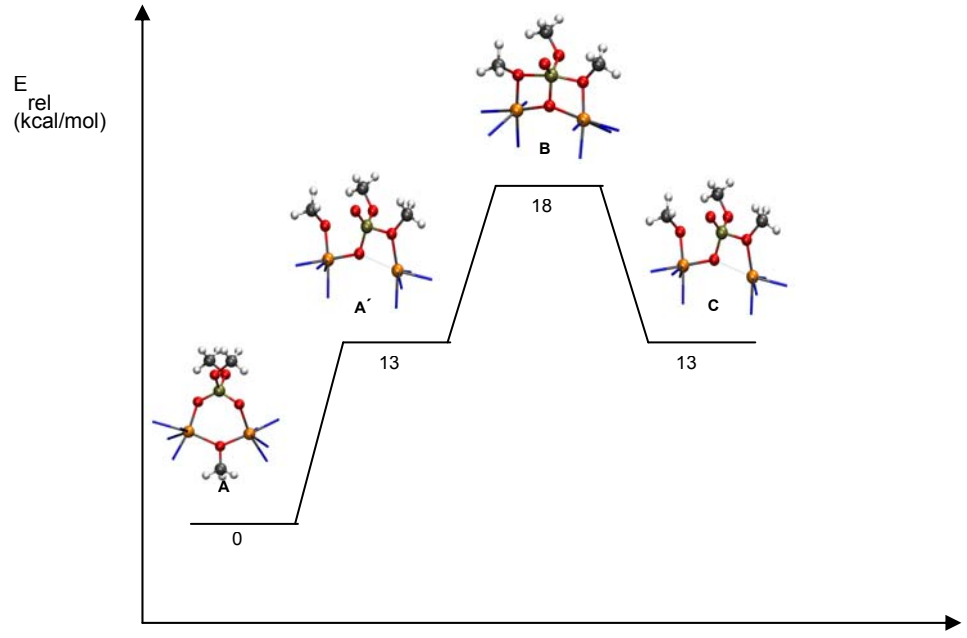

Scheme 3.5. Proposed pathway of LCu_2 promoted methanolysis of dimethyl phosphate. Energies of intermediates (**L** is omitted for clarity) were calculated by DFT methods.

Transition state (or intermediate) **B** is related to complex [**(L)**$Cu_3(\mu_3\text{-}OH)(\mu\text{-}CH_3O)_2(CH_3CN)_2](ClO_4)_3 \cdot CH_3CN$[47] in which **$LCu_2$** ´´incorporates`` a transition state analog of DMP methanolysis. Stabilization of the $-OCH_3$ leaving group by Cu^{2+} coordination would explain both the outstanding reactivity of **LCu_2** and the strong dependence of $O_2P(OR)_2^-$ cleavage rate on steric bulk of –OR. Chin[16a] pointed out that up to 6 orders of magnitude rate acceleration by leaving group stabilization can add up to the effects of double Lewis acid activaton, generation and positioning of metal coordinated nucleophile in dinuclear phosphoesterases. In scheme 3.4 a third equilibrium species **A''** of (**L**)Cu_2(DMP)(OCH_3) is proposed. Although low energy minimum (13 kcal/mol) of **A''**, the resulting transition state is ´´nonproductive`` since the system returns to the same ground state without exchange, i.e. it is the incoming OCD_3^- nucleophile which is released. The very large rate acceleration of DMP methanolysis by **1** would be difficult to explain without a contribution of leaving group stabilization. Molecular models show that the Cu^{2+} coordination of bulky –OR leaving groups in **B** is disfavored by interference with the N-CH_2-py methylene groups of the ligand.

4. Screening of ATP hydrolysis by Zr(IV) und Eu(III) complexes

4.1. Dephosphorylation of ATP

Hydrolysis of ATP by ATPases plays a key role in many biological processes. A number of studies have been devoted to the mechanisms of divalent metal ion[48] (in particular Cu^{2+}, Zn2+, Mg2+) or polyammonium macrocycle[33] promoted ATP dephosphorylation. ATP cleavage by high-valent metal ions such as Zr(IV) and Ce(IV) which display the highest phosphoesterase activities in DNA cleavage[49] and related reactions, is less well explored. While early investigations[50] describe cleavage of ATP by Zr hydroxide, there is a lack of detailed studies on homogeneous Zr complexes. In view of the rapid turnover of intracellular ATP, it would however be important to improve the efficiency of synthetic ATPases in order to produce significant biological effects. Therefore, the ATP dephosphorylation (ATP→ ADP + P_i, Figure 4.1) activities by various Zr(IV) and Eu(III) complexes was explored.

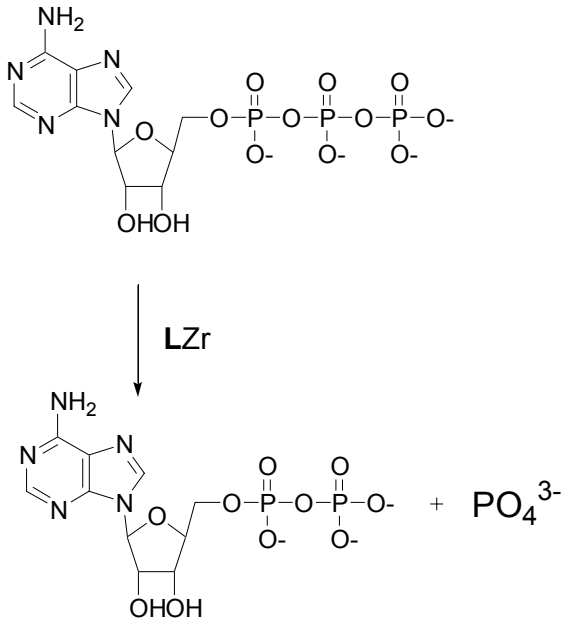

Figure 4.1. Dephosphorylation of ATP to ADP and P_i.

4.2. Ligands used in ATP hydrolysis

While aminoalcohols are good ligands for Zr^{4+} complexation without loss of activity in DNA cleavage, polycarboxylate ligands have been shown to quench strongly the phosphoesterase activity of the metal ion.[49] The structure of the ligands used in ATP hydrolysis is shown in scheme 4.1. **L1**-**L5** were commercially available. **L6** was prepared as described below. A sample of **L7** was provided by Dr. J. Brunner.

4.2.1. Synthesis of 2,6-Bis[N,N-bis(carboxymethyl)aminomethyl]-4-methylphenol (L6)

The ligand was synthesized by a published procedure[51]. To an aqueous solution of iminodiacetic acid and *p*-cresol in an ice-water bath NaOH was added. Upon dissolution, formaldehyde was added dropwise at 0°C. The solution was stirred for 30 min, heated at 70°C for 4 h, and then concentrated to dryness. Recrystallization of the solid from methanol yielded colourless crystals of sodium salt of **L6**.

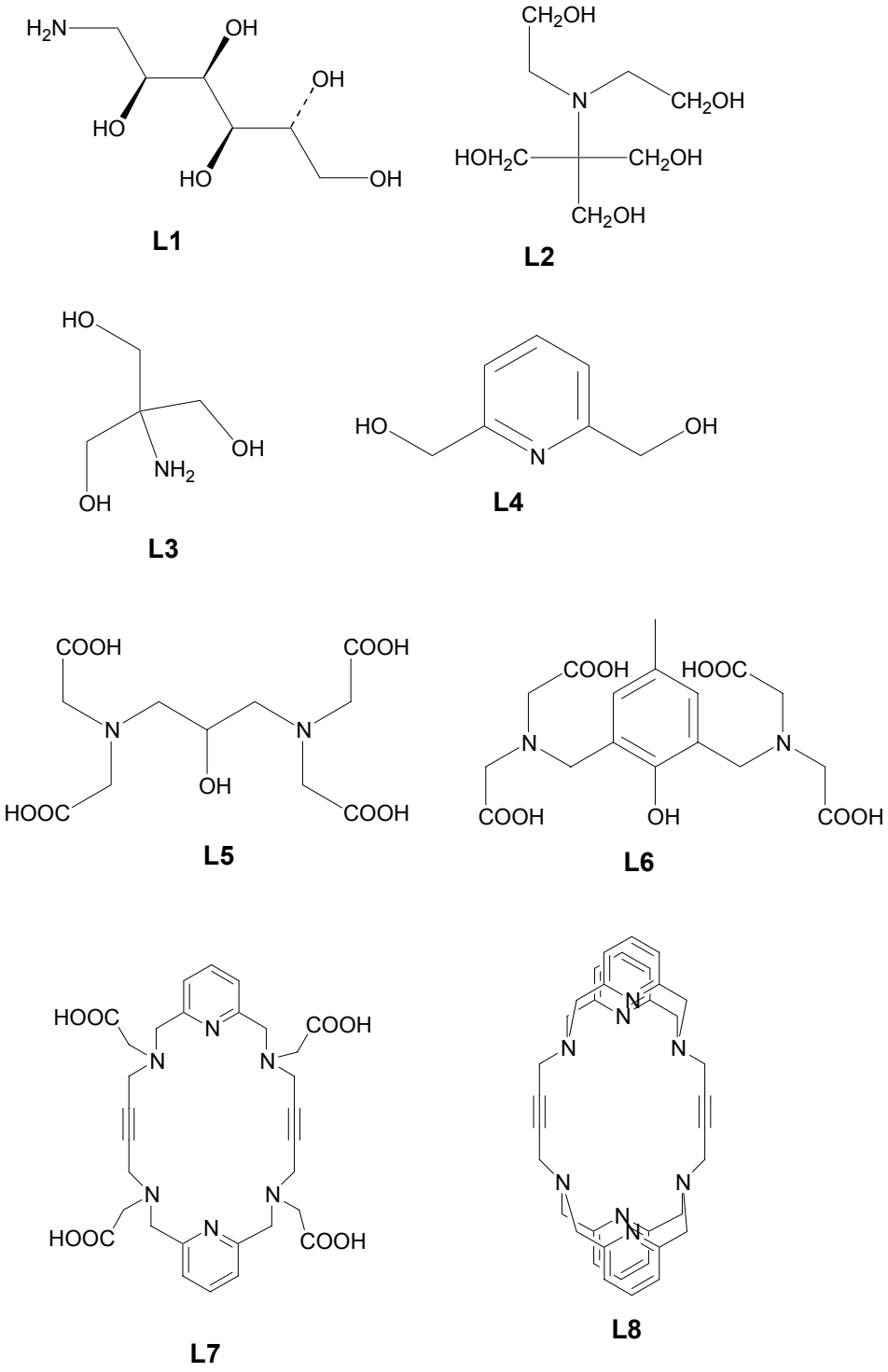

Scheme 4.1. Structure of the ligands used in ATP hydrolysis.

4.3. Determination of phosphate concentration in solution

The concentration of released phosphate was determined according to the Hirata-Appleman procedure[52] applied to a TECAN Genesis Workstation. Advantages of the method are simplicity of operational procedure, stability of the colour development, excellent reproducibility, and stability of the reagents over several months. There are four solutions used in the assay: molybdate reagent ($(NH_4)Mo_7O_{24} \cdot 4H_2O$ solution in water with addition of $HClO_4$), perchloric acid, ice cooled acetone and water, which are hold in the solution rack. A calibration curve was recorded in the absence and in the presence of Zr(IV) (Figure 4.2), indicating that the metal does not affect the colorimetric assay in spite of its high phosphate affinity.

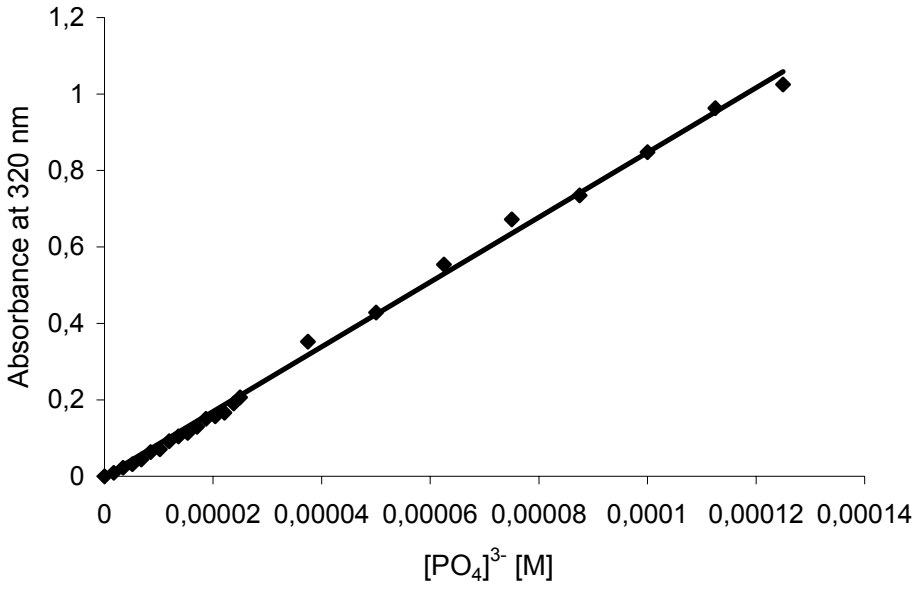

Figure 4.2. Calibration of colorimetric assay for phosphate detection by molybdophosphate reagent. Curves in the absence and presence (values shown) of 1mM $ZrCl_4$ (final concentration in assay mixture) are indistinguishable within error limits.

With use of the pipeting robot, ATP was added from a 10 mM stock solution (the pH of which was adjusted to either 4 or 7) to the reaction solution. The final ATP concentration was 1mM. Samples of reaction solutions were taken in appropriate time intervals and subjected to a colorimetric assay for phosphate determination. After 4 min the formation of yellow phosphomolybdate complex was detected with UV-Vis measurements at 320nm.

4.4. Kinetics of dephosphorylation of ATP

Reaction solutions were prepared by mixing ATP (1mM), $ZrCl_4$ (1 mM) and ligand **L1-L6** (2 mM) in water and adjusting the pH to either 4 or 7, and the temperature to 50°C. Activity of Zr(IV) in the absence of ligands could not be determined due to formation of precipitates. To prevent precipitation, two equivalents of ligand were added, although strong chelators **L5-L6** keep the metal ion in solution at 1 equiv. As observed previously in Zr catalyzed DNA cleavage,[49] dephosphorylation acticivity is strongly pH dependent and decreases when pH is raised from 4 to 7. This is attributed to extended formation of hydroxo clusters at higher pH which prevents access of the substrate to free sites of Zr. Initial rates of ATP dephosphorylation were recorded at 50°C. After prolonged reaction times, both ADP and AMP was qualitatively determined as cleavage products by electrospray mass spectrometry.

Clearly, ATPase activity of the metal is modulated by the ligands (fig. 2). Remarkably, the most efficient catalyst is the Zr complex of the tetracarboxylate ligand **L6** at both pH 4 and pH 7. This is in contrast to Zr promoted DNA hydrolysis where polycarboxylate ligands have been shown to quench strongly the phosphoesterase activity of the metal ion.[49] The activity of **L6**Zr is in the same order of magnitude as found for Cu^{2+} ions[48] and at pH 7 lower than of lanthanide ions, but importantly an active Zr(IV) complex of an efficient chelator (association constant log K = 24)[53] was found which should prevent loss of the metal ion in the presence

of competitive ligands. In view of applications in an "aggressive" biological environment, it is important to find ligands that form complexes of high thermodynamic and, ideally, kinetic stability.

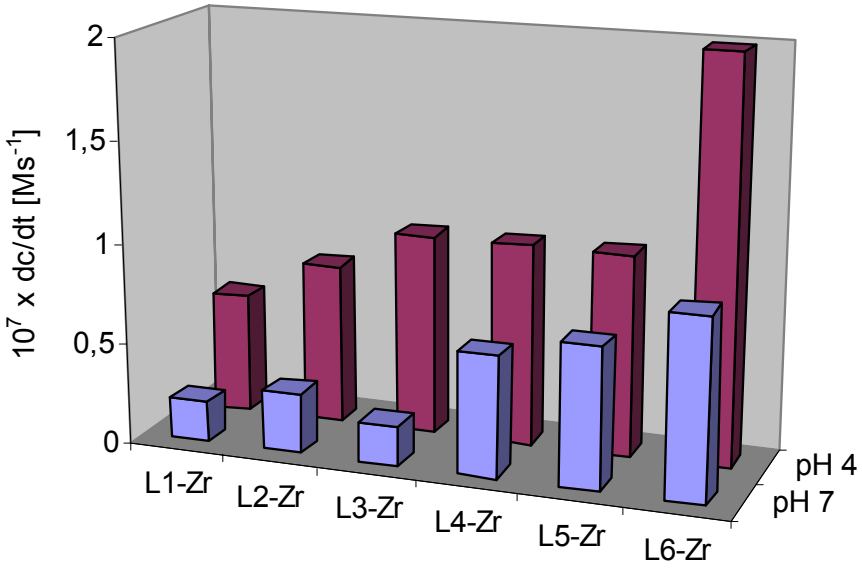

Figure 4.3. Increase of phosphate concentration with time (dc/dt) in solutions containing ATP (1 mM), $ZrCl_4$ (1 mM) and a ligand **Ln** (2 mM). pH was adjusted to either 4.0 or 7.0 with NaOH. T = 50°C. Data are average values of three independent measurements, reproducibility ± 20%.

The catalyst screening was expanded to Eu(III) and Cu(II) complexes of the macrocyclic ligand type **L7**/**L8**. The dinuclear Cu(II) complex of **L8** is the only available catalyst for transesterification of the highly inert substrate dimethyl phosphate.[44] In the crystallographically characterized dinuclear Eu(III) complex of **L7**[54], the metal ions appear to be ideally preorganized for multiple activation of the phosphate groups of ATP.

Unfortunately, none of the two complexes displayed significant activity toward ATP at pH 7, and the substantial activity of free Eu(III) ions is even supressed by **L7** (fig. 3).

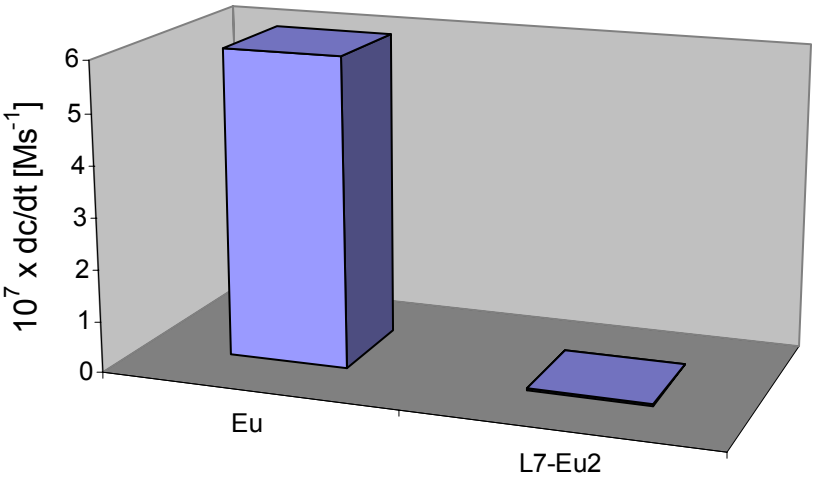

Figure 4.4. Increase of phosphate concentration with time (dc/dt) in solutions containing ATP (1 mM), $EuCl_3$ (1 mM) and a **L7** (0.5 mM). pH was adjusted to 7.0 with NaOH. T = 50°C. Data are average values of three independent measurements, reproducibility ± 20%.

5. Summary

Phosphoryl transfer reactions are ubiquitous in biology and are usually catalyzed by metalloenzymes. For a number of phosphoryltransfer enzymes, including the exonuclease subunit of DNA polymerase I, a mechanism involving two metal ions and double Lewis-acid activation of the substrate, combined with leaving group stabilisation, has been proposed.

Aim of this thesis was the study of low-molecular-weight models of phosphoryl transfer metalloenzymes. The focus was in particular on the macrocyclic dicopper(II) complex **LCu$_2$**, which is the first tansesterification catalyst for highly inert dialkyl phosphates and a mimic of the exonuclease subunit of DNA polymerase I.

For the first time, a crystal structure of **LCu$_2$** with a coordinated phosphodiester was obtained. [**L**Cu$_2$(1,3-μ-DMP)(NO$_3$)](NO$_3$)$_2$ (**2**) contains a 1,3- bridging phosphodiester.

By extensive UV-Vis and pH metric titrations, the metal complex species present in methanolic **LCu$_2$**/DMP solution have been identified. In particular it has been shown, that [**L**Cu$_2$(DMP)(OCH$_3$)]$^{2+}$ is the active species and that coordinated methanolate (and not free methanol or methanolate) is the nucleophile which attacks the P-atom of the substrate. DFT calculation (in cooperation with the group of Prof. Smith, IWR Heidelberg) confirm that the 1,3-DMP bridged complex is the dominant species in solution (Scheme 5.1, species **A**), and support the existence of energy rich intermediates **A´**, **A´´** and **B**.

By extensive kinetic studies including rate dependence on catalyst concentration, saturation kinetics, pH dependence of rate and dependence on rate on substrate structure, solid experimental data have been obtained which support the mechanistic proposal given in scheme 5.1.

The applicability of **LCu$_2$** as a catalyst for the phosphorylation of various alcohols by dimethyl phosphate has been evaluated. A unique functional group tolerance of the catalyst and selectivity for dialkyl phosphates over alkyl carboxylates is observed.

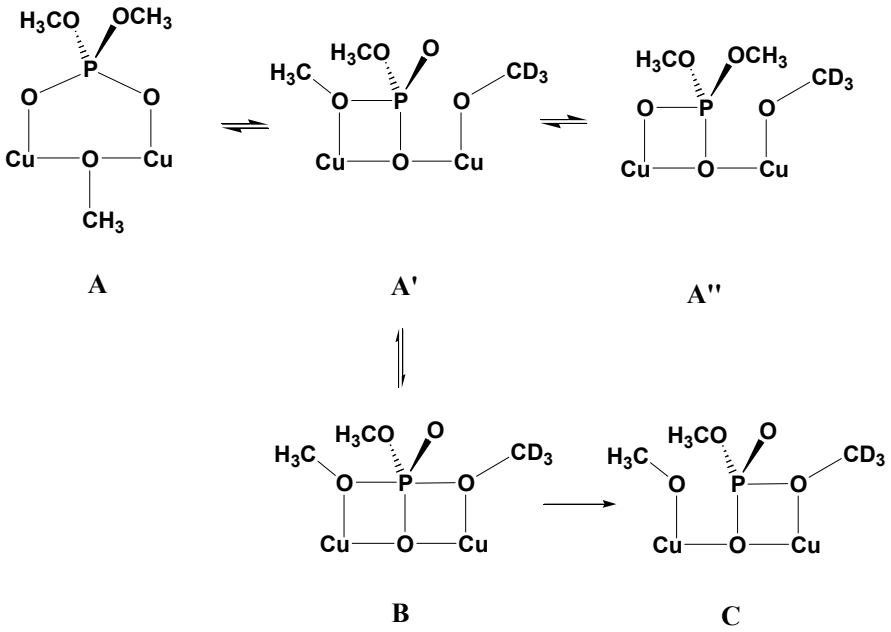

Scheme 5.1. Proposed mechanism for the transesterfication of $(CH_3O)_2PO_2^-$ in CD_3OD catalyzed by **LCu$_2$** (**L** is omitted for clarity).

Even if **LCu$_2$** is not applicable to the cleavage of biological substrates in aqueous systems, it supports the idea that cooperation of two divalent metal ions in the proposed manner might be crucial for the function of such enzymes, which often cleave phosphate esters with poor O-alkyl leaving groups.

Screening of ATP hydrolysis by Zr(IV) and Eu(III) complexes was examined using a robotic liquid-handling workstation. It was found that a phosphate detection assay using molybdate is compatible with the presence of these high-valent metal ions. ATPase activity of the metal is modulated by the ligands, and the most efficient catalyst is the Zr complex of the tetracarboxylate ligand **L6** (Fig. 5.1) at both pH 4 and pH 7. This is in contrast to Zr promoted DNA hydrolysis where polycarboxylate ligands have been shown to quench strongly the phosphoesterase activity of the metal ion. In conclusion, stable Zr(IV) complexes with ATPase activity were found, using a robotics-based automated screening assay for phosphate.

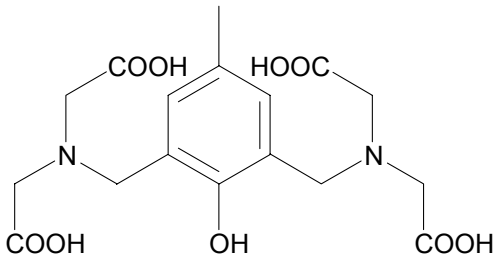

L6

Figure 5.1. Structure of the ligand showing the most efficient rate in ATP hydrolysis.

6. Experimental details

6.1. Equipment

All experiments were performed at Inorganic Chemistry Department of Heidelberg University using following equipment:

UV-Vis spectroscopy:

UV-Vis spectra were measured on a Varian Cary 100-Bio UV-Visible Spectrophotometer equipped with a temperature controller. For the measurements 1 cm quartz-cuvettes were used.

ESI - mass spectrometry:

Electrospray ionisation mass spectra were acquired using Waters ESI- Q- TOF Ultima API device (mobile phase: acetonitrile, flow rate: 50 µL/min).

HPLC Analysis:

HPLC analysis of **L** was performed on Waters Alliance liquid chromatograph equipped with UV-Vis Detector. A Macherey-Nagel Nucleosil C18 250 x 4,6 mm column with gradients of CH_3CN/water was used.

EPR spectroscopy:

EPR spectra were recorded on a Bruker ESP 300E spectrometer in methanol glass at 77K.

NMR spectroscopy:

^{1}H NMR spectra were acquired using a Bruker AC200 spectrometer (200 MHz). The chemical shifts are given in ppm, with reference to rest hydrogens signal of the deuterated solvents.

pH measurements:

The $CH_3OH_2^+$ concentration was determined using a Thermo-ORION 420A pH meter equipped with a ORION 7103SC combination (glass/calomel) electrode, calibrated with Acros Organic standard aqueous buffers (pH = 4 and pH = 7). Values of $^{s}{}_{s}$pH were obtained by addition of a correction constant 2.24 to the experimental pH meter reading, as reported by Bosch and co-workers.[40b]

High-Throughput Screening:

The concentration of released phosphate was determined with Hirata-Appleman procedure[51] applied to a TECAN Genesis Workstation 150 equipped with TECAN SpectraFluor Plus UV-Visible Spectrophotometer and temperature controller VARIOMAG 96 reaction block. UV-Vis spectra were measured in Greiner 96-wells microtiterplates. The automated assay for phosphate determination was programmed using Gemini 3.10 software.[55]

Structure Determination:

Intensities were collected using a Bruker AXS CCD Smart 1000 diffractometer, with graphite-monochromated Mo-Kα radiation (λ=0.71073 Å). Absorption corrections were performed based on multiple scans of equivalent reflections using the SADABS routine. The structure was solved by direct methods and refind by full-matrix least-squares (SHELXTL NT V.5.1.) anisotropically for all non-hydrogen atoms. Hydrogen atoms were located in difference Fourier maps and refined isotropically.

6.2. Materials

All reagents were purchased from Sigma-Aldrich or Acros. Unless otherwise indicated the reagents were of analytical grade and were used without further purification.

Sodium dimethyl phosphate (DMP) and sodium dibenzyl phosphate (DBP) were available in group of Prof. Krämer. A sample of macrocycle **L7** was provided by Dr. J. Brunner.

Deuterated solvents were purchased from Deutero GmbH.

6.3. Syntheses of ligands

6.3.2. Synthesis of

6.3.2.1. Synthesis of 2,6-pyridinedicarboxaldehyde[56]

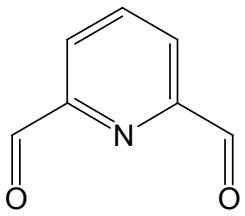

To a solution of 10 g (72 mmol) of 2,6-Bis(hydroxymethyl)pyridine in 160 ml dioxane 7.95 g (72 mmol) seleniumdioxide was added and the solution was stirring for 16 h at 90 °C. The solid was separate on a silica gel column with ethyl acetate as an eluent. The solvent was evaporated and the solid dried in vacuum. Recrystallization of the solid from the mixture of petroleum ether/chloroform (1:1) yielded colourless crystals of 2,6-pyridinedicarboxaldehyde. Yield 8.2g (61 mmol, 86%).

^{1}H NMR (200 MHz, CDCl3)

δ(ppm): 10.15 (s, 2H), 8.16 (m, 2H), 8.06 (m, 1H)

6.3.2.2. Synthesis of 1,4-diamine-2-Butyne[57]

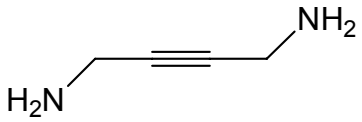

To a suspension of 57 g (0.34 mol) potassium phthalimide in 250 ml dimethylformamide, 15 ml (18.9 g, 15.5 mol) 1,4-dichloro-2-butyne was added dropwise and stirred for 7 h at 70 °C. After the solution was cooled down, 400ml water was added. The light brown precipitate of 1,4-Diphthalimide-2-butyne was filtered off, washed with water and dried in vacuum. Yield 51 g (0.14 mol, 95 %)

To a suspension of 25 g (0.08 mol) 1,4-Diphthalimide-2-butyne in 75 ml ethanol, 7 ml (7g, 0.15 mol) of hydrazine hydrate was added dropwise and refluxed. Gelatinous, hard to stir bulk was partially dissolved when 150 ml concentrated hydrochloric acid was added and the bulk was refluxed. Remaining solid was filtered off and washed with water. The filtrate was concentrated to dryness. Anhydrous ethanol was added and again evaporated. This was repeated until the solid was anhydrous. Recrystallization of the solid from the anhydrous methanol yielded brown crystals of 1,4-diamine-2-butyne-dihydrochlorid. Yield: 6.2 g (0.038 mol, 51 %).

^{1}H NMR (200 MHz, D_2O)

δ(ppm): 3.65 (s, 4H)

3 g (0.02 mol) of 1,4-diamine-2-butyne-dihydrochlorid was dissolved in anhydrous, hot methanol. After the solution was cooled down, 2.16 g (0.04 mol) of sodium methanolate in anhydrous methanol was added, warm up for 10 minutes and concentrated to dryness. Anhydrous ethanol was added and again evaporated. To the solid dichlormethane was added

and dried with Mg_2SO_4. NaCl and Mg_2SO_4 were filtered off. The filtrate was concentrated to dryness and light brown solid dried in vacuum. Yield: 1.2 g (0.014 mol, 71 %).

^{1}H NMR (200 MHz, D_2O)

δ(ppm): 3.19 (s, 4H)

6.3.2.3. Synthesis of 2,6-Bis(tosyloxymethyl)pyridine[58]

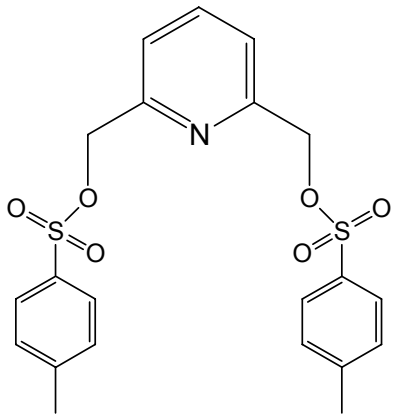

To a solution of 3.23 g (0.023 mol) 2,6-Bis(hydroxymethyl)pyridine in 35 ml anhydrous tetrahydrofurane, 5 g (0.063 mol) potassium hydroxide was added and kept in an ice bath. A solution of 9.8 g (0.051 mol) in 60 ml anhydrous tetrahydrofurane was added dropwise and stirred 5h at 0 °C and 12h at room temperature. The solid was filtered off and washed with diethyl ether. The filtrate was concentrated to dryness. Yield: 9.0 g (0.019 mol, 87 %).

^{1}H NMR (200 MHz, $CDCl_3$)

δ(ppm): 7.73 (d, 4H), 7.62 (t, 1H), 7.26 (d, 6H), 4.99 (s, 4H), 2.37 (s, 6H)

6.3.2.4. Synthesis of 3,8,16,21,27,28-Hexaazatricyclo[21.3.1.1^{10,14}]-octacosa-1(27),2,8,10,12,14(28),15,21,23,25-decaene-5,18-diine[36]

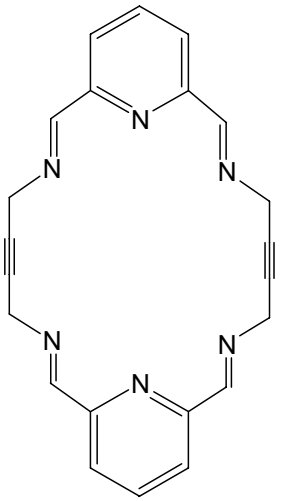

To a solution of 2.0 g (14.8 mmol) 2,6-pyridinedicarboxaldehyde in 75 ml anhydrous methanol, 1.24 g (14.8 mmol) 1,4-amine-2-butyne in 30 ml anhydrous methanol was added dropwise under continous stirring. The white precipitation was stirring for 15 min, filtered off and washed with little methanol. The white crystalline solid was dried in vacuum. Yield: 3.1 g (8.5 mmol, 57 %).

^{1}H NMR (200 MHz, $CDCl_3$)

δ(ppm): 9.11 (s, 4H), 8.10 (d, 4H), 7.82 (t, 2H), 4.81 (s, 8H)

6.3.2.5. Synthesis of 3,8,16,21,27,28-Hexaazatricyclo[21.3.1.1^{10,14}]-octacosa-1(27),10,12,14(28),23,25-hexaene-5,18-diine[36]

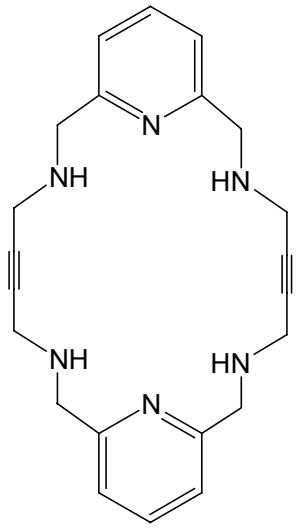

3.2 g (0.084 mol) of sodium tetraborate was added under stirring at 5 °C to 150 ml concentrated acetic acid. This solution was mixed at ice bath with suspention of 2.00 g (0.006 mol) 3,8,16,21,27,28-Hexaazatricyclo[21.3.1.110,14]-octacosa-1(27),2,8,10,12,14(28), 15,21, 23,25-decaene-5,18-diine in 100 ml chloroform. Concentrated NaOH was added to the mixture until the alkaline pH was achieved. After addition of 700 ml water and four times extraction with chloroform, the reaction mixture was dried with Mg_2SO_4. The extract was reduced to 20 ml, placed into silica gel column and eluated with chloroform/methanol (1:1). The eluate was evaporated to dryness. The solid was dissolved in 20 ml chloroform and precipitated by addition of 500 ml petroleum ether. The white precipitate was filtered off and dried in vacuum. Yield: 1.60 g (43 mmol, 78 %).

^{1}H NMR (200 MHz, CD_3OD)

δ(ppm): 7.67 (t, 2H), 7.24 (d, 4H), 3.91 (s, 8H), 3.45 (s, 8H)

6.3.2.6. Synthesis of L[58]

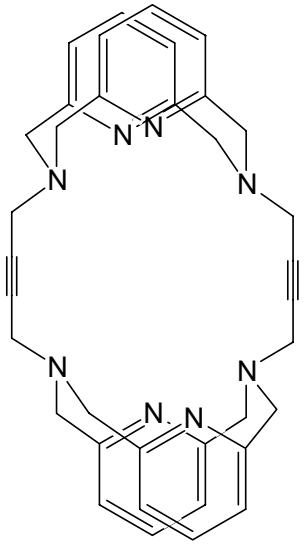

0.25 g (0.67 mmol) of 3,8,16,21,27,28-Hexaazatricyclo[21.3.1.1^{10,14}]-octacosa-1(27),10,12,14(28),23,25-hexaene-5,18-diine, 0.60 g (1.34 mmol) of 2,6-pyridinedimethyl ditosylate and 5.00 g (47.2 mmol) of Na_2CO_3 were suspended in 100 mL acetonitrile and supersonicized for 2 hours. After stirring for 4 days at room temperature, the solid was filtered off. The filtrate was reduced to 50 mL. 20 mL of water was added dropwise with stirring. The white precipitate was filtered off, washed with water, acetonitrile and diethyl ether and dried in vacuum. Yield: 191mg (0.330 mmol, 49%).

ESI-MS: m/z 581 [L + H^+]

^{1}H NMR ($CDCl_3$): δ [ppm] = 7.11 (t, 4H), 6.80 (d, 8H), 4.69 (d, 8H), 3.97 (d, 8H), 3.93 (s, 8H).

6.3.3. Synthesis of 2,6-Bis[N,N-bis(carboxymethyl)aminomethyl]-4-methylphenol (L6)[51]

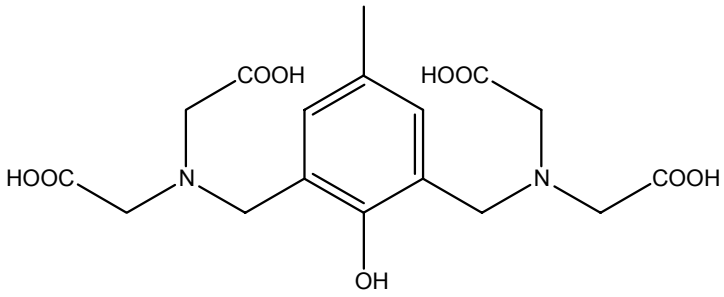

To a 50 mL aqueous solution of 8.35 g (0.063 mol) of iminodiacetic acid and 4.40 g (0.032 mol) of *p*-cresol was added 5.25 g (0.125 mol) of NaOH in 20 mL of water cooled in an ice-water bath. Upon dissolution, 7.5 mL of 37 % formaldehyde was added dropwise at 0 °C. The solution was stirred for 30 min, heated at 70 °C for 4 h, and then concentrated to dryness. Recrystallization of the solid from methanol yielded colourless crystals of Na_4**L6**. Yield: 10.74g (27 mmol, 85.7 %).

^{1}H NMR in D_2O (δ, ppm): 6.85 (s, 2H), 3.68 (s, 4H), 3.04 (s, 8H), and 2.05 (s, 3H).

6.4. Syntheses of metal complexes of L

[(L)$Cu_2(NO_3)_2$]$(NO_3)_2$ (1).[38] A methanolic solution of 16 mg (66 μmol) copper (II) nitrate trihydrate was added to a suspension of 20 mg (33 μmol) **L** in 2 ml methanol with stirring. A clear green solution was obtained. Layering with diethyl ether yielded a green powder and some green crystals of **1**. The crystals were mechanically separated from the powder. Yield 5-20%. ESI-MS: m/z 848 [**L**$Cu_2(NO_3^-)_2(OH^-)$+ H^+]

[(L)Cu_2(1,3-μ-DMP)(NO_3)$_2$] (NO_3)$_2$ · CH_3OH · H_2O (2). To 30 mg (49 μmol) **L**·2H_2O suspended in 4 mL methanol 24 mg (100 μmol) of $Cu(NO_3)_2 \cdot 3H_2O$ and 7.7mg (52 μmol) NaDMP was added. A green solution is obtained under stirring. Layering with diethyl ether yields some blue-green crystals of [(**L**)Cu_2(μ-DMP)(NO_3)$_2$](NO_3)$_2$. The yield was too small for full characterization, crystallization was not reproducible.

.

6.5. Spectrophotometric Titration

For the UV-Vis titrations only anhydrous solvents were used. A solution of $NaOCH_3$ was always prepared freshly from Na and CH_3OH. A volume correction of absorbance was not performed since total volume of added titrant do not exceed 2% of the reaction solution.

6.5.1. Titration of L with Cu(II)

For a titration of **L** with Cu(II) 10 mM **L** and 7 mM $Cu(NO_3)_2 \cdot 3H_2O$ stock solution were prepared. A mixture of methanol/chloroform (1:1) (the latter, to improve solubility of **L**) was used for preparation of all solutions. The solutions of L was diluted to 100 μM and aliquots of $Cu(NO_3)_2 \cdot 3H_2O$ stock solutions were added with stirring in steps of 0.1 equiv. While the 1:1 **L**Cu complex is formed smoothly, formation of **LCu_2** complex requires prolonged heating. The UV-Vis spectra upon addition of > 1 equiv. Cu(II) were equilibrated for 30 min at 50 °C (no further changes of the spectra were observed).

6.5.2. Titration of 1 with $NaOCH_3$ and DMP

For the titration of **1**, the following stock solutions in methanol were used: 5 mM **1** (prepared from separated crystals), 20 mM $NaOCH_3$ and 20 mM NaDMP. The stock solution of **1** was diluted to 100 μM and aliquots of stock solutions containing NaDMP or $NaOCH_3$ were added with stirring (in 0.1 equiv. steps). Immediately after addition, a UV spectrum of the solution was taken at 25°C.

6.5.3. Titration of 1/DMP with $NaOCH_3$

A 100 μM solution of **1** was prepared from 5 mM LCu_2 stock solution in methanol. Afterwards the solution was titrated with 20 mM NaDMP (0-1 equiv.) and 20 mM $NaOCH_3$ (1.1- 2 equiv.). Immediately after addition, a UV spectrum of the solution was taken at 25°C.

6.6. pH titrations

For the pH titrations only anhydrous, degassed methanol was used. The electrode was calibrated before each experiment with Acros Organic standard aqueous buffers (pH = 4 and pH = 7). A solution of $NaOCH_3$ was always prepared freshly from Na and CH_3OH. Titrations were made at 25 °C. pH meter reading was stable after about 30 s equilibration time. The recommended[40b] correction value 2.24 was added to the pH meter reading to obtain $^{s}_{s}$pH.

6.6.1. Titration of 1 with $NaOCH_3$

3 ml of a 1 mM solution of **1** in methanol was prepared. A 15 mM stock solution of $NaOCH_3$ in methanol was then added with stirring in steps of 0.1 equiv

6.6.2. Titration of 1/DMP (1:1) with $NaOCH_3$

A 3 mM solution of **1** and 10 mM solution of NaDMP in methanol were prepared. 1 ml of **1**, 0.3 ml of NaDMP solution and 1.7 ml of CH_3OH were mixed together. A 15 mM stock solution of $NaOCH_3$ in methanol was then added with stirring in steps of 0.1 equiv.

6.7. Catalytic transesterification of phosphate esters in CD_3OD

For catalytic transesterification of DMP, DBP and BNPP, a 2 mM stock solution of **1** in CD_3OD was prepared. In a typical kinetic assay, 7.4 mg (50 μmol) sodium dimethyl phosphate was added to 1 mL of a 2mM stock solution of **1** in CD_3OD and the solution transferred to an NMR tube. In the case of DBP and BNPP, 13.6 mg (50 μmol) and 19.5 mg (50 μmol) was added, respectively. The sample was kept at either 25°C or 55°C, and ^1H NMR spectra were recorded in appropriate time intervals. Conversion of $O_2P(OCH_3)_2^-$ to $O_2P(OCH_3)(OCD_3)^-$ was followed by integration of the signals of released methanol and residual methyl ester.

6.8. Dependence of initial rate of DMP cleavage on catalyst concentration.

A 3 mM stock solution of **1** was prepared in CD_3OD. 1ml of 1, 1.5, 2, 2.5 mM solutions of **1** were obtained by dilution of the 3 mM stock solution. 7.4 mg (50 μmol) sodium dimethyl phosphate was added to 1 mL of each solution. The $^s{}_s$pD value of the CD_3OD solutions at 25°C were 9.9 ± 0.2, adjusted by addition of *p*-toluonesulfonic acid to the solution at 1 and 1.5 mM **1.** To the pH meter reading of the CD_3OD solution, correction value of 2.24 was added. The solutions were transferred to an NMR tube and the samples were kept at 55°C. ^1H

NMR spectra were recorded in appropriate time intervals. Conversion of $O_2P(OCH_3)^{2-}$ to $O_2P(OCH_3)(OCD_3)$- was followed by integration of the signals of released methanol and residual methyl ester.

6.9. Saturation kinetics for the hydrolysis of DMP by 1

For the saturation kinetics 5 mM stock solution of **1** and 100 mM stock solution of NaDMP were prepared in CD_3OD. A series of reaction solutions containing 2, 5, 7, 10, 15, 20, 50 mM DMP solutions was prepared by addition of appropriate amount of sodium dimethyl phosphate stock solution (100 mM) to 0.4 ml solution of **1**. The final volume of reaction mixture was adjusted to 1 ml. The samples were transferred to an NMR tubes and kept at 55 °C. ^{1}H NMR spectra were recorded in appropriate time intervals. Conversion of $O_2P(OCH_3)_2$- to $O_2P(OCH_3)(OCD_3)^-$ was followed by integration of the signals of released methanol and residual methyl ester. The ^s_spD of the solution was 9.9 ± 0.3 at 25°C. To the pH meter reading of the CD_3OD solution, correction value of 2.24 was added. The pD of the solution dropped to < 9.5 when [DMP]<10 mM, therefore data at <10mM DMP were not included.

6.10. Dependence of DMP transesterification rate on pH

For this experiment following stock solution were prepared both in methanol and CD_3OD: 2 mM **1**, 100 mM $NaOCH_3$ (or $NaOCD_3$), 100 mM *p*-toluenesulfonic acid. To the samples in CH_3OH, 7.4 mg (50 μmol) sodium dimethyl phosphate was added and then ^s_spH was adjusted by addition of $NaOCH_3$ or *p*-toluenesulfonic acid stock solutions in CH_3OH. Then the same amount of $NaOCD_3$ and *p*-toluenesulfonic acid were added to the reaction solution in CD_3OD. The samples were transferred to an NMR tubes and kept at 55 °C. ^{1}H NMR spectra were

recorded in appropriate time intervals. Conversion of $O_2P(OCH_3)^{2-}$ to $O_2P(OCH_3)(OCD_3)^-$ was followed by integration of the signals of released methanol and residual methyl ester.

6.11. Catalytic transesterification of dimethyl phosphate in other alcohols.

For a transesterification of DMP, the following alcohols were used as solvents (min. 99%): benzyl alcohol, allyl alcohol, 2,2,2-trifluoroethanol, propane-1,3-diol and DL-Phenethyl. In a typical reaction, 3.8 mg (3.8 μmol) of **1** was dissolved in 2 ml of the alcohol and 15 mg (100 μmol) sodium dimethyl phosphate was added. The light green solution was kept at 55°C.

For ESI-MS spectrometry 10 μl of the reaction solution were mixed with 240 μL methanol. Except in the case of benzyl alcohol, 10 μl of 5 mM sodium dibenzyl phosphate in methanol was added as an internal standard. For the reaction in benzyl alcohol, 10 μl of 5 mM bis(p-nitrophenyl)phosphate was used.

6.11.1. Catalytic transesterification of dimethyl phosphate in benzyl alcohol in the presence of methyl 4-(hydroxymethyl) benzoate

3.8 mg of crystalline **1** (3.8μmol) was dissolved in 2 ml 99,9% benzyl alcohol. 15mg (100 μmol) sodium dimethyl phosphate and 3g (18 mmol) of methyl 4-(hydroxymethyl) benzoate was added. For ESI-MS spectrometry 10 μl of the reaction solution were mixed with 240 μl methanol. 10 μl of 5mM sodium dibenzyl phosphate in methanol was added as an internal standard.

6.12. Assay for phosphate determination

For phosphate determination following reagents were used: molybdate solution (1.25 g $(NH_4)_6Mo_7O_{24} \cdot 4H_2O$ + 0.4 ml 70 % $HClO_4$ + 500 ml H_2O), 70 % $HClO_4$, ice-cooled acetone and distilled H_2O (HPLC grade). 20 µl of the probe to be analyzed for phosphate was taken and placed in the microtiterplate. 40 µl of molybdate reagent, 80 µl of ice cooled acetone, 10 µl of 70 % $HClO_4$ and 50 µl of H_2O were then added allowing 4 minutes for equilibration. The formation of the phosphomolybdate complex was detected with UV-Vis measurements at 320nm. All manipulations were performed with use of the pipeting roboter of the Tecan Genesis Workstation.

6.12.1. Calibration curve

There were 2 stock solutions in water of standard NaH_2PO_4 prepared: 20 µM and 430 µM. These stock solutions were then diluted in a microtiterplate with water to obtain standard phosphate solutions in the range 4 - 430 µM and volume 70 µl. 40 µl of molybdate reagent, 80 µl of ice cooled acetone, 10 µl of 70 % $HClO_4$ were then added, allowing 4 minutes for equilibration. The formation of the phosphomolybdate complex was detected as usual.

The procedure was repeated in the presence of 1 mM $ZrCl_4$. NaH_2PO_4 stock solutions were diluted in the microtiterplate with water to obtain standard phosphate solution in the range 4 - 430 µM and volume 60 µl. 10 µl of 25mM $ZrCl_4$ stock solution, 40 µl of molybdate reagent, 80 µl of ice cooled acetone, 10 µl of 70 % $HClO_4$ were then added, allowing 4 minutes for equilibration. The formation of the phosphomolybdate complex was detected as described earlier.

6.12.2. Kinetics of ATP hydrolysis

10 mM stock solutions of ATP, $ZrCl_4$, $EuCl_3 \cdot 6H_2O$ and **L1-L8** were prepared in water. For kinetic assays, 300 µl $ZrCl_4$ (or 300 µl $EuCl_3 \cdot 6H_2O$), 600 µl **Ln** stock solution and 1.8 ml H_2O were mixed together. These solutions and ATP stock solution were adjusted to either pH 4 or 7 by addition of 0.1M NaOH or 0.1M HCl, and were kept in the reaction block under continous stirring at 50°C. With use of the pipeting robot, 300 µl ATP stock solution was added (concentration to be 1mM) and 20µL aliquots of the reaction solution were transferred to a microtiter plate to be anlyzed for phosphate. The formation of the phosphomolybdate complex was detected as described earlier.

6.13. DFT calculation

The calculations were performed in a collaborative project by the group of Prof. J. Smith using the program package TURBOMOLE 5.7.[59] The B3LYP[60] density functional together with the LANL2DZ[61] basis set with an effective core potential for the copper atoms and the SVP[62] all electron basis set for all the other atoms was applied.

The computations started from the crystal structure of the $[(\mathbf{L})Cu_2(DMP)(NO_3)]^{2+}$ replacing the nitrate ion with a methanolate ion. This starting structure was fully optimized in vacuum. Further vacuum minimum energy structures were obtained from starting structures derived by modification of the latter (terminally coordinated methanolate, bridging phosphate etc.). Minimizations were carried out stepwise: First the methanolate-oxygen-copper distance and the O-Cu-O (phosphate) angle were fixed while all other degrees of freedom were optimized. Subsequently, the fixed internal coordinates were relaxed and the structures were fully optimized to a convergence criterion of 10^{-6} a.u. and 10^{-4} a.u./Bohr for energy and gradient, respectively.

Solvent effects were treated implicitly, making use of the conductor like screening model (COSMO) as implemented in TURBOMOLE. This approach is a dielectric continuum solvation model in which the mutual polarization of the solute and the solvent is represented by screening charges on the surface of the solute cavity. These charges are derived under the simplified boundary condition that the electrostatic potential vanishes for a conductor and then are scaled to account for the finite dielectric constant of a real solvent (here methanol). All minimum energy structures, except **B** (Scheme 3.5), obtained from vacuum calculations were re-optimized in implicit methanol to 10^{-6} a.u. and 10^{-3} a.u./Bohr for energy and gradient, respectively. For **B** no stable vacuum minimum could be trapped. Thus, optimization of this structure in implicit solvent started from the initial starting structure for the vacuum calculations. Analytical second derivatives with subsequent normal mode analyses were carried out on the optimized structures to verify the minima.

7. Crystal structure parameters for 2

Table 7.1. Atomic coordinates (x 10^4) and equivalent isotropic displacement parameters (Å^{2}x 10^3) **2**. U(eq) is defined as one third of the trace of the orthogonalized U^{ij} tensor.

	x	y	z	U(eq)
C(1)	5041(4)	4573(3)	956(2)	28(2)
C(2)	4450(4)	4430(3)	557(2)	22(2)
C(3)	3971(5)	4385(3)	224(2)	26(2)
C(4)	3398(4)	4422(3)	-187(2)	28(2)
C(5)	1682(5)	3260(3)	2269(2)	29(2)
C(6)	1111(5)	3598(3)	1935(3)	30(2)
C(7)	672(4)	3874(3)	1652(3)	31(2)
C(8)	149(4)	4176(3)	1277(2)	27(2)
C(9)	5400(4)	4403(3)	1762(2)	24(2)
C(10)	4787(4)	4685(3)	2133(2)	25(2)
C(11)	3412(5)	4555(3)	2540(2)	22(2)
C(12)	3674(4)	4995(3)	2863(2)	29(2)
C(13)	4512(5)	5301(3)	2809(2)	32(2)
C(14)	5071(4)	5147(3)	2431(2)	23(2)
C(15)	2524(4)	4185(3)	2563(2)	24(2)
C(16)	3223(4)	3104(3)	2558(2)	29(2)
C(17)	3961(4)	2833(3)	2249(2)	22(2)
C(18)	4955(4)	3018(3)	1625(2)	27(2)
C(19)	5483(5)	2502(3)	1749(2)	29(2)
C(20)	5236(5)	2138(3)	2123(2)	32(2)
C(21)	4459(5)	2304(3)	2381(2)	30(2)
C(22)	5183(4)	3472(3)	1234(2)	25(2)
C(23)	-408(4)	4183(3)	497(2)	35(2)
C(24)	-189(5)	4046(3)	-6(2)	31(2)
C(25)	1000(5)	4053(3)	-531(2)	29(2)
C(26)	473(5)	3755(3)	-875(2)	33(2)
C(27)	-429(5)	3610(3)	-764(2)	32(2)
C(28)	-760(5)	3750(3)	-321(2)	35(2)
C(29)	2007(5)	4197(3)	-593(2)	36(2)
C(30)	2800(4)	3336(3)	-169(2)	28(2)

C(31)	2005(5)	2918(3)	-40(2)	24(2)
C(32)	719(4)	2847(3)	445(2)	25(2)
C(33)	504(5)	2256(3)	267(2)	29(2)
C(34)	1062(5)	1996(3)	-73(2)	31(2)
C(35)	1817(5)	2327(3)	-231(2)	28(2)
C(36)	210(4)	3182(3)	824(2)	28(2)
C(37)	3271(5)	5913(3)	658(2)	33(2)
C(38)	1964(5)	5918(3)	1790(2)	38(2)
C(39)	5192(6)	1583(4)	3527(3)	65(3)
Cu(1)	3400(1)	3881(1)	1651(1)	22(1)
Cu(2)	1622(1)	4065(1)	453(1)	25(1)
N(1)	2601(4)	3556(3)	2322(2)	27(1)
N(2)	4170(3)	3160(2)	1868(2)	22(1)
N(3)	4912(3)	4143(2)	1348(2)	25(1)
N(4)	3943(4)	4405(2)	2168(2)	25(1)
N(5)	297(3)	3895(2)	809(2)	24(1)
N(6)	1473(4)	3173(2)	299(2)	25(1)
N(7)	671(4)	4214(2)	-117(2)	30(2)
N(8)	2552(4)	4025(2)	-161(2)	24(1)
N(9)	2601(5)	1391(3)	3022(2)	39(2)
N(10)	7456(4)	4104(3)	1057(2)	36(2)
N(11)	2868(4)	2797(3)	1081(2)	33(2)
O(1)	2604(3)	4584(2)	1499(1)	27(1)
O(2)	1893(3)	4877(2)	704(1)	26(1)
O(3)	3259(3)	5469(2)	1037(1)	26(1)
O(4)	1675(3)	5587(2)	1374(1)	27(1)
O(5)	2994(3)	3417(2)	1079(1)	29(1)
O(6)	2497(4)	2542(2)	1423(2)	52(2)
O(7)	3139(4)	2479(2)	750(2)	48(2)
O(8)	7385(3)	4641(3)	1239(2)	46(1)
O(9)	7291(3)	4050(2)	636(2)	37(1)
O(10)	7700(5)	3651(3)	1297(2)	97(3)
O(11)	3336(4)	1068(2)	3031(2)	54(2)
O(12)	2222(4)	1531(3)	3390(2)	65(2)
O(13)	2278(4)	1558(2)	2644(2)	50(2)
O(14)	4535(4)	1232(4)	3796(2)	92(2)
O(15)	8243(5)	2486(4)	1165(3)	137(3)
P(1)	2351(1)	5083(1)	1148(1)	24(1)

Table 7.2. Bond lengths [Å] and angles [°] for **2**.

C(1)-N(3)	1.453(7)	C(14)-H(14)	0.9500
C(1)-C(2)	1.464(8)	C(15)-N(1)	1.487(7)
C(1)-H(1A)	0.9900	C(15)-H(15A)	0.9900
C(1)-H(1B)	0.9900	C(15)-H(15B)	0.9900
C(2)-C(3)	1.189(8)	C(16)-N(1)	1.474(7)
C(3)-C(4)	1.450(9)	C(16)-C(17)	1.505(8)
C(4)-N(8)	1.489(7)	C(16)-H(16A)	0.9900
C(4)-H(4A)	0.9900	C(16)-H(16B)	0.9900
C(4)-H(4B)	0.9900	C(17)-N(2)	1.326(7)
C(5)-C(6)	1.452(9)	C(17)-C(21)	1.375(8)
C(5)-N(1)	1.484(8)	C(18)-C(19)	1.370(8)
C(5)-H(5A)	0.9900	C(18)-N(2)	1.374(7)
C(5)-H(5B)	0.9900	C(18)-C(22)	1.507(8)
C(6)-C(7)	1.186(9)	C(19)-C(20)	1.364(9)
C(7)-C(8)	1.461(9)	C(19)-H(19)	0.9500
C(8)-N(5)	1.482(7)	C(20)-C(21)	1.400(9)
C(8)-H(8A)	0.9900	C(20)-H(20)	0.9500
C(8)-H(8B)	0.9900	C(21)-H(21)	0.9500
C(9)-N(3)	1.486(7)	C(22)-N(3)	1.491(7)
C(9)-C(10)	1.512(8)	C(22)-H(22A)	0.9900
C(9)-H(9A)	0.9900	C(22)-H(22B)	0.9900
C(9)-H(9B)	0.9900	C(23)-N(5)	1.490(8)
C(10)-C(14)	1.354(8)	C(23)-C(24)	1.509(9)
C(10)-N(4)	1.368(8)	C(23)-H(23A)	0.9900
C(11)-N(4)	1.356(7)	C(23)-H(23B)	0.9900
C(11)-C(12)	1.360(8)	C(24)-N(7)	1.342(8)
C(11)-C(15)	1.511(8)	C(24)-C(28)	1.376(9)
C(12)-C(13)	1.389(9)	C(25)-N(7)	1.325(8)
C(12)-H(12)	0.9500	C(25)-C(26)	1.397(9)
C(13)-C(14)	1.396(8)	C(25)-C(29)	1.511(9)
C(13)-H(13)	0.9500	C(26)-C(27)	1.388(9)
C(26)-H(26)	0.9500	C(39)-H(39B)	0.9800
C(27)-C(28)	1.391(9)	C(39)-H(39C)	0.9800
C(27)-H(27)	0.9500	Cu(1)-O(1)	1.922(4)
C(28)-H(28)	0.9500	Cu(1)-N(2)	1.978(5)
C(29)-N(8)	1.517(8)	Cu(1)-O(5)	1.996(4)
C(29)-H(29A)	0.9900	Cu(1)-N(4)	2.008(5)

C(29)-H(29B)	0.9900	Cu(1)-N(1)	2.352(5)
C(30)-N(8)	1.484(7)	Cu(1)-N(3)	2.435(5)
C(30)-C(31)	1.499(8)	Cu(2)-O(2)	1.883(4)
C(30)-H(30A)	0.9900	Cu(2)-N(6)	1.924(5)
C(30)-H(30B)	0.9900	Cu(2)-N(7)	2.169(5)
C(31)-N(6)	1.353(7)	Cu(2)-N(5)	2.218(5)
C(31)-C(35)	1.377(8)	Cu(2)-N(8)	2.227(5)
C(32)-N(6)	1.361(8)	N(9)-O(12)	1.227(7)
C(32)-C(33)	1.371(8)	N(9)-O(13)	1.235(7)
C(32)-C(36)	1.491(8)	N(9)-O(11)	1.268(7)
C(33)-C(34)	1.382(9)	N(10)-O(10)	1.222(7)
C(33)-H(33)	0.9500	N(10)-O(9)	1.237(7)
C(34)-C(35)	1.379(9)	N(10)-O(8)	1.242(7)
C(34)-H(34)	0.9500	N(11)-O(7)	1.224(7)
C(35)-H(35)	0.9500	N(11)-O(6)	1.241(7)
C(36)-N(5)	1.493(7)	N(11)-O(5)	1.306(7)
C(36)-H(36A)	0.9900	O(1)-P(1)	1.496(4)
C(36)-H(36B)	0.9900	O(2)-P(1)	1.502(4)
C(37)-O(3)	1.430(6)	O(3)-P(1)	1.583(4)
C(37)-H(37A)	0.9800	O(4)-P(1)	1.581(4)
C(37)-H(37B)	0.9800	O(14)-H(14A)	0.8400
C(37)-H(37C)	0.9800	N(3)-C(1)-C(2)	113.9(5)
C(38)-O(4)	1.443(7)	N(3)-C(1)-H(1A)	108.8
C(38)-H(38A)	0.9800	C(2)-C(1)-H(1A)	108.8
C(38)-H(38B)	0.9800	N(3)-C(1)-H(1B)	108.8
C(38)-H(38C)	0.9800	C(2)-C(1)-H(1B)	108.8
C(39)-O(14)	1.433(9)	H(1A)-C(1)-H(1B)	107.7
C(39)-H(39A)	0.9800	C(3)-C(2)-C(1)	172.7(7)
C(2)-C(3)-C(4)	172.4(7)	C(11)-C(12)-H(12)	120.6
C(3)-C(4)-N(8)	114.1(5)	C(13)-C(12)-H(12)	120.6
C(3)-C(4)-H(4A)	108.7	C(12)-C(13)-C(14)	119.7(6)
N(8)-C(4)-H(4A)	108.7	C(12)-C(13)-H(13)	120.1
C(3)-C(4)-H(4B)	108.7	C(14)-C(13)-H(13)	120.1
N(8)-C(4)-H(4B)	108.7	C(10)-C(14)-C(13)	118.4(6)
H(4A)-C(4)-H(4B)	107.6	C(10)-C(14)-H(14)	120.8
C(6)-C(5)-N(1)	112.6(5)	C(13)-C(14)-H(14)	120.8
C(6)-C(5)-H(5A)	109.1	N(1)-C(15)-C(11)	111.4(5)
N(1)-C(5)-H(5A)	109.1	N(1)-C(15)-H(15A)	109.3
C(6)-C(5)-H(5B)	109.1	C(11)-C(15)-H(15A)	109.3

N(1)-C(5)-H(5B)	109.1	N(1)-C(15)-H(15B)	109.3
H(5A)-C(5)-H(5B)	107.8	C(11)-C(15)-H(15B)	109.3
C(7)-C(6)-C(5)	177.5(7)	H(15A)-C(15)-H(15B)	108.0
C(6)-C(7)-C(8)	175.6(8)	N(1)-C(16)-C(17)	114.2(5)
C(7)-C(8)-N(5)	114.9(5)	N(1)-C(16)-H(16A)	108.7
C(7)-C(8)-H(8A)	108.5	C(17)-C(16)-H(16A)	108.7
N(5)-C(8)-H(8A)	108.5	N(1)-C(16)-H(16B)	108.7
C(7)-C(8)-H(8B)	108.5	C(17)-C(16)-H(16B)	108.7
N(5)-C(8)-H(8B)	108.5	H(16A)-C(16)-H(16B)	107.6
H(8A)-C(8)-H(8B)	107.5	N(2)-C(17)-C(21)	121.3(6)
N(3)-C(9)-C(10)	115.0(5)	N(2)-C(17)-C(16)	117.2(6)
N(3)-C(9)-H(9A)	108.5	C(21)-C(17)-C(16)	121.2(6)
C(10)-C(9)-H(9A)	108.5	C(19)-C(18)-N(2)	120.5(6)
N(3)-C(9)-H(9B)	108.5	C(19)-C(18)-C(22)	124.3(6)
C(10)-C(9)-H(9B)	108.5	N(2)-C(18)-C(22)	115.2(5)
H(9A)-C(9)-H(9B)	107.5	C(20)-C(19)-C(18)	119.5(7)
C(14)-C(10)-N(4)	122.3(6)	C(20)-C(19)-H(19)	120.2
C(14)-C(10)-C(9)	122.9(6)	C(18)-C(19)-H(19)	120.2
N(4)-C(10)-C(9)	114.6(6)	C(19)-C(20)-C(21)	119.6(7)
N(4)-C(11)-C(12)	122.2(6)	C(19)-C(20)-H(20)	120.2
N(4)-C(11)-C(15)	114.0(5)	C(21)-C(20)-H(20)	120.2
C(12)-C(11)-C(15)	123.8(6)	C(17)-C(21)-C(20)	118.7(6)
C(11)-C(12)-C(13)	118.8(6)	C(17)-C(21)-H(21)	120.6
C(20)-C(21)-H(21)	120.6	N(8)-C(30)-C(31)	111.8(5)
N(3)-C(22)-C(18)	111.7(5)	N(8)-C(30)-H(30A)	109.3
N(3)-C(22)-H(22A)	109.3	C(31)-C(30)-H(30A)	109.3
C(18)-C(22)-H(22A)	109.3	N(8)-C(30)-H(30B)	109.3
N(3)-C(22)-H(22B)	109.3	C(31)-C(30)-H(30B)	109.3
C(18)-C(22)-H(22B)	109.3	H(30A)-C(30)-H(30B)	107.9
H(22A)-C(22)-H(22B)	107.9	N(6)-C(31)-C(35)	121.7(6)
N(5)-C(23)-C(24)	110.7(5)	N(6)-C(31)-C(30)	113.2(5)
N(5)-C(23)-H(23A)	109.5	C(35)-C(31)-C(30)	125.1(6)
C(24)-C(23)-H(23A)	109.5	N(6)-C(32)-C(33)	121.3(6)
N(5)-C(23)-H(23B)	109.5	N(6)-C(32)-C(36)	113.2(6)
C(24)-C(23)-H(23B)	109.5	C(33)-C(32)-C(36)	125.5(6)
H(23A)-C(23)-H(23B)	108.1	C(32)-C(33)-C(34)	118.8(7)
N(7)-C(24)-C(28)	121.8(7)	C(32)-C(33)-H(33)	120.6
N(7)-C(24)-C(23)	112.1(6)	C(34)-C(33)-H(33)	120.6
C(28)-C(24)-C(23)	126.0(7)	C(35)-C(34)-C(33)	120.5(6)

N(7)-C(25)-C(26)	123.1(6)	C(35)-C(34)-H(34)	119.7
N(7)-C(25)-C(29)	114.0(6)	C(33)-C(34)-H(34)	119.7
C(26)-C(25)-C(29)	122.8(7)	C(31)-C(35)-C(34)	118.4(6)
C(27)-C(26)-C(25)	117.2(7)	C(31)-C(35)-H(35)	120.8
C(27)-C(26)-H(26)	121.4	C(34)-C(35)-H(35)	120.8
C(25)-C(26)-H(26)	121.4	C(32)-C(36)-N(5)	113.9(5)
C(26)-C(27)-C(28)	119.5(7)	C(32)-C(36)-H(36A)	108.8
C(26)-C(27)-H(27)	120.2	N(5)-C(36)-H(36A)	108.8
C(28)-C(27)-H(27)	120.2	C(32)-C(36)-H(36B)	108.8
C(24)-C(28)-C(27)	119.0(7)	N(5)-C(36)-H(36B)	108.8
C(24)-C(28)-H(28)	120.5	H(36A)-C(36)-H(36B)	107.7
C(27)-C(28)-H(28)	120.5	O(3)-C(37)-H(37A)	109.5
C(25)-C(29)-N(8)	111.6(6)	O(3)-C(37)-H(37B)	109.5
C(25)-C(29)-H(29A)	109.3	H(37A)-C(37)-H(37B)	109.5
N(8)-C(29)-H(29A)	109.3	O(3)-C(37)-H(37C)	109.5
C(25)-C(29)-H(29B)	109.3	H(37A)-C(37)-H(37C)	109.5
N(8)-C(29)-H(29B)	109.3	H(37B)-C(37)-H(37C)	109.5
H(29A)-C(29)-H(29B)	108.0	O(4)-C(38)-H(38A)	109.5
O(4)-C(38)-H(38B)	109.5	N(7)-Cu(2)-N(8)	78.32(19)
H(38A)-C(38)-H(38B)	109.5	N(5)-Cu(2)-N(8)	153.07(19)
O(4)-C(38)-H(38C)	109.5	C(16)-N(1)-C(5)	109.7(5)
H(38A)-C(38)-H(38C)	109.5	C(16)-N(1)-C(15)	113.3(5)
H(38B)-C(38)-H(38C)	109.5	C(5)-N(1)-C(15)	110.2(5)
O(14)-C(39)-H(39A)	109.5	C(16)-N(1)-Cu(1)	104.8(4)
O(14)-C(39)-H(39B)	109.5	C(5)-N(1)-Cu(1)	119.0(4)
H(39A)-C(39)-H(39B)	109.5	C(15)-N(1)-Cu(1)	99.5(3)
O(14)-C(39)-H(39C)	109.5	C(17)-N(2)-C(18)	120.0(5)
H(39A)-C(39)-H(39C)	109.5	C(17)-N(2)-Cu(1)	121.4(4)
H(39B)-C(39)-H(39C)	109.5	C(18)-N(2)-Cu(1)	118.6(4)
O(1)-Cu(1)-N(2)	174.5(2)	C(1)-N(3)-C(9)	109.5(5)
O(1)-Cu(1)-O(5)	90.31(17)	C(1)-N(3)-C(22)	112.0(5)
N(2)-Cu(1)-O(5)	93.40(19)	C(9)-N(3)-C(22)	112.9(5)
O(1)-Cu(1)-N(4)	89.47(19)	C(1)-N(3)-Cu(1)	122.2(4)
N(2)-Cu(1)-N(4)	87.4(2)	C(9)-N(3)-Cu(1)	103.4(3)
O(5)-Cu(1)-N(4)	171.9(2)	C(22)-N(3)-Cu(1)	96.2(3)
O(1)-Cu(1)-N(1)	96.05(18)	C(11)-N(4)-C(10)	118.2(6)
N(2)-Cu(1)-N(1)	78.7(2)	C(11)-N(4)-Cu(1)	118.9(4)
O(5)-Cu(1)-N(1)	112.77(18)	C(10)-N(4)-Cu(1)	122.4(4)
N(4)-Cu(1)-N(1)	75.3(2)	C(8)-N(5)-C(23)	106.6(5)

O(1)-Cu(1)-N(3)	107.22(17)	C(8)-N(5)-C(36)	110.8(5)
N(2)-Cu(1)-N(3)	76.57(19)	C(23)-N(5)-C(36)	111.1(5)
O(5)-Cu(1)-N(3)	94.87(17)	C(8)-N(5)-Cu(2)	118.8(4)
N(4)-Cu(1)-N(3)	77.48(19)	C(23)-N(5)-Cu(2)	105.1(4)
N(1)-Cu(1)-N(3)	143.75(18)	C(36)-N(5)-Cu(2)	104.2(4)
O(2)-Cu(2)-N(6)	168.86(19)	C(31)-N(6)-C(32)	119.3(6)
O(2)-Cu(2)-N(7)	107.17(18)	C(31)-N(6)-Cu(2)	118.7(4)
N(6)-Cu(2)-N(7)	83.8(2)	C(32)-N(6)-Cu(2)	120.3(4)
O(2)-Cu(2)-N(5)	98.56(18)	C(25)-N(7)-C(24)	119.1(6)
N(6)-Cu(2)-N(5)	81.5(2)	C(25)-N(7)-Cu(2)	114.2(5)
N(7)-Cu(2)-N(5)	79.2(2)	C(24)-N(7)-Cu(2)	112.4(4)
O(2)-Cu(2)-N(8)	102.10(18)	C(30)-N(8)-C(4)	109.7(5)
N(6)-Cu(2)-N(8)	81.5(2)	C(30)-N(8)-C(29)	110.2(5)
C(4)-N(8)-C(29)	105.2(5)	P(1)-O(1)-Cu(1)	146.4(3)
C(30)-N(8)-Cu(2)	101.3(4)	P(1)-O(2)-Cu(2)	132.6(3)
C(4)-N(8)-Cu(2)	121.6(4)	C(37)-O(3)-P(1)	119.5(4)
C(29)-N(8)-Cu(2)	108.6(4)	C(38)-O(4)-P(1)	118.4(4)
O(12)-N(9)-O(13)	121.3(7)	N(11)-O(5)-Cu(1)	121.3(4)
O(12)-N(9)-O(11)	119.3(7)	C(39)-O(14)-H(14A)	109.5
O(13)-N(9)-O(11)	119.4(6)	O(1)-P(1)-O(2)	118.8(2)
O(10)-N(10)-O(9)	122.6(7)	O(1)-P(1)-O(4)	109.8(2)
O(10)-N(10)-O(8)	118.9(7)	O(2)-P(1)-O(4)	105.1(2)
O(9)-N(10)-O(8)	118.5(6)	O(1)-P(1)-O(3)	106.4(2)
O(7)-N(11)-O(6)	121.6(6)	O(2)-P(1)-O(3)	110.4(2)
O(7)-N(11)-O(5)	119.2(6)	O(4)-P(1)-O(3)	105.5(2)
O(6)-N(11)-O(5)	119.3(6)		

Table 7.3. Anisotropic displacement parameters ($Å^2 x\ 10^3$)for **2**. The anisotropic displacement factor exponent takes the form: $-2p^2[\ h^2a^{*2}U^{11} + ... + 2\ h\ k\ a^*\ b^*\ U^{12}\ ]$

	U^{11}	U^{22}	U^{33}	U^{23}	U^{13}	U^{12}
C(1)	13(4)	24(4)	48(5)	10(4)	2(3)	-4(3)
C(2)	19(4)	19(4)	29(4)	8(3)	-1(3)	3(3)
C(3)	24(4)	21(4)	32(4)	2(3)	8(4)	-3(3)
C(4)	15(3)	34(4)	36(4)	5(3)	8(4)	-7(4)
C(5)	29(4)	16(4)	41(4)	4(3)	0(4)	-6(4)
C(6)	16(4)	31(5)	44(5)	-10(4)	14(4)	-14(4)

C(7)	18(4)	29(4)	46(5)	-4(4)	7(4)	-14(4)
C(8)	18(4)	28(4)	33(4)	-2(3)	5(3)	-4(3)
C(9)	22(4)	13(4)	38(4)	4(3)	-3(3)	-3(3)
C(10)	21(4)	18(4)	36(4)	7(3)	1(3)	6(3)
C(11)	21(4)	15(4)	31(4)	3(3)	-4(4)	-1(3)
C(12)	26(4)	22(4)	39(4)	0(3)	8(3)	-2(3)
C(13)	36(5)	20(4)	41(5)	-2(3)	-4(4)	6(4)
C(14)	17(4)	16(4)	36(4)	0(3)	-1(3)	-5(3)
C(15)	20(4)	13(4)	40(4)	1(3)	6(3)	-5(3)
C(16)	31(5)	25(4)	30(4)	0(3)	1(3)	1(3)
C(17)	18(4)	18(4)	28(4)	3(3)	-4(3)	-8(3)
C(18)	23(4)	19(4)	38(4)	-7(3)	-4(4)	0(3)
C(19)	23(4)	16(4)	47(5)	-8(3)	-2(3)	-2(3)
C(20)	23(4)	20(4)	52(5)	-5(4)	-12(4)	1(3)
C(21)	25(4)	14(4)	50(5)	3(3)	-7(4)	-7(3)
C(22)	15(4)	21(4)	39(4)	1(3)	2(3)	7(3)
C(23)	16(4)	45(5)	44(5)	2(4)	1(4)	9(3)
C(24)	22(4)	22(4)	49(5)	7(4)	-2(4)	6(4)
C(25)	28(4)	19(4)	41(5)	4(4)	-3(4)	2(3)
C(26)	27(4)	25(4)	47(5)	11(4)	-6(4)	3(4)
C(27)	30(4)	24(4)	44(5)	5(4)	-17(4)	4(4)
C(28)	19(4)	32(5)	52(5)	10(4)	-7(4)	7(3)
C(29)	30(4)	33(5)	45(5)	-8(4)	-2(4)	-10(4)
C(30)	22(4)	19(4)	42(4)	2(3)	7(3)	3(3)
C(31)	29(4)	7(4)	38(4)	1(3)	-2(3)	6(3)
C(32)	20(4)	21(4)	33(4)	6(3)	0(3)	2(3)
C(33)	26(4)	14(4)	46(5)	2(3)	-10(4)	-5(3)
C(34)	38(5)	18(4)	38(5)	-1(3)	-10(4)	5(4)
C(35)	35(5)	19(4)	30(4)	-1(3)	-5(3)	9(3)
C(36)	12(4)	24(4)	48(5)	0(3)	4(3)	-7(3)
C(37)	34(4)	16(4)	48(4)	14(3)	1(4)	-13(4)
C(38)	40(5)	26(4)	47(5)	-10(4)	1(4)	3(4)
C(39)	62(7)	78(7)	56(6)	10(5)	-2(5)	21(6)
Cu(1)	17(1)	17(1)	34(1)	2(1)	1(1)	-1(1)
Cu(2)	20(1)	16(1)	39(1)	-1(1)	0(1)	0(1)
N(1)	21(3)	23(3)	36(3)	3(3)	5(3)	-6(3)
N(2)	15(3)	13(3)	38(4)	3(3)	2(3)	-1(2)
N(3)	18(3)	22(3)	35(3)	3(3)	3(3)	-2(3)
N(4)	18(3)	18(3)	38(4)	-1(3)	5(3)	4(3)

N(5)	20(3)	19(3)	35(3)	4(3)	2(3)	3(3)
N(6)	18(3)	19(3)	39(3)	3(3)	-2(3)	8(3)
N(7)	30(4)	21(4)	38(4)	0(3)	-2(3)	1(3)
N(8)	24(3)	13(3)	36(3)	0(3)	-2(3)	-6(3)
N(9)	49(5)	22(4)	47(4)	-2(3)	20(4)	-5(3)
N(10)	15(3)	33(4)	61(5)	8(4)	-6(3)	-7(3)
N(11)	23(3)	34(4)	43(4)	-3(4)	-5(3)	-1(3)
O(1)	23(3)	17(3)	42(3)	5(2)	2(2)	4(2)
O(2)	25(3)	19(3)	35(3)	1(2)	-6(2)	-1(2)
O(3)	17(3)	16(2)	45(3)	8(2)	4(2)	-1(2)
O(4)	22(3)	21(3)	39(3)	-2(2)	0(2)	6(2)
O(5)	34(3)	15(3)	38(3)	5(2)	2(2)	2(2)
O(6)	66(4)	32(3)	57(4)	6(3)	9(3)	-10(3)
O(7)	65(4)	36(3)	44(3)	-9(3)	1(3)	24(3)
O(8)	47(4)	49(4)	41(3)	-5(3)	9(3)	-15(3)
O(9)	23(3)	49(3)	40(3)	-13(3)	-4(2)	0(3)
O(10)	95(6)	70(5)	127(6)	56(5)	-43(5)	5(4)
O(11)	28(3)	58(4)	78(4)	-6(3)	10(3)	18(3)
O(12)	65(4)	81(5)	50(4)	14(3)	18(3)	46(4)
O(13)	45(4)	54(4)	53(4)	-6(3)	3(3)	1(3)
O(14)	58(5)	145(7)	74(5)	39(5)	-12(4)	19(5)
O(15)	110(7)	180(9)	122(6)	-20(6)	0(6)	-9(6)
P(1)	20(1)	14(1)	38(1)	2(1)	1(1)	-2(1)

Table 7.4. Hydrogen coordinates (x 10^4) and isotropic displacement parameters (Å^{2}x 10^3) for **2**.

	x	y	z	U(eq)
H(1A)	5688	4549	854	34
H(1B)	4922	5018	1059	34
H(4A)	3761	4284	-460	34
H(4B)	3221	4875	-238	34
H(5A)	1756	2810	2167	35
H(5B)	1371	3257	2575	35
H(8A)	311	4637	1266	32

H(8B)	-511	4146	1354	32
H(9A)	5832	4738	1656	29
H(9B)	5766	4053	1902	29
H(12)	3291	5090	3121	35
H(13)	4703	5614	3028	39
H(14)	5638	5362	2384	28
H(15A)	2357	4113	2893	29
H(15B)	2030	4440	2417	29
H(16A)	2856	2746	2685	35
H(16B)	3516	3327	2823	35
H(19)	6017	2399	1575	34
H(20)	5589	1773	2207	38
H(21)	4279	2056	2643	36
H(22A)	5850	3457	1173	30
H(22B)	4862	3334	948	30
H(23A)	-430	4653	547	42
H(23B)	-1017	4005	575	42
H(26)	721	3655	-1171	39
H(27)	-818	3417	-989	39
H(28)	-1371	3643	-238	42
H(29A)	2087	4659	-661	43
H(29B)	2245	3952	-862	43
H(30A)	3310	3259	51	33
H(30B)	3015	3219	-485	33
H(33)	-19	2030	375	34
H(34)	924	1585	-197	38
H(35)	2198	2152	-467	33
H(36A)	439	3027	1128	33
H(36B)	-446	3067	802	33
H(37A)	2988	5715	384	49
H(37B)	3906	6029	586	49
H(37C)	2929	6299	744	49
H(38A)	2101	5605	2034	56
H(38B)	1474	6204	1895	56
H(38C)	2515	6171	1722	56
H(39A)	4917	1985	3419	98
H(39B)	5380	1326	3258	98
H(39C)	5729	1678	3720	98
H(14A)	4119	1095	3620	13

8. References

1. Thompson, P.R.; Philip, A.C., *PNAS* **2001,** 98(15), 8170-8171
2. Knowles, J.R., *Annu. Rev. Bioch*em. **1980**, 49, 877-919
3. Joyce, C. M.; Steitz, T.A., *Annu. Rev. Biochem.* **1994**, 63, 777-822
4. Doublie, S.; Sawaya, M.R.; Ellenberger, T. *Structure* **1999**, 7, R31-R35
5. Ollis, D. L.; Brick, P.; Hamlin, R.; Xuong, N. G.; Steitz, T.A. *Nature* **1985**, 313, 762-766
6. Rodriguez, A.C.; Park, H.W.; Mao, C.; Beese, L.S., *J. Mol. Biol*. **2000**, 299, 447-462
7. Brautigam, C.A.; Steitz, T.A., *Curr. Opin. Struct. Biol.* **1998**, 8, 54-63
8. Kim, E.E; Wyckoff, H.W. J., *Mol. Biol.* **1991**, 218, 449-464
9. C.A. Brautigam, T.A. Steitz *J. Mol. Biol.* **1998**, *277*, 363
10. Derbyshire, V.; Freemont, P.S.; Sanderson, M.R.; Beese, L.S.; Freidman, J.M.; Steitz, T.A.; Joyce, C.M. *Science* **1988**, 240, 199-201
11. Kim, E.E.; Wyckoff, H.W.*J. Mol. Bio.* **1991**, *218*, 449-464
12. Kovall, R.A.; Matthews, B.W., *Curr. Opin. Chem. Biol.* **1999**, *3*, 578-583
13. Steitz, T.A., *J. Biol. Chem.* **1999**, *247*, 17395-17398
14. Steitz, T.A., *Nature*, **1998**, *391*, 231-232
15. Steitz, T.A.; Steitz , J.A., *Proc. Natl. Acad. Sci. USA*, **1993**, *90*, 6498-6502
16. a) Williams, N.H.; Takasaki, B.; Chin, J., *Acc. Chem. Res*., **1999**, *32*, 485-493. b) Blasko, A.; Bruice, T.C., *Acc. Chem. Res.*, **1999**,*32,* 475-484. c) Krämer, R.; Gajda, T., *Persp. Bioinorg. Chem.*, **1999**, 4, 209-240 d) Kimura, E. *Current Opinion in Chemical Biology* **2000**, 4(2), 207-213 e) Calama, M.C.; Timmermann, P.; Reinhoudt, D.N., *Chem. Soc. Rev.* **2000**, *29,* 75-86
17. More recent examples of dicopper(II) systems: a) Mancin, F.; Rampazzo, E.; Tecilla, P.; Tonellato, U. Eur. J. Org. Chem. **2004**, 2, 281-288. b) Jancso, A.; Mikkola, S.;

Lonnberg, H.; Hegetschweiler, K.; Gajda, T. *Chem. Eur. J.* **2003**, 9(21), 5404-5415. c) Fry, F.H.; Spiccia, L.; Jensen, P.; Moubaraki, B.; Murray, K.S.; Tiekink, E.R.T. *Inorg. Chem.* **2003**, 42(18), 5594-5603. d) Scarpellini, M.; Neves, A.; Hoerner, R.; Bortoluzzi, A.J.; Szpoganics, B.; Zucco, C.; Silva, R.A.N.; Drago, V.; Mangrich, A.S.; Ortiz, W.A.; Passos, Wagner A.C.; De Oliveira, M.C. B.; Terenzi, H. *Inorg. Chem.* **2003**, 42(25), 8353-8365. e) Gajda, T.; Duepre, Y.; Toeroek, I.; Harmer, J.; Schweiger, A.; Sander, J.; Kuppert, D.; Hegetschweiler, K. *Inorg. Chem.* **2001**, 40(19), 4918-4927. f) Deal, K.A.; Park, G.; Shao, J.; Chasteen, N. D.; Brechbiel, M.W.; Planalp, R.P. *Inorg. Chem.* **2001**, 40(17), 4176-4182.

18. More recent examples of dizink(II) systems : a)Yang, M.Y.; Iranzo, O.; Richard, J.P.; Morrow, J.R. *J. Am. Chem. Soc*. **2005**, 127(4), 1064-1065 b)Bauer-Siebenlist, B. Meyer, F. Farkas, E. Vidovic, D. Cuesta-Seijo, J.A.; Herbst-Irmer, R.; Pritzkow, H. *Inorg. Chem*. **2004**, 43(14), 4189-4202 c)Yashiro, M.; Kaneiwa, H.; Onaka, K.; Komiyama, M. *Dalton Trans*. **2004**, 4, 605-610 d) Iranzo, O.; Richard, J.P.; Morrow, J.R.. *Inorg. Chem.* **2004**, 43(5), 1743-1750 e) Arca, M.; Bencini, A.; Berni, E.; Caltagirone, C.; Devillanova, F.A.; Isaia, F.; Garau, A.; Giorgi, C.; Lippolis, V.; Perra, A.; Tei, L.; Valtancoli, B. *Inorg. Chem*. **2003**, 42(21), 6929-6939
19. Trawick, B.N.; Daniher, A.T.; Bashkin, J.K. Chem. Rev., **1998**, 98, 939
20. Breslow, R.; Singh, S.; *Bioorg. Chem.* **1988**, 16, 408
21. Yashiro, M.; Ishikubo, A.; Komiyama, M. *Chem. Comm.,* **1995**,17,1793-4
22. Matsuda, S.; Ishikubo, A.; Kuzuya, A.; Yashiro, M.; Komiyama, M., *Angew. Chem. Int. Ed.*, **1998**, 37, 3284
23. Wall, M.; Hynes, R.C.; Chin, J., *Angew. Chem. Int. Ed*., **1993**, 32, 1633
24. a) He, C.; Lippard, S.J. *J. Am. Chem. Soc.*, **2000**, *122*, 184-185 b) He, C.; Gomez, V.; Spingler, B.; Lippard, S.J. *Inorg. Chem*., **2000**, *39*, 4188-4189
25. Kim, J. H.; Chin, J., *J. Am. Chem. Soc.* **1992**, *114*, 9792

26. Moss, R.A.; Ragunathan, K.G., *Chem. Commun.* **1998**, 17, 1871-1872

27. Kuo, L.Y.; Barnes, L.A., *Inorg. Chem.* **1999**, 38, 814-817

28. Sträter, N.; Lipscomb, W.N.; Labunde, T.K.; Krebs, B., *Angew. Chem. Inter. Ed*., **1996**, 35, 2024-2055

29. Wilcox, D.E., *Chem. Rev*. **1996**, 96, 2435-2458

30. Williams, N.H., *J. Am. Chem. Soc.*, **2000**, 122, 12023-12024

31. Dietrich, B.; Hosseini, M.W.; Lehn, J.-M. Sessions, R.B., *J. Am. Chem. Soc.* **1981**, 103, 1282-1283

32. Peter, F.; Gross, H.;Hosseini, M.W.; Lehn, J.-M. Sessions, R.B. *Chem. Comm.* **1981**, 1067-1069

33. Hosseini, M.W.; Lehn, J.-M.; Jones, K.C.; Plute, K.E.; Mertes, K.B.; Mertes, M.P. *J. Am. Chem. Soc.*, **1989**, 111, 6330-6335

34. a) Coprehensive Inorganic Chemistry, **1973**, Vol 3, 449-453 b) Coprehensive Coordination Chemistry II, **2004**, Vol. 4, 128-130

35. Clearfield, A.; Vaughan, P.A.; *Acta Cryst*., **1956**, 9, 555

36. Warzeska, S.; Kraemer, R.. *Chem. Ber*., **1995**, 128, 115-119

37. Warzeska, S., PhD thesis, **1997**

38. Warzeska, S.; Kraemer, R.. *Chem. Comm*., **1996,** 499-500

39. Peisach, J.; Blumberg, W.E., *Arch. Biochem. Biophys.*, **1974**, 165(2), 691-708

40. a) Neverov, A.A.; Brown, R.S., *Inorg. Chem.* **2001,** 40, 3588-3595 b) Bosch, E.; Rived, F.; Roses, M.; Sales, J., *J. Chem. Soc Perkin Trans. 2*,**1999**, 1953-1958

41. a) Fronczek, F.R.; Mamo, A.; Pappalardo, S. *Inorg. Chem.* **1989**, 28(7), 1419-22. b) Che, C.M.; Li, Z.Y.; Wong, K.Y.; Poon, C.K.; Mak, T.C. W.; Peng, S.M. *Polyhedron* **1994**, 13(5), 771-6 c) Krueger, H.J. *Chem. Ber.* **1995**, 128(6), 531-9

42. Tsang, J. S. W.; Neverov, A. A.; Brown, R. S., *J. Am. Chem Soc*. **2003**, 125, 7602-7607

43. Dean, J. A. *Handbook of Organic Chemistry*; McGraw-Hill Book Co.: New York, **1987**

44. Kuehn, U., Warzeska, S.; Kraemer, R. *J. Am. Chem. Soc*. **2001**, 123(33), 8125-8126

45. Imhof, P., Fischer, S.; Krämer, R.; Smith, J. C., *J. Mol. Struct. Theochem,* **2005,** 713, 1-5

46. Kirby, A.J.; Younas, M. *J. Chem. Soc.(B*), **1970**, 6, 1165-1172

47. Kühn, U., PhD thesis, **2003**

48. a) Tetas, M.; Lowenstein, J.M., *Biochemistry* 2 (**1963**), 350-357 b) Sigel, H.; Amsler, P. E., *J. Am. Chem. Soc.* 98 (**1976**) 7390-7400 c) Sigel, H.; Hofstetter, F.; Martin, R.B.; Milburn, R.B.; Scheller-Kratinger, V.; Scheller, K. H., *J. Am. Chem. Soc.* 106 (**1984**) 7935-7946 d) Ge, R.; Lin, H.; Xu, X.; Sun, X.; Lin, H.; Zhu, S.; Ji, B.; Li, F.; Wu, H., *J. Inorg. Biochem*. 98 (**2004**),917-924

49. a) Krämer, R. *Appl. Microbiol*. *Biotechnol*. 52 (**1999)**, 761-767 b) Ott, R.; Krämer, R. *Angew. Chem. Int. Ed*., 37 (**1998)**,1957-1959

50. Trapmann, H.; Devani, M., Zeitschr. Physiol. Chem. 328 (**1962**) 207-211

51. Branum, M.E.; Tipton, A.K.; Zhu, S.; Que, L, *J.Am. Chem. Soc.,* **2001**, 123, 1898

52. Hirata, A.A.; Appleman, D. *Anal.Chem.* **1959**, 31(12), 2097-2099; See also Cogan, E. B.; Birell, G. B.; Griffith, O.H., Anal. Biochem. 271 (**1999**) 29-35

53. Tikhonova, L. *Zhur. Neorg. Khim*. **1967,** 12 , 494

54. Brunner, J.; Pritzkow, H.; Krämer, R. *Dalton Trans*. **2005**, 2, 338-343

55. Gemini 3.10, **1998-1999** Tecan Software GmbH

56. Alcock, N.W.; Kingston, R G.; Moore, P.; Pierpoint, C. *J. Chem. Soc. Dalton Trans.* **1984**, 1937

57. Fraser, M.M.; Raphael, R.A. *J. Chem. Soc.* **1952**, 226

58. Bradshaw, J.S.; Husztky, P.; McDaniel, C.; Zhu, C.Y.; Dalley, N.K.; Izatt, R. *J. Org. Chem.* **1990**, 55, 3134

59. Electronic Structure Calculations on Workstation Computers: The Program System TURBOMOLE. Ahlrichs, R.; Bar, M.; Haser, M.; Horn, H.;Kolmel, C.; *Chem. Phys. Letters*, **1989,** 162, 165

60. a) Becke, A.D., *J. Chem. Phys*. **1993**, 98, 5648-5652 b) Lee, C.; Yang, W.; Parr, R.G., *Phys. Rev. B*. **1988**, 37, 785-789 c) Miehlich, B.; Savin, A.; Stoll, H.; Preuss, H. *Chem. Phys. Lett.* **1989**, 157, 200

61. a) Dunning, T. H. Jr.; Hay, P. J. *Modern Theoretical Chemistry*, Ed. H. F. Schaefer III, Plenum Press (New York, USA), **1976**, 1-28 b) Hay, P. J.; Wadt, W. R. *J. Chem. Phys.*,**1985**, *82*, 270 c) Wadt, W. R.; Hay, P. J. *J. Chem. Phys.*,**1985**, *82*, 284 d) Hay, P. J.; Wadt, W. R. *J. Chem. Phys.*, **1985**, *82*, 299

62. Dunning, T. H.; Hay, P. J. in Methods of Electronic Structure Theory, Vol. 3, H.F. Schaefer III, Ed. Plenum Press **1977**

Aus dieser Arbeit hervorgegangene Publikationen:

"Screening of ATP hydrolysis by Zr(IV) and Eu(III) complexes"
Malgorzata Jagoda, Roland Krämer *Inorg. Chem. Comm.*, **2005**, 8, 697-699

"Catalytic transesterification of dialkyl phosphates by a bioinspired dicopper(II) macrocyclic complex"
Malgorzata Jagoda, Sabine Warzeska, Hans Pritzkow, Hubert Wadepohl, Petra Imhof, Jeremy C. Smith, Roland Kraemer *J. Am. Chem. Soc.*, **2005**, in press

An dieser Stelle möchte ich mich bei allen Personen bedanken, die zum Gelingen der vorliegenden Arbeit beigetragen haben.

Bei Heike Vongerichten, Karin Gabel, Claudia Dienemann und Beate Termin möchte ich mich für die Organisation des „alltäglichen“ Laborbetriebs und für die Unterstützung bei den ESI-MS und NMR Messungen bedanken.

Meiner Arbeitsplatznachbarin Mareike Göritz möchte ich herzlich für die gute Atmosphäre und die langen Unterhaltungen danken, die mich immer wieder motiviert und aufgebaut haben.

Meinen Laborkollegen Dr. Iris Boll, Dr. Jens Brunner, Mareike Göritz, Nora Graf, Elmar Jentzsch, Radek Kierat, Ann-Kathrin Marguerre, Dr. Andriy Mokhir, Dr. Patrick Plitt, Dr. Stefan Wörl, Dr. Felix Zelder danke ich für das gute “Teamwork“.

Nora Graf und Dr. Jens Brunner gilt mein Dank für das Korrekturlesen dieser Arbeit.

Meiner Lehramtskandidatin Nadine Ehret danke ich für die Unterstützung und Unterhaltung im Labor.

Tobias Graf danke ich, dass er der dafür gesorgt hat, die Arbeit an den Computern möglichst einfach zu machen.

Bei meinen zahlreichen Anorganik- und Organikpraktikanten möchte ich mich ebenfalls für die Hilfe im Labor bedanken.

Allen übrigen Arbeitskreis-Mitgliedern danke ich für die gute Zusammenarbeit.

Besonderer Dank an meine Eltern, meine Schwestern, meine Familie und meinen Freund Jens für die Unterstützung und das Verständnis während der Promotion.

Erklärungen gemäß § 7 (3) b) und c) der Promotionsordnung:

a) ich erkläre hiermit, dass ich die vorgelegte Dissertation selbst verfasst und mich dabei keiner anderen als der von mir ausdrücklich bezeichneten Quellen und Hilfen bedient habe,

b) ich erkläre hiermit, dass ich an keiner anderen Stelle ein Prüfungsverfahren beantragt bzw. die Dissertation in dieser oder anderer Form bereits anderweitig als Prüfungsarbeit verwendet oder einer anderen Fakultät als Dissertation vorgelegt habe.

Heidelberg, den 23.08.2005 .....

(Malgorzata Jagoda)